DEGREE PROJECT IN ELECTRIC POWER ENGINEERING 120 CREDITS, SECOND CYCLE

STOCKHOLM, SWEDEN 2016

Analysis of load models used in black-start studies

ALBANE SCHWOB

KTH ROYAL INSTITUTE OF TECHNOLOGY

SCHOOL OF ELECTRICAL ENGINEERING

TRITA-EE 2016:016

MASTER THESIS

Albane Schwob

Analysis of load models used in black-start studies

2015-2016

Supervisors
KTH : Luigi Vanfretti and Maxime Baudette
RTE : Yannick Filion

Acknowledgements

This research project would not have been possible without the help of many people.

I would like to express my sincere gratitude to my tutor at RTE, Yannick Fillion, who guided me all along my work. His suggestions have contributed immensely to the evolution of the project.

I am very thankful to Simon Deschanvres and David Petesch who were always eager to help me out. I wish to thank Pierre Rault who has been most helpful with the use of EMTP. More generally, I wish to thank all the people working in the Mesh division.

I would also like to thank Maxime Baudette, who has given me advices throughout my work. Finally, I want to thank my tutor at KTH, Luigi Vanfretti, who has been kind enough to accept the role of being my supervisor at KTH.

Abstract

This research project has been conducted at RTE in order to study the influence of the load model in black start studies.

After a black-out, a procedure called black-start is led in order to restore voltage on the grid. Transient harmonic overvoltages are likely to appear during this procedure. Therefore black start studies are carried out to determine the overvoltage likely to appear at the primary of the transformer energized.

In the past, the representation of key components in the black start study (alternator, 400 kV lines) have been extensively studied. However, the representation of the load was never much considered. Until now, only one load model has been used in black-start. This load model is very basic and it is not known if a more precise load model would improve the results of the black-start studies.

The approach used in the scope of this Thesis is based on comparisons with the results of black start studies using a more detailed load model. First, a detailed model of the load is built. The point is to use the results of the black start study with the detailed load model as a reference. Starting from the detailed load model and simplifying it, simplified load models are built. Then the results of the black start studies using the different load models are compared with the reference in order to determine the influence of the load model on black start studies. Finally, a new load model is suggested for black start studies.

Table of contents

List of Figures

List of Tables

List of Acronyms

TSO Transmission System Operator
DSO Distribution System Operator
RTE the French transmission system operator

Chapter 1. Introduction

1.1 Background

This Thesis deals with the load models used in black start studies. A black start is a procedure to restore voltage on the electric grid, after a widespread incident, without the help of another grid. High overvoltages must be avoided during the energizing of the network. They can damage the electric equipment and thus be responsible for the failure of the restoration procedure**.** Black start studies are carried out to analyze the overvoltages during the restoration phase.

The restoration phase must be as quick as possible in order to limit the social and economic impacts of the electricity shortage. An outage affects everyone: households and firms. Households suffer economic losses due for instance to the food spoiled. Industries and services may suffer economic losses due to a loss of output, damages in the equipment. The consequences on social life are inconveniences. The transportation system is out of order making it hard for people to commute to work. Governmental services such as airports, police stations, hospitals and clinics are considered as priority clients and energized first. For hospitals, electricity is a matter of life or death. Some patients rely on equipment fed by electricity to live. After a widespread incident leading to the loss of voltage on the grid, hospitals switch to back-up power sources for electric supply but this solution has a limited life time so it is vital to restore power quickly.

For practical reasons, it is unthinkable to carry out a black start on the actual power grid. Clients do not accept to be disconnected from the electric grid unless they receive a financial compensation. Besides, some expensive electric equipment might get damaged during the restoration process. That is the reason for entirely relying on computer simulation for this kind of studies.

Modeling the electric grid for black start studies is a challenge. When the model used is not complex enough, the results may not be representative of the real behavior, by missing overvoltages. However, a complex model will lengthen the simulation time of the study. Much work was put in modeling the 400kV grid, but the load model used on lower voltages levels has traditionally been a simple model. A study is needed to determine whether the current load model is satisfactory and whether a different load model could significantly improve the fidelity of black start studies.

1.2 Problem definition and objectives

After a major incident leading to voltage collapse on the electric grid, the Transmission System Operator (TSO) will energize the grid. There is a risk of overvoltages during energizing of an unloaded transformer. Black start studies are carried out to analyze this risk. Current black start studies use a very basic load model to represent the 225 kV and lower voltage level grids. The reason for keeping this basic load model is that black-start studies require about 10 000 scenarios spanning lots of grid parameters variations. In such conditions, a detailed load model would require a too large computing time.

The problem is that we don't know if the basic load model used in a grid during black-start gives realistic results for the overvoltages.

The analysis carried out in this work will study the difference between the basic model currently used, a detailed model and load models with a mixed complexity level, that we will call "simplified models".

A first objective is to determine whether using a load model more precise than the basic one can improve black-start studies. A second objective is to study how such a load model with a mixed complexity level could be elaborated without having to build a detailed load model.

1.3 Overview of the report

The principle for network restoration and the phenomenon of transient harmonic overvoltages are presented in Chapter 2.

Chapter 3 is focused on the load picked-up during black-start. The different load models are presented. As no measurements of a real black start are available, a detailed load model is built. The results of the black start studies using this detailed load model will be used as a reference. Then the basic load model currently used in black-start studies is presented. Finally, mixed level complexity load models, called simplified load models, are built. These simplified models are derived from the detailed model through successive simplification steps.

Chapter 4 is focused on a grid including the load picked-up during black-start. Frequency and time-domain analysis are carried-out on this grid using the different load models. The results of the analysis of the grid using the basic and simplified load models are compared with the reference.

In Chapter 5, a new load model is proposed, which does not stem from the detailed load model. This model is compared to the reference.

Appendices I to IV give technical details on the detailed load model. Appendix V gives more information on the parameters of the simulations. Appendix VI gives more information about the harmonic analysis performed in Chapter 4. Appendix VII gives technical details on the line models used in Chapter 3 and 4. Appendix VIII presents the frequency dependent network equivalent. Appendix IX gives additional simulations results for Chapter 5.

Chapter 2. Electromagnetic transients during network restoration

2.1 Network restoration

The procedure to restore the electric grid to its state of normal operation is built to ensure the security of people and avoid any further collapse of the network which is not as robust as usual [1]. Before the restoration phase, the grid is prepared by splitting it into load pockets. A load pocket must be small enough to be restored by a single generation unit but large enough to damp the resonance and avoid transient harmonic overvoltages. In case of voltage collapse, the grid is automatically split into load pockets by specific programmable logic controllers, called "zero-voltage automatic devices », according to the « zero-voltage plan ». Zero-voltage devices automatically open the breaker they command when they detect a loss of voltage. A diagnosis of the situation is performed to determine the most fitted strategy for network restoration. If a strong network is available, restoration is performed starting from this strong network. The strategy is called “top-down”.

Otherwise, networks are restored using the main regional structure, a “bottom-up” strategy. A main regional structure is a predetermined 400 kV backbone that links the nuclear and hydro power plants of the region to the main consumption areas of the region. A map depicting the seven main regional structures is shown on Figure 1. The restoration is based on generation units with black start capability (dedicated black start units and in house load operation units). The 400 kV backbone is energized, load pockets are energized and the load is restored, starting with priority customers and extending to all customers. The network restoration plan is the guideline used by the dispatcher to restore the network in the aftermath of a widespread outage in the grid.

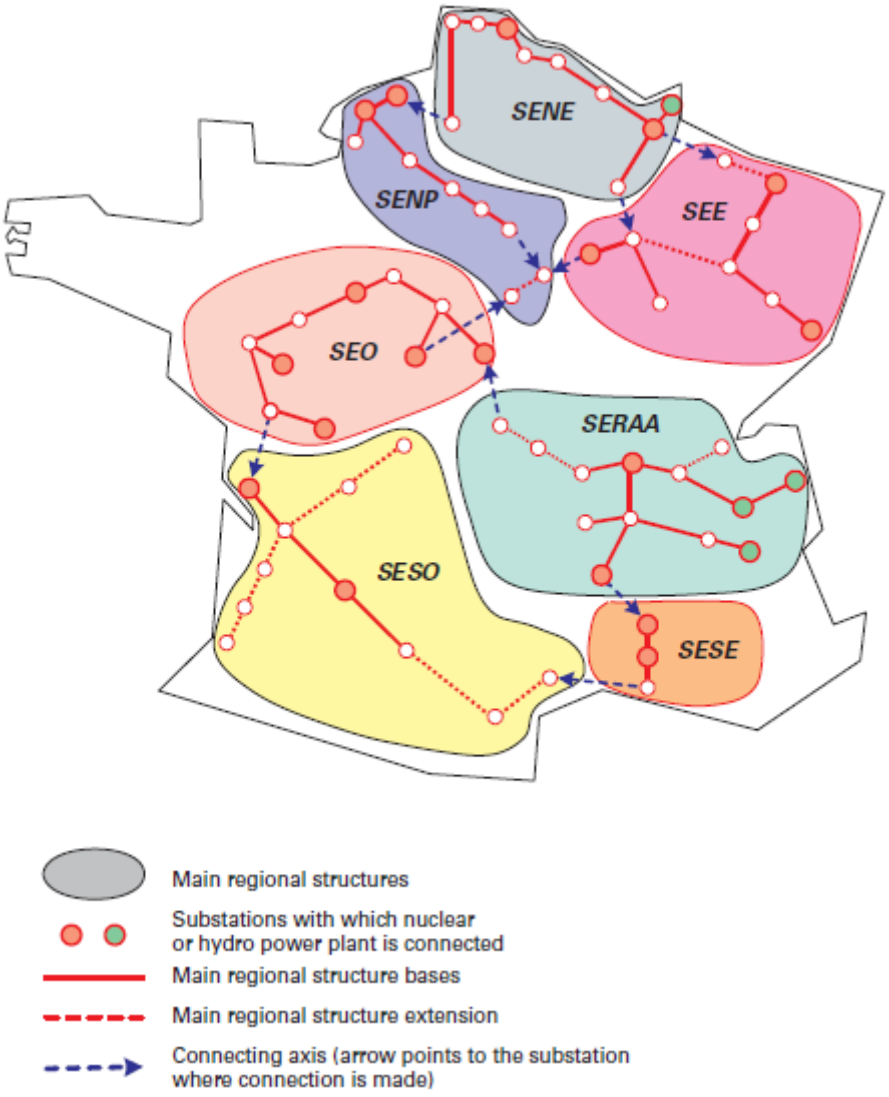

Figure 1 Map of main regional structures

The network restoration aims at restoring the main regional structure, energizing using local power plants and picking up the load for priority customers. Load pick-up for non-priority customers is carried out in a later stage. The load of different customers is divided into 5 categories, depending on their priority levels. Hospitals and critical industries (SEVESO) are considered as priority level 5, the highest priority level. They have backup power sources such as standby generators, which will automatically start up when electrical power is lost. Load pick-up aims at connecting priority clients back to the grid. The load shedding plan is revised once a year in winter. It surveys the active power at each priority level on that day.

2.2 Transient harmonic overvoltage

Generation units are on the 400 kV grid and the load is spread on lower voltage grids of 225 kV, 90 or 63 kV. Thus, several step-down transformers have to be energized to restore the load. However, when energizing a transformer, transient harmonic overvoltages may occur. A simplified way of modeling a transformer is a non-linear inductance. Energizing a non-linear inductance, such as

depicted on Figure 2, produces a current containing harmonics. According to Faraday's law, $e = \frac{d\varphi}{dt}$, the flux is deduced by integrating the voltage. At $t = 10\,ms$, the switch is closed. At that time, voltage is minimum and it is assumed that there is no remanent flux, so the flux is zero. The corresponding point on the saturation curve is (0,0). The saturation curve of the non-linear inductance is displayed on Figure 3 and the evolution of voltage, flux and current with time after the switch's closure on Figure 2. 4 phases are delimited for a better understanding of the generation of harmonic current. These phases are indicated by numbered arrows on Figure 3 and Figure 4.

- Phase 1 : Voltage is negative so flux decreases and current moves along the first segment of the saturation curve.
- Phase 2 : When flux reaches $-12.5\,Wb$, current moves along the second segment of the saturation curve. The slope is smaller so the current increases sharply in absolute value.
- Phase 3 : Voltage gets positive, so flux increases and current moves backward on the second segment of the saturation curve.
- Phase 4 : When flux reaches again $-12.5\,Wb$, current moves backward on the first segment of the saturation curve.

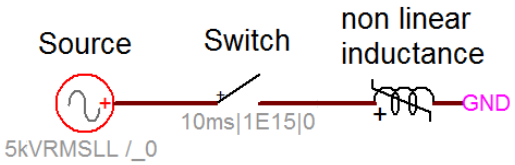

Figure 2 Switching of a non-linear inductance

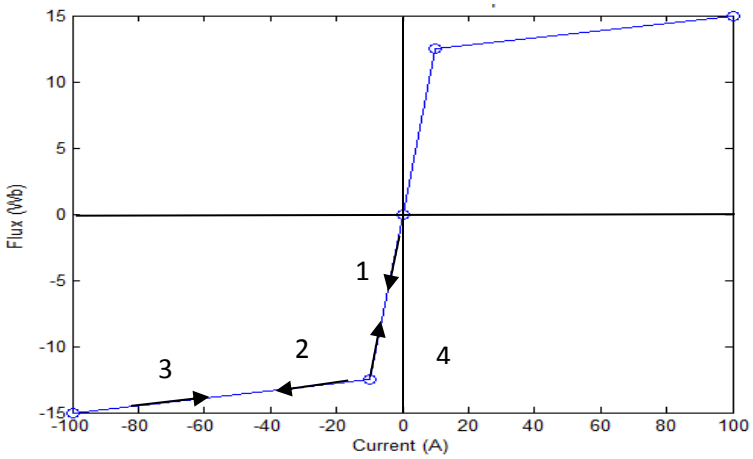

Figure 3 Saturation curve of a non-linear inductance

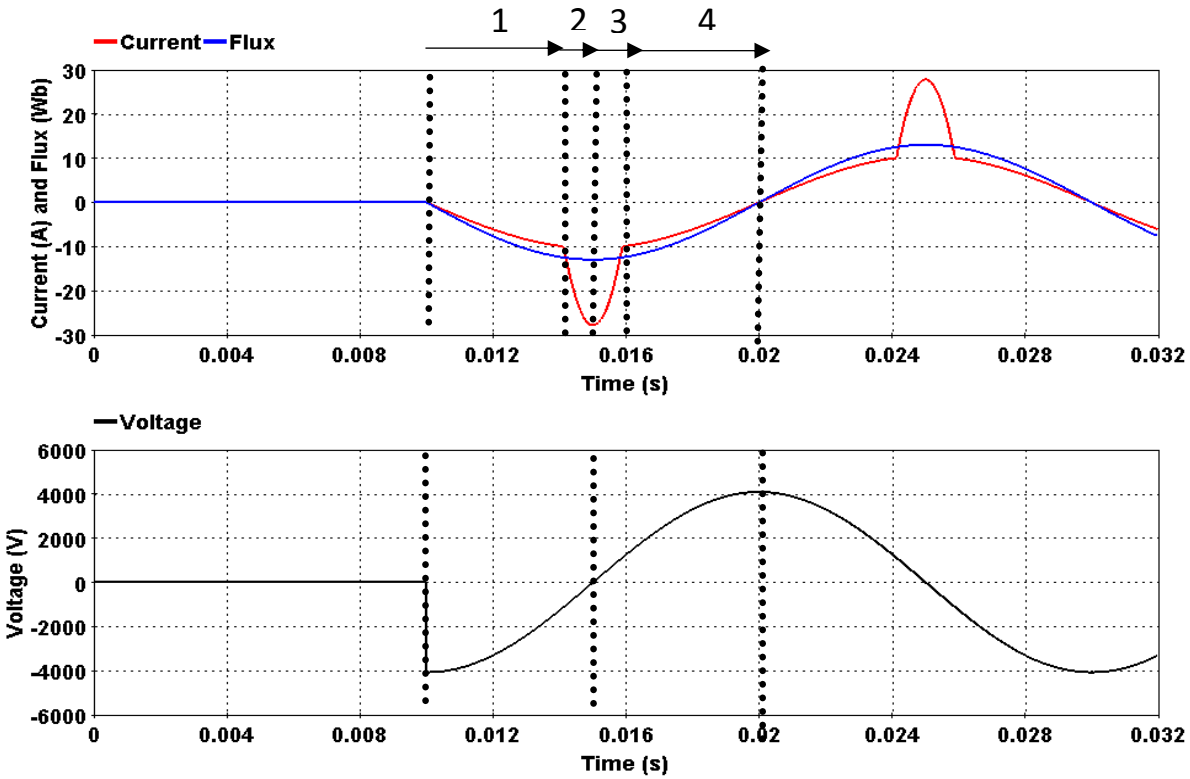

Figure 4 Current, flux and voltage when switching a non-linear inductance

A current containing harmonics is not a pure sinusoid. In addition to the fundamental, it also contains harmonics of higher ranks. When energizing a transformer, the amplitude of the harmonic current is proportional to the inverse of the harmonic's rank. Thus, the high transient harmonic overvoltages occur at low frequencies. The transformer, modeled by a non-linear inductance (Figure 5), is switched from a network equivalent and produces harmonic current (Figure 6).

The network is composed of a sinusoidal power source, cables which are capacitive components and transformers, lines which are inductive components. Ferroresonance can occur in such a configuration, depending on the initial conditions of the system. Ferroresonance is a non-linear phenomenon which should not be confused with linear resonance. The network which is composed of capacitances and inductances can have several linear resonant frequencies. In some circuits, the linear resonant frequency occurs when the impedance of the network is at a maximum, in others at zero. If the network impedance's resonance (Figure 7) occurs for a harmonic contained in the harmonic current (Figure 6), then the current harmonic is amplified. At that frequency, network impedance has a resonance and current is amplified so, according to Ohm's law, the voltage is amplified. This phenomenon of amplification is the ferroresonance. The resulting three phase voltages are called transient harmonic overvoltages and the typical allure of the overvoltages is displayed on Figure 8.

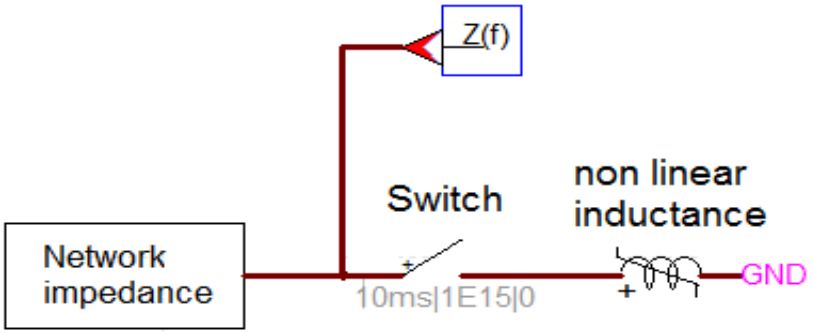

Figure 5 Switching of non-linear inductance with network resonance at 150 Hz

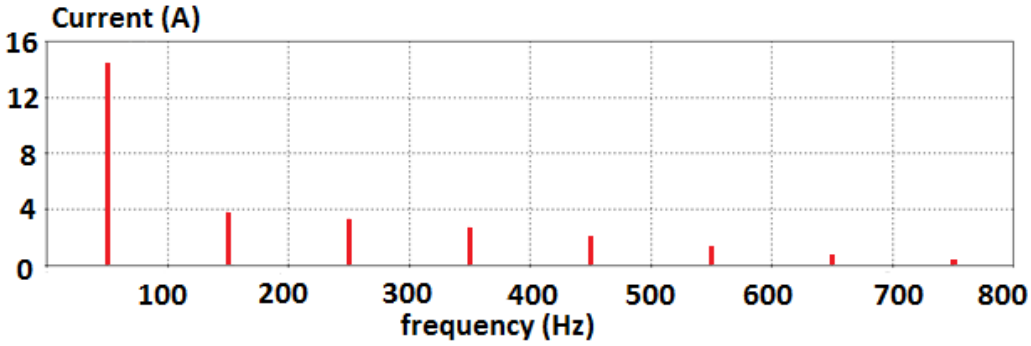

Figure 6 Harmonic analysis of current over one period

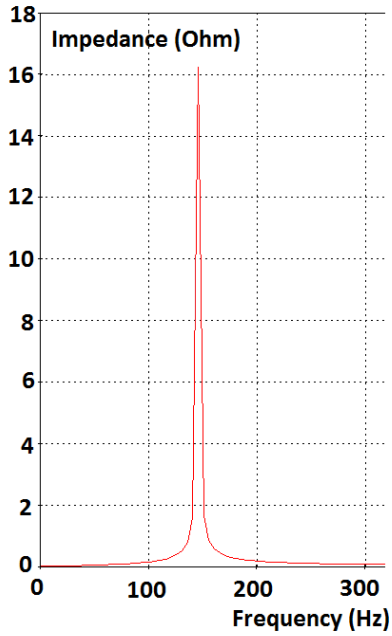

Figure 7 Network Impedance

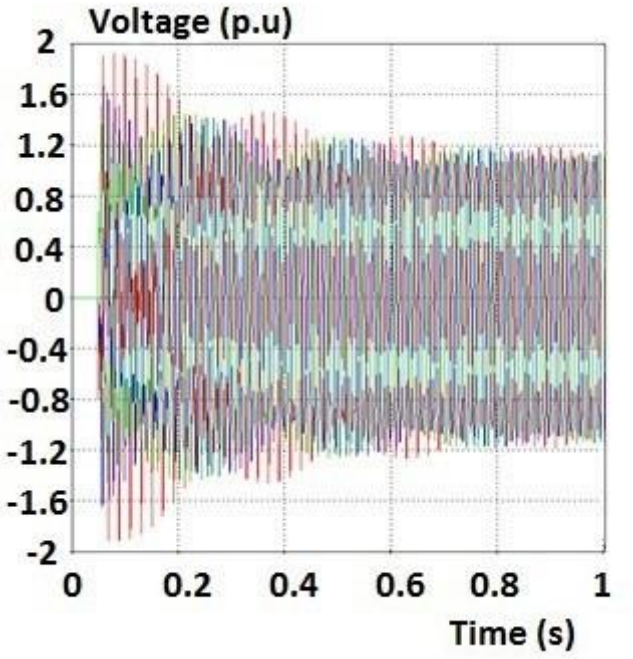

Figure 8 Phase-to-earth overvoltages for the three phases when switching a non-linear inductance

The distance between the transformer to be energized and the unit in black-start or the last energized transformer is compared to a critical distance [2]. With distances higher than the critical distance, transient harmonic overvoltages are likely to happen. The critical distances were determined by internal studies. The critical distance is 45 km for energizing of a transformer and 90km for energizing of an autotransformer. If the distance is higher than the critical distance, picking up more load is an efficient way of damping the resonance and reducing transient harmonic overvoltages.

2.3 Frequency and time windows in frequency and time analysis

In the scope of this Thesis, high frequencies are not a matter of interest. The amplification of a harmonic is inversely proportional to the rank so low order harmonics are more amplified. Therefore, grid's resonance at high frequencies do not lead to overvoltages. Moreover, at high frequencies, the models used for cables, lines and transformers are not valid anymore since they do not take into account high frequency phenomena such as the skin effect. For these two reasons, the frequency window is limited to 1000 Hz in high frequencies. In low frequencies, the window is limited to 50Hz, the fundamental frequency for signals in France. Sometimes the window is reduced in high frequency and takes into account only the first resonance(s).

Transient overvoltages are likely to appear within the first seconds after energizing the transformer. Considering the networks used in this Thesis, the simulation time is chosen to be 1 second.

2.4 Network restoration using Normandy's regional structure

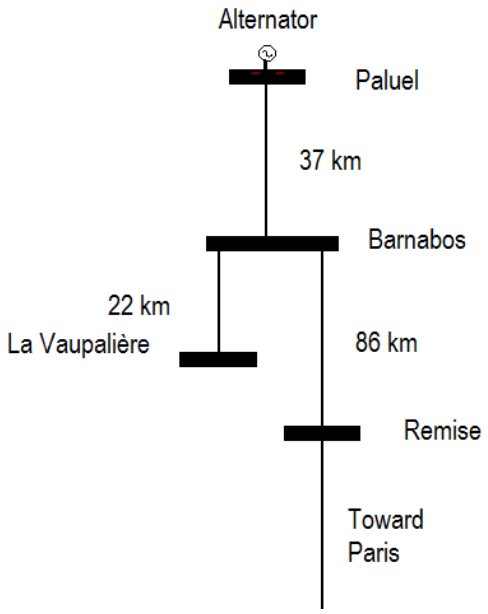

Figure 9 Normandy 400 kV backbone

The Normandy's 400 kV backbone is displayed on Figure 9. This regional structure is built starting from the nuclear power plant at Paluel and progressively energizing 400 kV lines toward Paris. The path is chosen by minimizing the distance between the no-load transformers energized in order to to limit the risk of overvoltages. When the distance between the no-load transformer energized is too long, load is picked-up.

Before starting restoration phase, the network has been split into load pockets according to the zero-voltage plan. At La Vaupalière, zero-voltage devices created two load pockets, a 225 kV load pocket, highlighted in grey on Figure 10 and a 90 kV load pocket highlighted in purple on Figure 11 (for confidentiality reasons, some information were hidden on these figures). Figure 10 shows that as soon as the 90 kV load pocket is energized, some priority customers are automatically supplied again at Dieppedalle, Harcanville and Grand Quevilly (circled in red on Figure 11). Once the 225 kV load pocket has been energized and later once the 90 kV load pocket has been energized, load pick-up is performed by closing the appropriate switches.

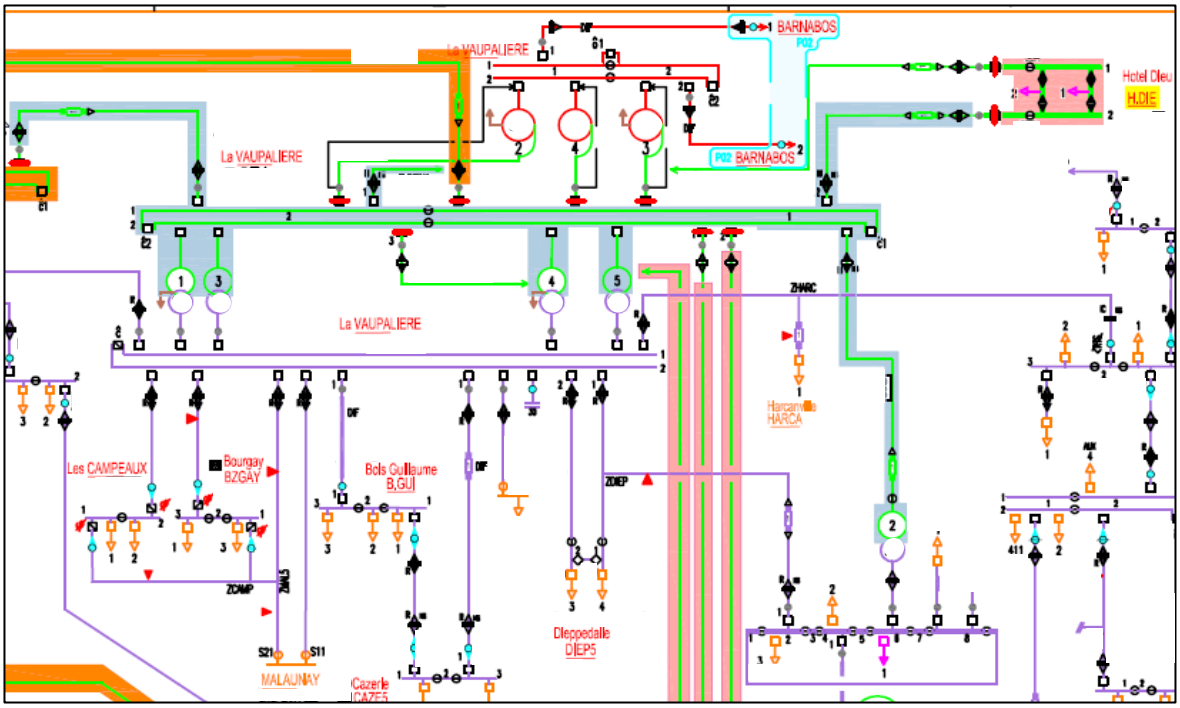

Figure 10 225 kV Load pocket highlighed in grey

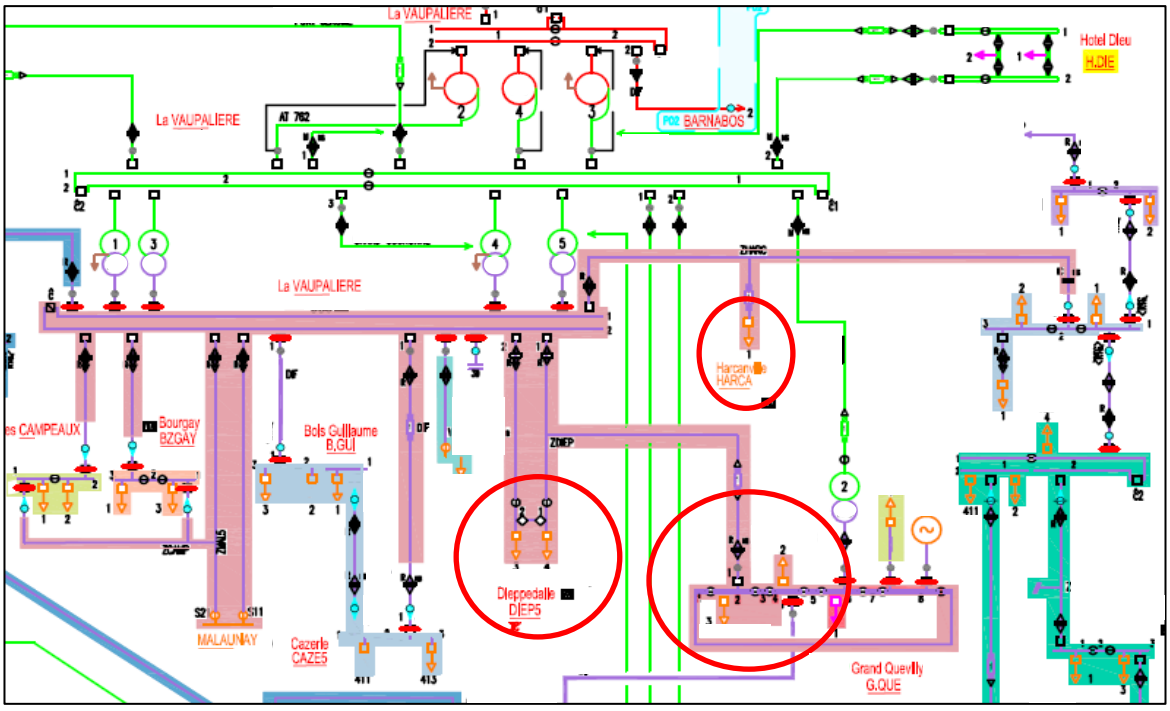

Figure 11 90 kV load pocket highligthed in purple

In the event of power loss on the grid, there are several ways to restore the regional structure, depending on the availability of the nuclear power plants. In the scope of this Thesis, we considered the case where the nuclear power plant at Paluel is used in black-start.
To minimize transient harmonic overvoltages, energizing is always performed at 90% of nominal voltage. Transient harmonic overvoltages are likely to occur if the distance between the transformer to be energized and the unit in black-start or the last energized transformer is big. In that case, picking up some load is an efficient way of damping the resonance and reducing the overvoltages.

The restoration process is illustrated on Figure 12 and the different steps of the network restoration plan are explained below.

1- Barnabos 400 kV is energized. The distance between Paluel and Remise, 123 km, is higher than the critical distance (45 km), so energizing a transformer at Remise can lead to transient harmonic overvoltages. To minimize the risk of harmonic overvoltages and damp the resonance, it is decided to pick-up load at La Vaupalière before energizing the transformer at Remise.
2- La Vaupalière 400 kV is energized.
3- An autransformer 400/225 kV is energized. After energizing the autotransformer at La Vaupalière, the 225 kV load pocket is automatically energized.
4- Priority load is picked-up at Hotel-Dieu.
5- One transformer 225/90 kV is energized, preferably the transformer with the smallest nominal power so as to minimize the risk of overvoltages. La Vaupalière 90 kV load pocket is automatically energized.
6- Load is picked-up at Bourgay, Campeaux, Bois-Guillaume and Grand Quevilly.
7- The transformer 400/63 kV at Remise is energized.

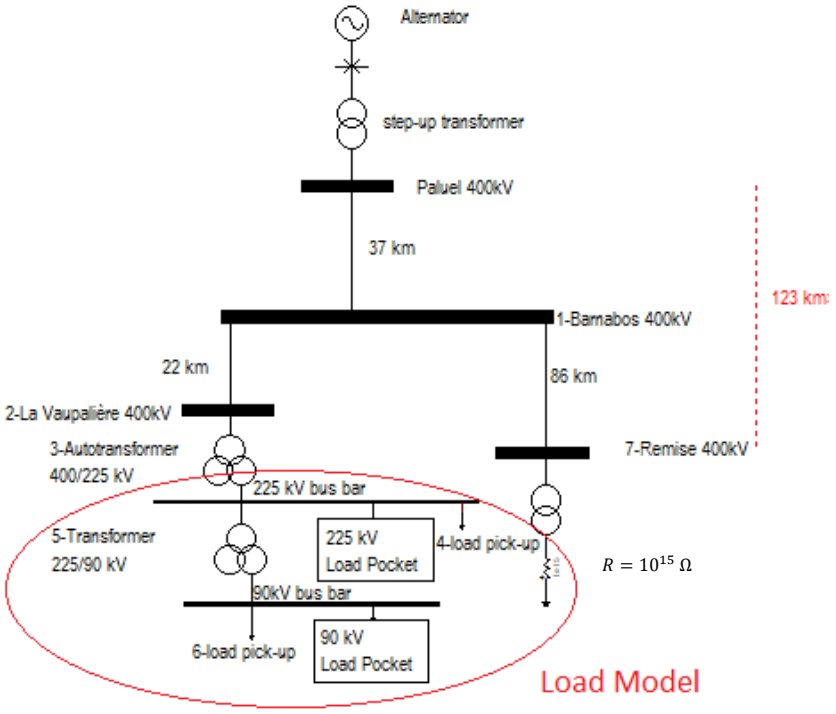

Figure 12 Network restoration plan for Normandy's Backbone

2.5 Load

The Normandy backbone was chosen as the case study in this work because there is a known risk of transient harmonic overvoltage when energizing the transformer at Remise (step 7 of the restoration plan). Since the case study presents a located risk of overvoltages, the focus of the analysis can be on a specific bus bar of the backbone. Specifically, the study will be on the influence of the load model at this bus bar. The load is circled in red in Figure 12. Currently, this load is represented by a very basic model, a simple inductance in parallel with a resistance, depicted on Figure 13.

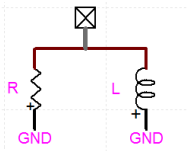

Figure 13 Basic load model

The goal is to determine whether a more precise load model would improve the results of the black-start studies. We build a detailed load model and use it as a reference for comparisons. Three load models are built (presented in Chapter 3), derived from the detailed load model through successive simplification steps.

2.6 Conclusion of chapter 2

After a black-out, the voltage is restored on the grid through a procedure, called network restoration. This procedure involves the energizing of a no-load transformer, which may cause transient harmonic overvoltages. It is necessary to study this phenomenon as overvoltages may damage the equipment and lead to the failure of the network restoration. That is why black-start studies are performed. The load in black-start studies has always been represented using a very basic load model. Would a more precise load model change the results of the black-start studies? And if so, what new load model should be used in black-start studies? The method used is based on comparisons: a detailed load model and simplified load models are built. Then, the results of the black-start studies using the different load models, basic and simplified, are compared with the results of the black start studies using the detailed load model.

Chapter 3. Load models

3.1 Detailed load model

3.1.1 Presentation

A detailed model of the load at La Vaupalière is built. It is used as a reference for comparisons with other load models throughout the Thesis. This load model is not used in black start studies for two reasons: it is too long to create and given the level of detail, the simulation time of the backbone using the detailed load model is very long.

The detailed model represents the load seen at La Vaupalière from the 225 kV bus bar. It is composed of the 225 kV load pocket, the 90 kV load pocket and the priority load picked-up at La Vaupalière 225 kV and 90 kV, as depicted on Figure 12. For the priority load pick-up, it is assumed the values of active power given in the load shedding plan. The load shedding plan is revised once a year by the distribution system operator (DSO). Therefore, the detailed load model is built using the load data from this particular day.

Convergence[1] was used to check the validity of the detailed model. Load flow results of the detailed EMTP[2] load model were compared with Convergence's situation on the same day.

The detailed EMTP load model was built in 3 steps. First, the 225 kV load pocket was created, then the 90 kV load pocket was created, finally, the load pick-up was added. To compare load flow results with Convergence after step 1, the 225 kV load pocket was created on Convergence, starting from the situation of the day of the load shedding plan and changing the state of the appropriate switches. The same procedure was used to check load flow results after step 2. It is uninteresting to check load flow results with Convergence after step 3. Indeed, the load shedding plan gives the active power of the load behind the 90 kV/20 kV transformer whereas Convergence uses data for load taking into account the 90/20 kV transformer.

The boundaries of the load model are determined with the help of the load pockets plans and the network restoration plan. The result is the schematic version of the detailed model presented on Figure 14. With Convergence, it is possible to get a more precise idea of the structure of each substation.

[1] Convergence is a software developed by RTE, which performs load flow calculations, based on the Newton-Raphson algorithm. A situation with data for a particular day and time of the year can be loaded in Convergence, displaying the active and reactive power consumptions at each substation and the state of each switch in the network. Both can be charged in the program's interface, but the actions remain purely fictive.

[2] EMTP is a software developed by RTE to study electromagnetic transients in the time scale from microseconds to seconds. The simulation is based on numerical methods. The models used for the devices are described by algebraic, differential and partial differential equations.

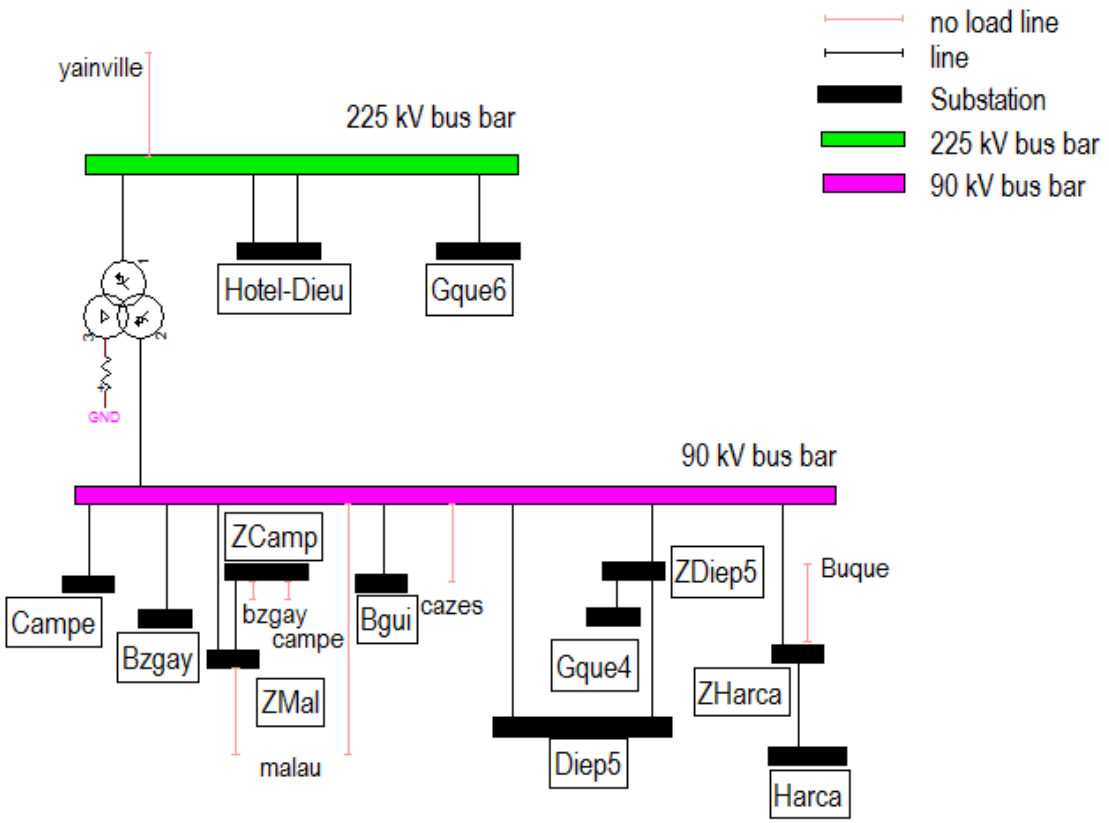

Figure 14 Schematic detailed load model

3.1.2 Assumptions

The load model is a representation of the real load seen from the 225 kV bus bar. The representation is not exact for two reasons: it is unnecessary to reach a very accurate representation and the information available is limited. Low voltage level grids have less influence on the load as they are far away from the point of connection of the load, the 225 kV bus bar. The detailed load model includes the load picked-up which is located behind the 90/20 kV transformers. As a consequence, the detailed representation of the load includes the 20 kV voltage level grid but leaves aside lower voltage level grids.

The TSO owns the transmission system, from the 400 kV grid down to the 63 kV grid. The transformers with a secondary winding on the 20 kV voltage level are part of the distribution system and owned by the DSO. The TSO does not have access to this data. Therefore, assumptions have to be made regarding the representation of the 90/20 kV transformers and the 20 kV voltage level grid. These assumptions are described in appendix II.

Among the data needed to build the detailed load model, there is the active and reactive power picked-up at the different substations. Table 1 shows the active power on Convergence and on the load shedding plan.

Table 1 Convergence and load shedding plan active power

Substation	Convergence P (MW)	Convergence Q (MVar)	Convergence Power factor	Load shedding plan all priority levels (MW)	Difference Load shedding plan/Convergence ΔP (MW)
Hotel-Dieu	85,04	8,67	0,9948	90.6	5.56
Bzgay	29,50	2,82	0,9955	32.8	3.30
Campe	40,12	2,68	0,9978	39.5	-0.62
Bgui	34,94	6,23	0,9845	41.7	6.76
Gque4	55,69	6,98	0,9922	30.6	-25.09
Diep5	23,84	3,16	0,9913	35.5	11.66

Contrary to Convergence, the load shedding plan's values for active power are corrected to take into account aleas such as work on the grid. This leads to differences in the active power given by Convergence and the load shedding plan.

According to the restoration plan, the load pick-up is about $50\ MW$ for one load pocket so $100\ MW$ in total. Load pick-up starts with priority levels 5 and 4. If the $100\ MW$ are not reached, other priority levels are added in decreasing order. Load pick-up for priority levels 4 and 5 at La Vaupalière is summarized in Table 2. The total load pick-up, $103\ MW$, is above the $100\ MW$ minimum, so there is no need to pick up priority level 3.

There is no mention of the reactive power for load pick-up on the load shedding plan. That is why an estimation of the power factor has to be made. Convergence's power factor is computed at each substation and displayed on Table 1. The power factor found rounded at two decimal is $0{,}99$. This power factor is unusually high. According to RTE's operation teams, in general in the grid the usual power factor is 0.97 in winter. The latter power factor is used as it is more representative of a usual winter day situation. According to Convergence, the load pick-up is always inductive in this area. Thus, it is assumed that $Q > 0$ when computing the reactive power.

Table 2 Load pick-up for priority levels 4 and 5

substations	P (MW) Load shedding plan Priority level 4 and 5	Q ($MVar$) Load factor 0.97
Hotel-Dieu	39,90	10,00
Bzgay	9,20	2,31
Campe	11,80	2,96
Bgui	19,50	4,89
Gque4	16,59	4,16
Diep5	4,7	1,18
Harca	1,70	0,43
Addition	6,40	
Total	**103,39**	

3.1.3 Load flow and frequency analysis

The load flow is performed at 50 Hz on the detailed load model seen from the 225 kV bus bar and the result is displayed in Table 3. Though only inductive load has been picked-up ($Q > 0$), the total reactive power seen from the 225 kV bus bar is capacitive ($Q < 0$). It means that the reactive power produced by the underground cables and no load lines is prevailing at 50 Hz. In other words, the load has a capacitive behavior at 50 Hz.

Table 3 Load flow at 50Hz for detailed load model

	Active power P (MW)	Reactive power Q (MVar)
detailed model	104.58	-6.94

The frequency analysis (impedance as function of the frequency) is performed seen from the 225 kV bus bar and the result is shown on Figure 15. It is pointed out that the frequency analysis is performed on the load alone at La Vaupalière without the network. The presence of inductive elements such as transformers and overhead lines together with capacitive elements such as underground cables explains the resonance. This resonance occurs at 323 Hz with an amplitude of $716\ \Omega$.

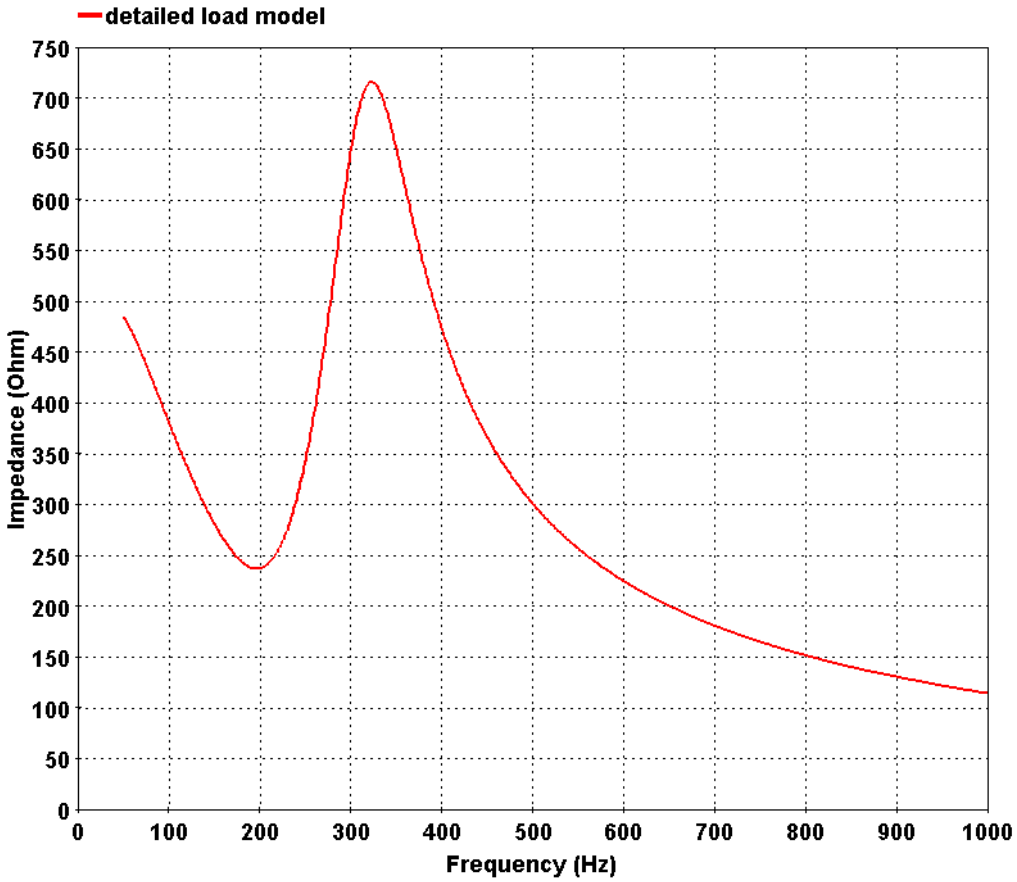

Figure 15 Frequency analysis for the detailed load model

3.1.4 Modeling the detailed load on EMTP

Transformers:
One has to keep in mind that during restoration of the main regional structure, voltages should be kept low, so as to avoid overvoltages. However, the voltages should not be too low, because the load will increase at later stages of the restoration, as non-priority clients are connected back to the grid, leading to a voltage drop. Besides, the dispatcher is used to operating the grid with a voltage slightly higher than the nominal voltage rather than slightly lower, while remaining in the allowed range of voltage variation. Indeed, the higher the voltage is and the lower the losses are.

Below are displayed the allowed ranges of variation for the voltage:
- $[220; 245]$
- $90\ \text{kV} \pm 8\%$ so $[82.8; 97.2]$
- $20\ \text{kV} \pm 5\%$ so $[19; 21]$
- $15\ \text{kV} \pm 5\%$ so$[14.25; 15.75]$

There are several transformers between la Vaupalière 225 kV and la Vaupalière 90 kV. During restoration phase, only one transformer is energized to speed-up the restoration. Besides, whenever possible, it is chosen to energize the transformer with the smallest nominal power, as it is less likely to cause overvoltages. At La Vaupalière, the transformer with the smallest nominal power, 70 MVA, is thus energized.

The tap position of a transformer controls the transformer's ratio. A tap position matches a set of parameters (see appendix I to IV for details about the computation of transformer's parameters). The transformer's tap position is chosen so as to best fit in the allowed range of voltage variation and be as close as possible to the target nominal voltage. Short-circuit tests results used for computation of transformer's parameters are only available for 3 tap positions. Thus, for computation of parameters' value, the closest short-circuit test results available are used. The results are displayed in Table 4 for all transformers in the detailed load model.

Table 4 Tap position of other transformers

Transformer	Tap position	Tap position for computation of parameters
La Vaupalière 225/90 kV	7	1
Grand Quevilly	8	14
Hotel Dieu	13	13
90/20 kV	9	9

Lines :
The constant parameter model is used for the lines of the load. It neglects the frequency dependence of the resistance, inductance and capacitance. Phenomena such as skin effect or ground resistivity are not taken into account. The model assumes a continuously transposed, distributed LC line, with the total resistance lumped in three (R/2 in the middle of the line and R/4 at each end) and no shunt conductance G. More information on the Constant parameter model can be found in appendix VII.

The load, used in black start studies, is far from the transformer energized on the 400 kV grid. Therefore, it is not relevant to use a more precise model, such as the wide band model, which takes into account the frequency dependence of the resistance and inductance.

3.1.5 The detailed load model on EMTP

The detailed load model built on EMTP is shown on Figure 16.

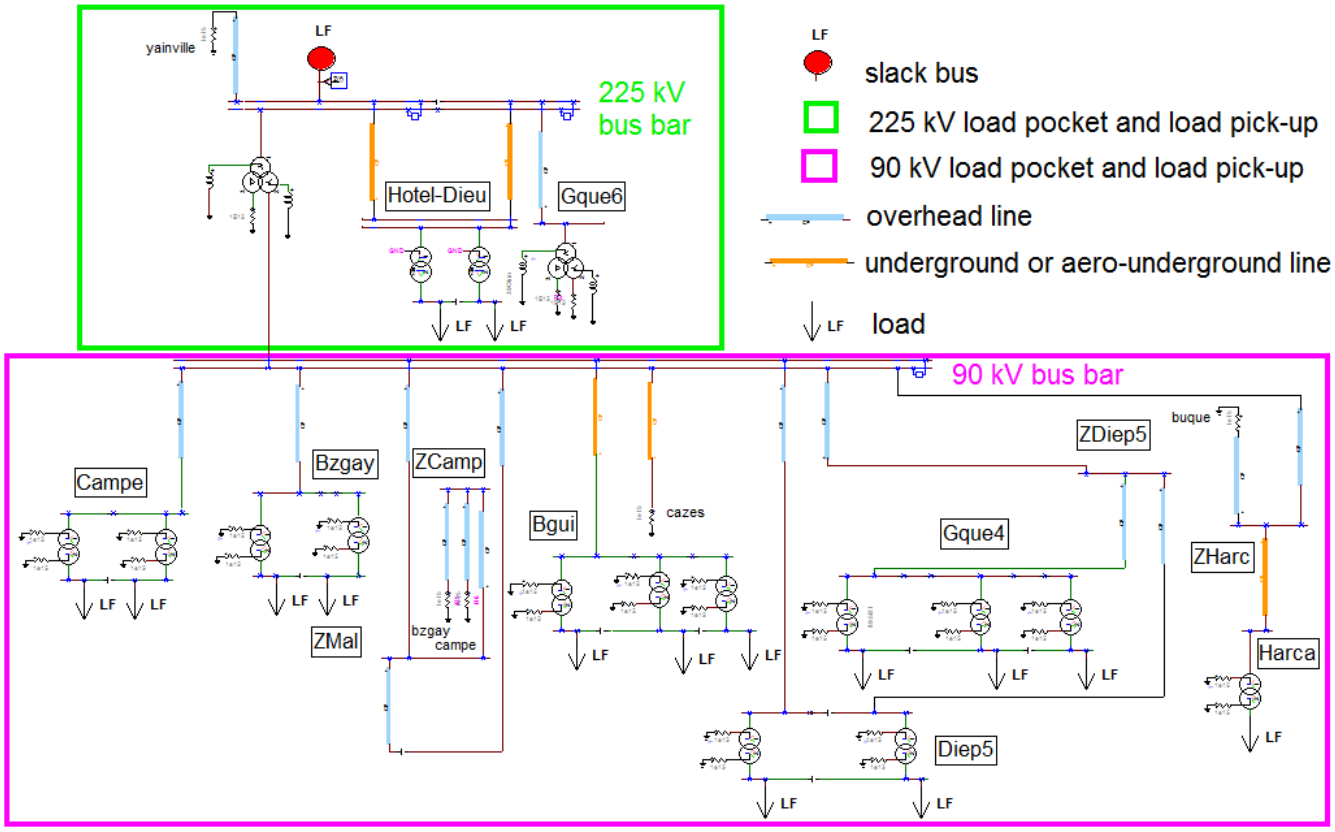

Figure 16 Detailed load model

3.2 Basic load model

3.2.1 Presentation

The basic model is the load model currently used in black start studies. The only information needed to build this model are in the load shedding plan.
The following assumptions are made:

- The active power represents the load pick up with priority levels 4 and 5. It adds up to $103.39\ MW$ in the case of the Normandy backbone.
- The load has an inductive behavior at $50\ Hz$ ($Q > 0$). In the case of the Normandy's backbone, this assumption is wrong! According to the detailed model, the load has rather a capacitive behavior at $50\ Hz$.
- The reactive power is computed with the usual power factor for a winter situation, 0.97, assuming an inductive load.

In some black start studies, the information of the load shedding plan is not used. It is assumed that the active power picked up is $100\ MW$ and the reactive power is $30\ MVar$.

The basic model is an inductance in parallel with a resistance as shown in Figure 17.

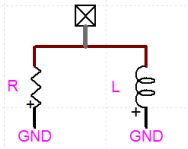

Figure 17 Basic load model

The parameters R and L are computed using (1).

$$\boldsymbol{R = \frac{U^2}{P} \; and \; L = \frac{U^2}{Q2\pi f}} \qquad \textbf{(1)}$$

3.2.2 Load flow and frequency analysis

The load flow at $50\ Hz$ is $P = 103.39\ MW$ and $Q = 26.01\ MVar$.
The frequency analysis is displayed on Figure 18. It represents the impedance of the load as function of the frequency :
$Z(f) = \frac{RjfL}{2\pi R + jfL}$.
$\lim_{f\to 0} Z(w) = \frac{jfL}{2\pi}$: the model behaves as an inductance for low frequencies
$\lim_{f\to \infty} Z(w) = R$: the model behaves as a resistance for high frequencies

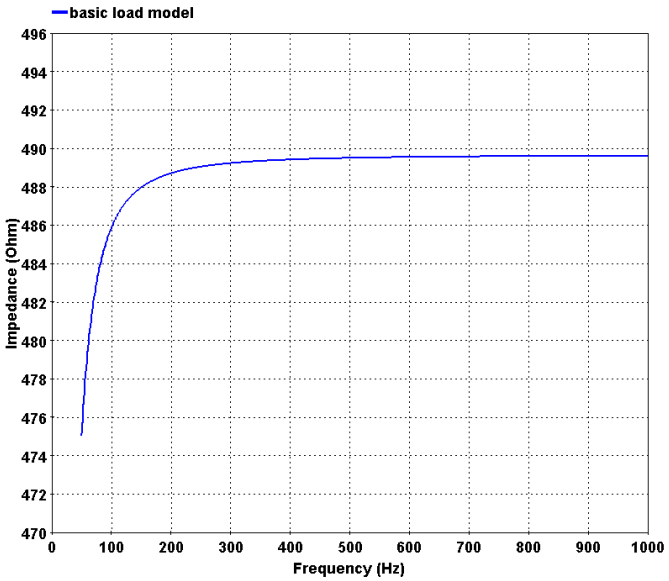

Figure 18 Frequency analysis of the basic load model

3.4 Simplified load model

3.4.1 Presentation

The aim is to find load models that are more accurate than the basic model but less complicated than the detailed model. To create these load models, the detailed model is simplified. The simplified load models are compared with the detailed load model. The load flow and frequency analysis should be as close as possible to the detailed model's. To check whether the frequency analysis of the simplified load model is close to the frequency analysis of the detailed model, an envelope is built surrounding the frequency analysis of the detailed load model.

3.4.2 Method for simplification

Presentation

Capacitive elements have a strong influence on the frequency analysis so they are carefully identified before starting the simplification of the detailed load model. The underground cables and the main areo-undergound cables, highlighted in orange in Figure 16, are displayed in Table 5. The last column indicates the percentage of the cable which is underground. The higher that percentage is and the more influence the line has on the frequency analysis. The information regarding the line to Hotel-Dieu2 is missing, but it is assumed to be about the same information as the line to Hotel-Dieu1 and result in a similar underground percentage. No load lines are shown in Table 6.

Table 5 Underground and main aero-underground cables at La Vaupalière

From	To	$\boldsymbol{R}$ (Ω)	$\boldsymbol{L}$ (Ω)	$\boldsymbol{C}$ $(\boldsymbol{nF})$	length (km)	overhead length (km)	underground length (km)	% underground
Vaupa90	BGui	0,373	1,782	3488,7	11.3	0	11.3	100
ZHarc	Harca	1,4	5,12	913	24.176	2.606	21.57	89.22
Vaupa225	HDieu1	0,54	2,122	550	6.827	2.285	4.542	66.53
Vaupa90	Cazes	2,557	7,636	3899,3	26.078	11.3	14.778	56.67

Table 6 No load lines at La Vaupalière

From	To	$\boldsymbol{R}$ (Ω)	$\boldsymbol{L}$ (Ω)	$\boldsymbol{C}$ $(\boldsymbol{nF})$
Vaupa90	ZMal	4.689	0.592	44.563
ZMal	Malau	1.952	0.435	19.099
Vaupa90	Malau	6.328	1.25	57.423
ZMal	ZCamp	1.576	0.232	12.732
ZCamp	Bzgay	2.13	0.32	19.099
ZCamp	Campe	?	0.87	50.93
Zharc	Buque	3.77	11.95	283.296
Vaupa225	Yainville	1.43	6.58	187.803

The detailed model is connected to the 225 kV bus bar. The 225 kV grid is very close to the point of connection and thus has a strong influence on the frequency analysis. The 90 kV grid is further away from the point of connection so has less influence on the frequency analysis. As a consequence, the

225 kV simplification should be finer than the 90 kV simplification to get accurate results for frequency analysis. A finer representation is obtained by using the Cigré model instead of a parallel RLC. The Cigré model is displayed on Figure 19 and further presented in the 225 kV simplification.

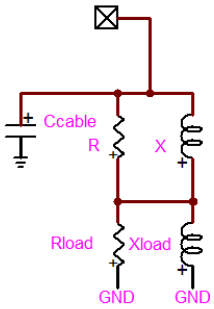

Figure 19 Cigré model

Three simplified models are built and Table 7 summarizes the differences between them.

Table 7 Differences between simplified load models 1, 2 and 3

Simplified load model	Substation Cazes	90 kV grid	Transformer 225/90	225 kV grid
1	CLC	RLC parallel and Cazes	detailed	Cigré
2	C	RLC parallel	RL serie	Cigré
3	C	RLC parallel	L serie	RLC parallel

Substation Cazes :

Simplified load model 1 represents the underground line to Cazes (represented on Figure 16) with the PI model, neglecting the serie resistance. Simplified load models 2 and 3 represent Cazes with a shunt capacitance. This capacitance is included in the capacitance of the equivalent RLC for the $90\ kV$ grid.

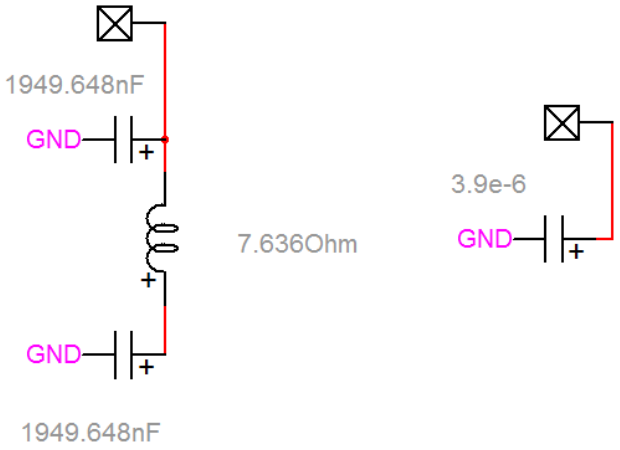

Figure 20 Underground cable to Cazes in simplified load model 1 (on the left) and 2 (on the right)

Transformer 225/90 kV

Simplified load model 1 represents the transformer as depicted in appendix I. Simplified load model 2 represents the transformer with a serie inductance X_{serie} and resistance R_{serie}. The serie inductance is the inductance between primary and secondary winding referred to the primary when primary is powered and secondary is short-circuited. It is referred to as $X_{scHV/MV}$ in appendix I. $X_{scHV/MV} =$

112.26 Ω in the case of transformer 225/90 kV. The third winding is open-circuited so there is no need to take it into account. Model 3 neglects the serie resistance. Figure 21 summarizes the simplification of the transformer 225/90 kV.

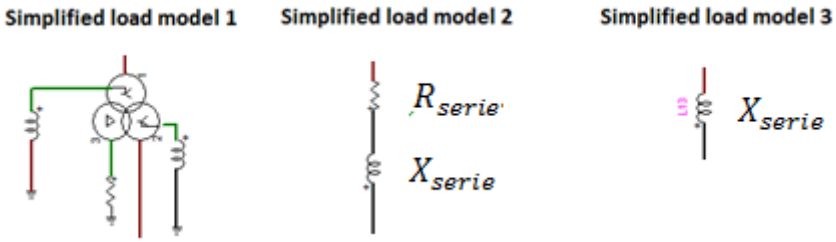

Figure 21 Simplification of the transformer 225/90 kV

Envelope

The envelope is displayed on Figure 22. It is built varying the impedance's amplitude of the detailed load model from $\pm 2.5\%$. Between 202Hz and the resonance, the impedance's slope is high so the envelope is pressed against the detailed model. That is why, from 202Hz on, the impedance's amplitude is changed with a step of 5.10^{-4} Ω up to $\pm 5\%$ until the resonance is reached. From the resonance on, the impedance's amplitude is changed with a step of 5.10^{-4} Ω back to $\pm 2.5\%$ again.

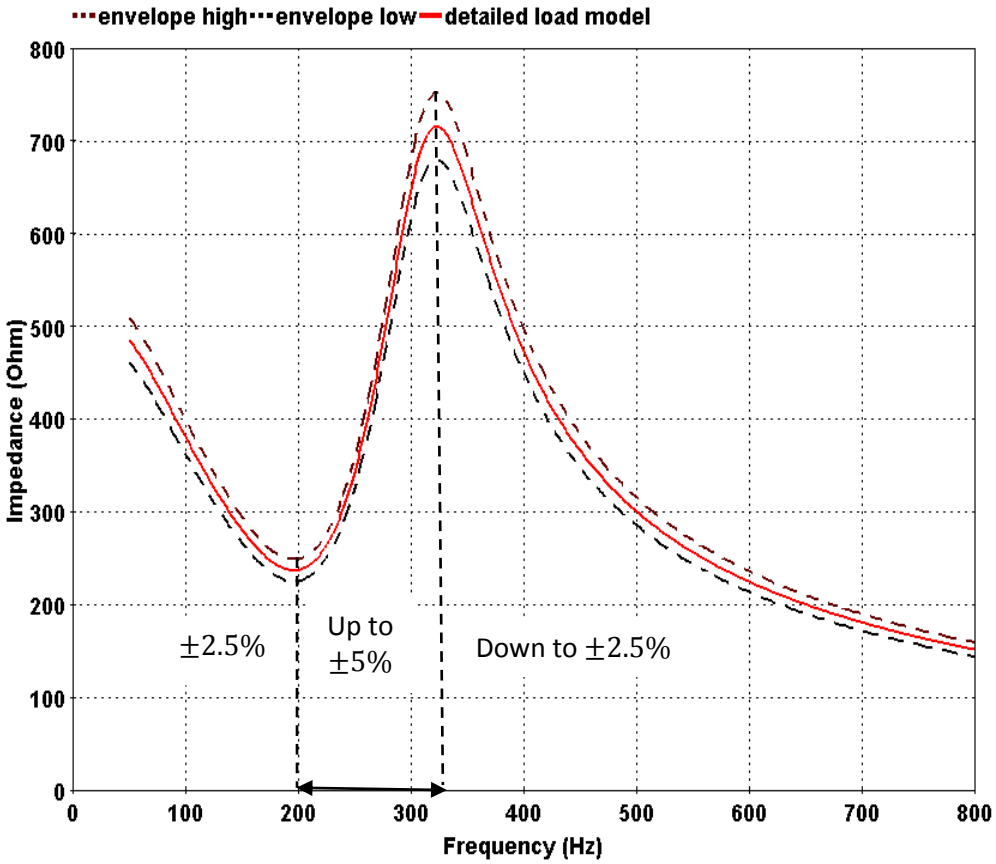

Figure 22 Envelope and frequency analysis of detailed load model

90 kV simplification

The 90 kV grid is simplified as a parallel resistance, inductance and capacitance at the 90 kV bus bar. The purely capacitive elements on the 90 kV grid are identified and taken away, as shown on Figure 23. A load flow is performed at 50 Hz and with (1) it is deduced an equivalent of the 90 kV grid

without the capacitive elements as a parallel resistance and inductance, depicted on Figure 24. The results of the computation of the resistance and inductance are displayed in Table 8. The purely capacitive elements on the 90 kV grid are modeled with a shunt capacitance.

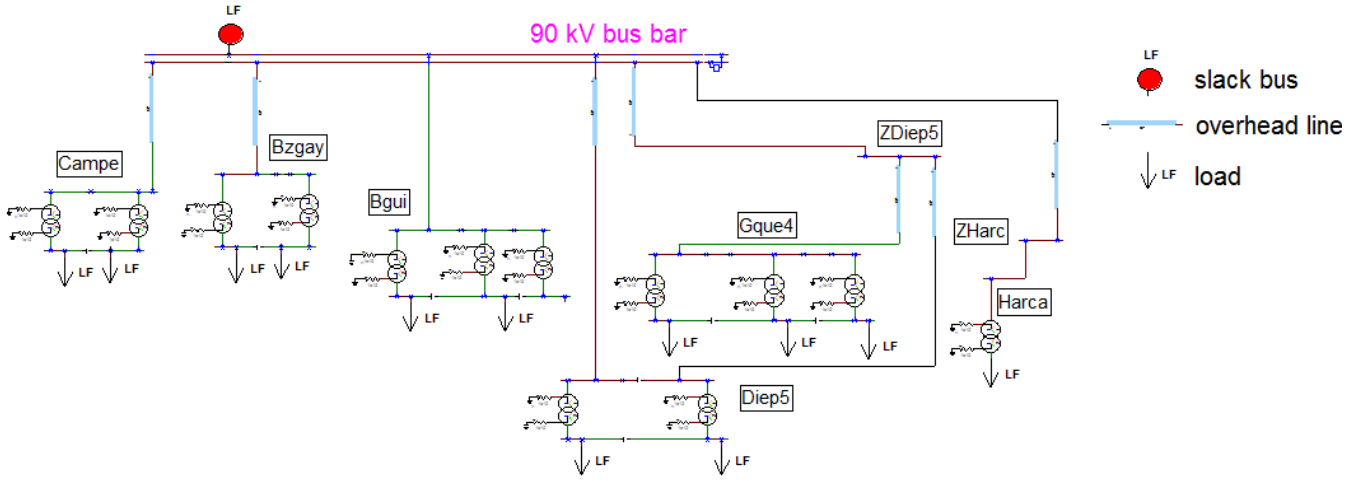

Figure 23 Detailed load model, 90 kV grid without capacitive elements

Table 8 Equivalent RL for 90 kV grid without capacitive elements

P (MW)	Q ($MVar$)	U (kV)	R (Ω)	L (H)
63.95	16.40	90.8	**128,95**	**1,60**

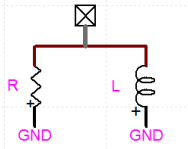

Figure 24 Parallel RL equivalent

Figure 25 explains how the simplification process is performed at Harca. Highlighted in grey are inductive elements which are simplified as described in Table 8.

1- Detailed model
2- The no load line behaves as a capacitor and is modeled with a shunt capacitor. The aero-underground line is modeled with the PI model.
3- The resistance and inductance of the PI model are negligible compared to the capacitances. The resulting capacitance is the sum of all capacitances.
4- The resulting capacitance is moved to bus bar 2. The capacitance's new position introduces inaccuracy by slightly moving the frequency analysis.

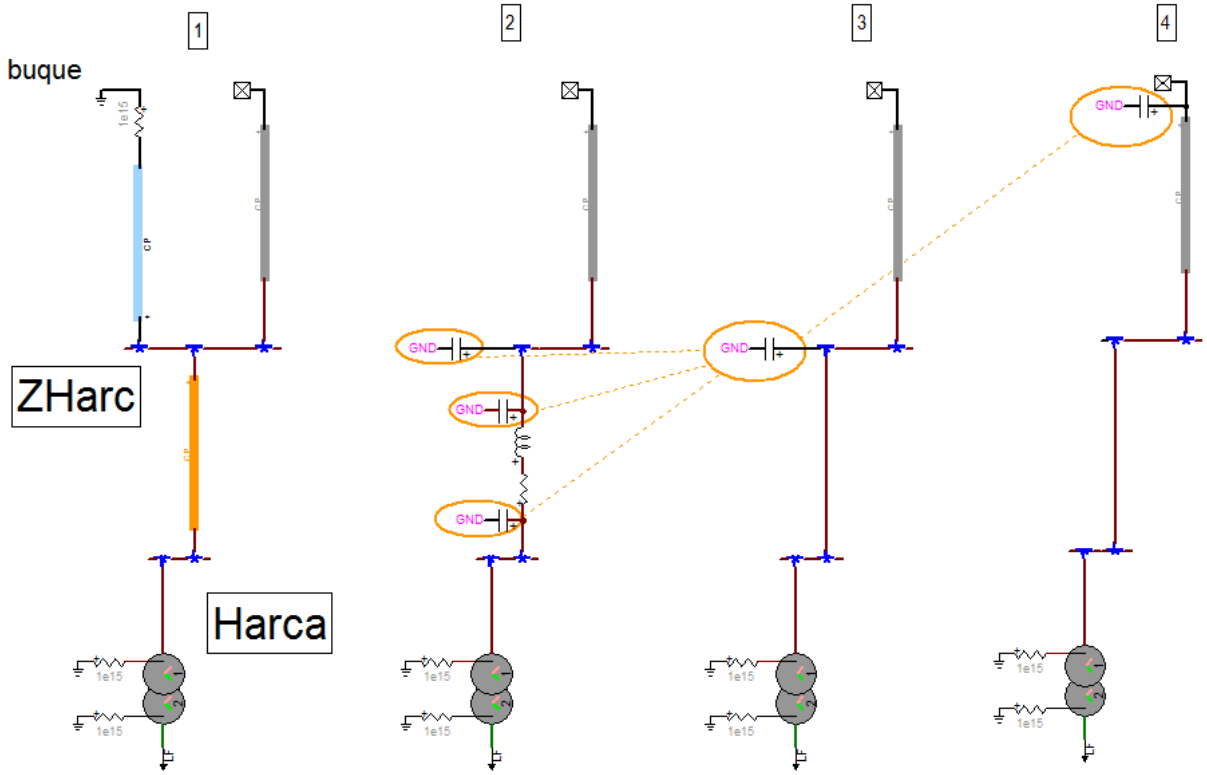

Figure 25 Simplification at Harca

A similar method is applied to simplify Malau and Bois-Guillaume.
The 90 kV capacitance is obtained by adding the capacitances, deduced from a load flow or found in RTE's database.

Table 9 Computation of Capacity for 90 kV grid from reactive power or capacitance's data

Element simplified	reactive production Q ($MVar$)	U (kV)	Capacitance C (nF)
no load line from Vaupa 90 kV to Malau	0.53	90.8	204
no load line from Vaupa 90 kV to Harca	0.85	90.8	326

Element simplified	Capacitance C (nF)
aero-underground cable from Vaupa 90 kV to Harca	914
cable from Vaupa 90 kV to B.GUI	3490

Total	Capacitance C (nF)
no load lines, aero-underground cables and cables	4930
Cazes simplified load model 1 Cazes simplified load model 2	1950 3900
with simplified load model 1 referred to 90 kV with simplified load model 2 referred to 90 kV	**6880** **8830**

In the simplified load model 2 and 3, the simplified 90 kV grid is referred to the primary of the transformer following (2).

$$R_{referred\ 225kV} = R_{referred\ 90kV}\left(\frac{U_{225}}{U_{90}}\right)^2 \qquad (2)$$

$$L_{referred\ 225kV} = L_{referred\ 90kV}\left(\frac{U_{225}}{U_{90}}\right)^2$$

$$C_{referred\ 225kV} = \frac{C_{referred\ 90kV}}{\left(\frac{U_{225}}{U_{90}}\right)^2}$$

Therefore, the final value of resistance, inductance and capacitance in simplified load model 2 and 3 are :

$R = 791\ \Omega, \quad L = 9.8\ H \quad and\ C = 1407\ nF$

225 kV simplification

The 225 kV grid is close to the 225 kV bus bar and direct simplification in a parallel RLC does not give accurate results for the frequency analysis. The capacitive elements are the aero-underground lines to Hotel-Dieu, the no load line to Yainville and the no load transformer at Grand Quevilly. The aero-underground lines at Hotel-Dieu have a strong influence on the frequency analysis. That is why a more accurate model, the Cigré model [3], is used.

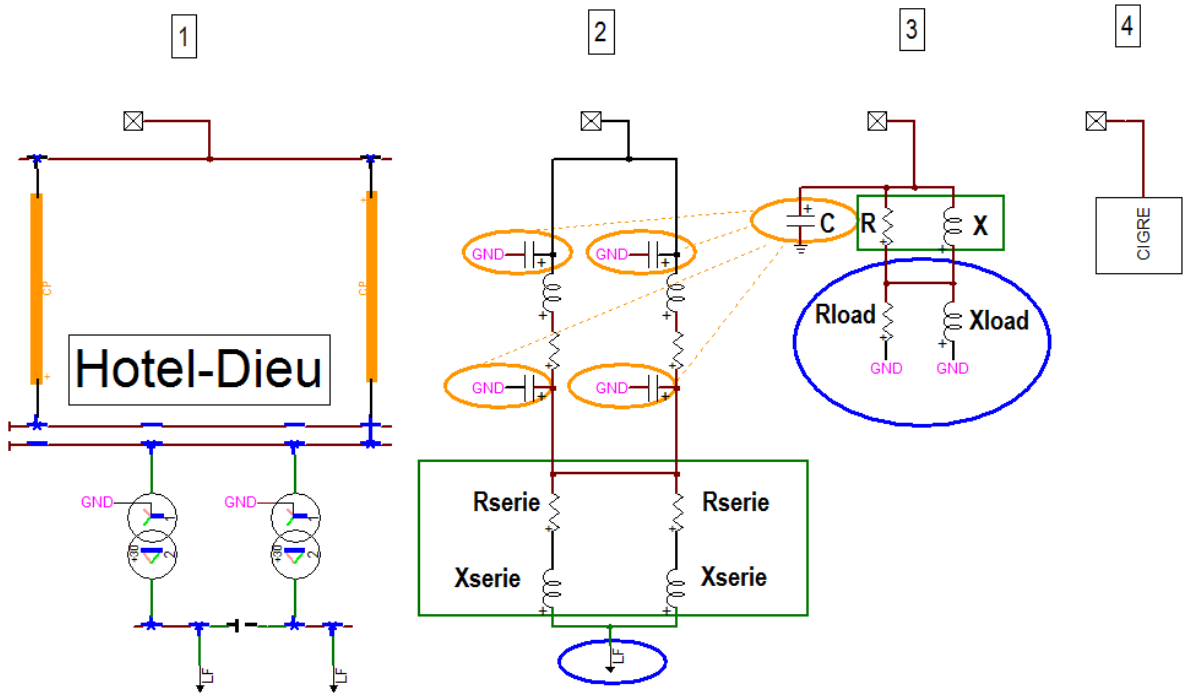

Figure 26 Cigré model applied at Hotel Dieu

Figure 26 explains how Hotel-Dieu is simplified using the Cigré model.

1- Detailed model

2- Lines are simplified with the PI model. Each transformer is modeled with the mean resistance and reactance in series referred to the primary: R_{serie} and X_{serie}. The load is referred to the primary of the transformer.

Computation of the mean series resistance and inductance :
- U_{HT} the phase to phase voltage on the primary : 227 kV
- U_{MV} the phase to phase voltage on the secondary : 15.75 kV
- R_{HT} , X_{HT} the resistance and reactance on the primary
- R_{MV} , X_{MV} the resistance and reactance on the secondary

The total resistance and reactance refered to the primary of transformer 1 are :

$$R^1_{serie} = R_{HT} + R_{MV}\frac{U_{HT}}{U_{MV}} \text{ and } X^1_{serie} = X_{HT} + X_{MV}\frac{U_{HT}}{U_{MV}}$$

The total resistance and reactance refered to the primary of transformer 2, R^2_{serie} and X^2_{serie} are computed similarly. A mean value R_{serie} and X_{serie} is then used.

3- The capacitance C_{cable} is the sum of the capacitances of the lines. The resistance and inductance of the lines are small compared to the capacitance and can be neglected. The series resistance and reactance of the transformers are changed into a parallel resistance R and reactance X. The inductive load is represented with a parallel resistance R_{load} and reactance X_{load} referred to the primary.

The equivalent parallel R and X are derived from :

$$\frac{\mathbf{2}}{\boldsymbol{R_{serie} + j\, X_{serie}}} = \frac{\mathbf{1}}{\boldsymbol{R}} + \frac{\mathbf{1}}{\boldsymbol{j\, X}} \qquad \textbf{(3)}$$

which gives

$$\boldsymbol{R} = \frac{\boldsymbol{R_{serie}}^2 + \boldsymbol{X_{serie}}^2}{\boldsymbol{2\, R_{serie}}} \qquad \boldsymbol{X} = \frac{\boldsymbol{R_{serie}}^2 + \boldsymbol{X_{serie}}^2}{\boldsymbol{2\, X}} \qquad \textbf{(4)}$$

The load referred to the primary of transformers becomes :

$$\boldsymbol{R_{load}} = \frac{\boldsymbol{U_{HT}^2}}{\boldsymbol{P}} \quad \boldsymbol{X_{load}} = \frac{\boldsymbol{U_{HT}^2}}{\boldsymbol{Q}} \qquad \textbf{(5)}$$

with P and Q the active and reactive three phase power of the load

4- The Cigré model is defined as a subcircuit.

Table 10 Values of Parameters for the Cigré model at Hotel-Dieu

$\boldsymbol{R_{serie}}(\Omega)$	$\boldsymbol{X_{serie}}(\Omega)$	**R** (Ω)	$\boldsymbol{X}$ (Ω)
9,43	130,00	**900,78**	**65,34**

$\boldsymbol{R_{line}}(\Omega)$	$\boldsymbol{X_{line}}(\Omega)$	$\boldsymbol{C}$ (nF)
0,54	2,12	550,68
0,54	2,12	502,93
		1053,61

$\boldsymbol{P_{load}}(\boldsymbol{MW})$	$\boldsymbol{Q_{load}}(\boldsymbol{MVar})$	$\boldsymbol{U}$ $(\boldsymbol{kV\ RMS\ LL})$	$\boldsymbol{R_{load}}$	$\boldsymbol{X_{load}}$
39.90	10	225.45	**1273,88**	**5082,77**

The no load line to Yainville and the aero-underground cable to Grand Quevilly are simplified with a

shunt capacitance, which is added to the capacitance of the Cigré model. The final value of the capacitance for the Cigré model at Hotel-Dieu is given in Table 11.

Table 11 Final value of the capacitance for the Cigré model at Hotel-Dieu

	C_{cable}
no load line to Yainv	1,88E-07
Aero-underground cable to GQUE6	2.23E-07
Cigré at HDIEU	1,05E-06
equivalent Cigré	**1,46E-06**

The third simplified model represents the 225 kV grid with a parallel RLC. The capacitance value is the same as Cigré's capacitance. The resistance and reactance are deduced from the active and reactive power produced by the Cigré model when removing the capacitance. The results are displayed in Table 12.

Table 12 Values of Parameters for model 3

$P\ (MW)$	$Q\ (MVar)$	$U\ (kV)$	$R\ (\Omega)$	$X\ (\Omega)$
38.67	11.74	225.45	**1313**	**4326**

3.4.3 Comparison of simplified load models with the detailed load model

The simplified load models are shown on Figure 27 from the most accurate model (simplified load model 1) to the least accurate model (simplified load model 3) and the basic load model is recalled. The inside of the CIGRE model is depicted on Figure 28.

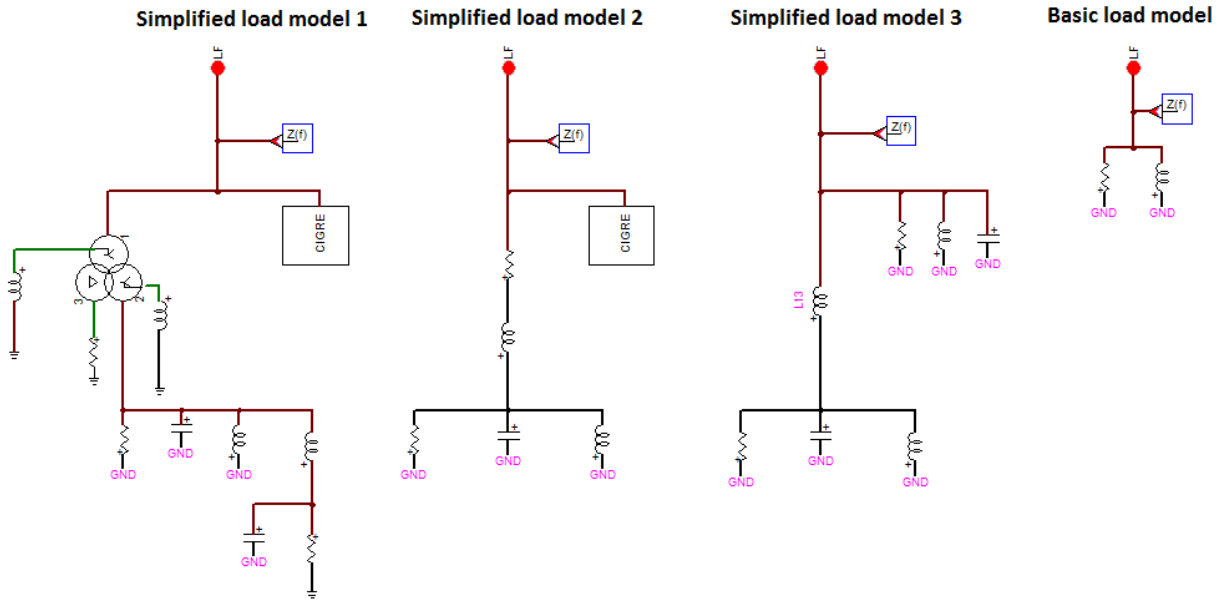

Figure 27 Load models

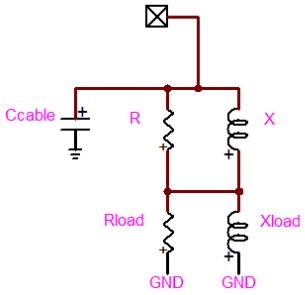

Figure 28 CIGRE model

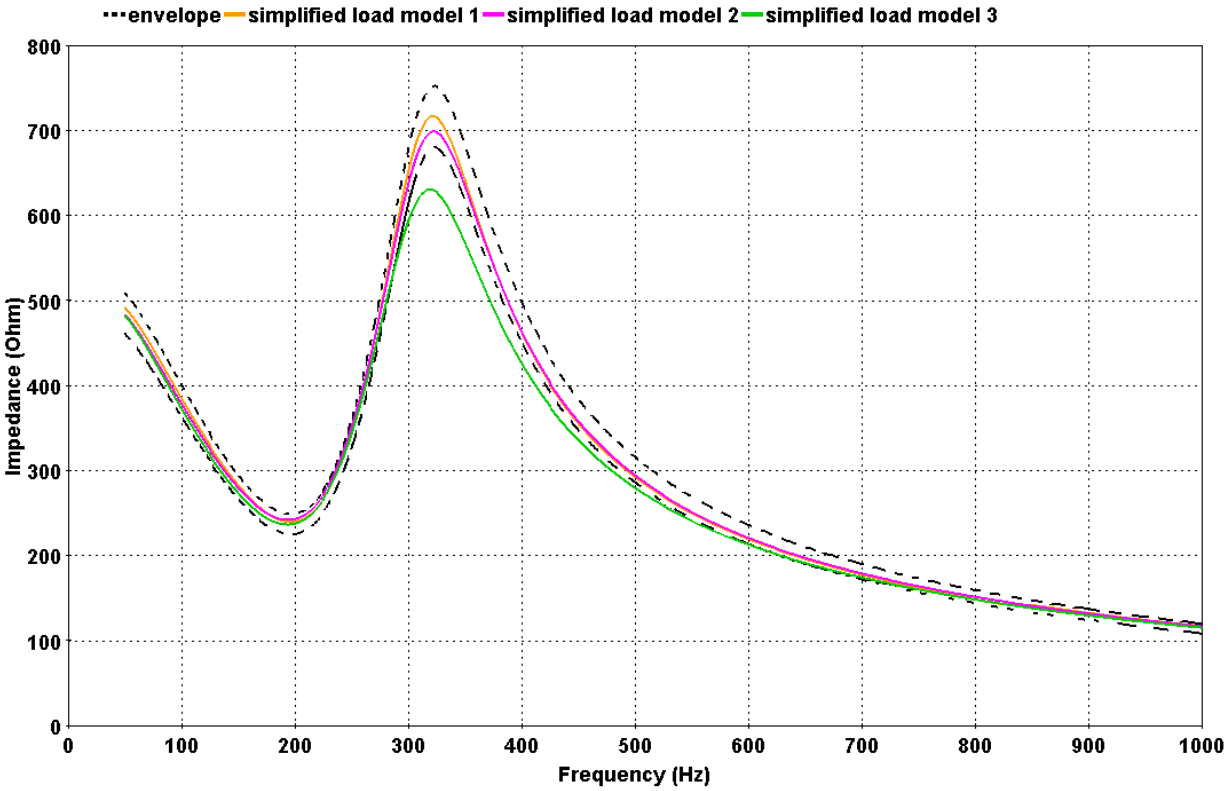

Figure 29 Comparison of simplified models with the envelope

The simplified load models introduced previously are compared to the detailed load model built in Section 3.1. The comparison is done using the envelope in the frequency response presented in Section 3.5 and shown on Figure 29. One can notice that simplified load models 1 and 2 are within the envelope on the studied frequency range, while simplified load model 3 is out above 300 Hz. Simplified load model 2's 90 kV grid's simplification in a parallel RLC is rough and the 225 kV grid's simplification in a Cigré model is finer. The resulting frequency analysis of load model 2 is a good approximation, inside the envelope, since the 90 kV grid is far away from the 225 kV bus bar. However, simplified load model 3's 225 kV grid's simplification in RLC has much clearer impact on the frequency response since the 225 kV grid is close to the 225 kV bus bar. This is the reason why the frequency analysis of simplified load model 3 is outside the envelope.

3.5 Load flow and frequency analysis

The load flow is performed on a load model seen from the 225 kV busbar. The reference is the detailed model's load flow. Due to the simplification, simplified load models do not have the exact same load flow as the reference. The difference for the active power is small, about 2 MW, which represents less than 2%. Regarding the reactive power, the difference is about 2MVar but it represents a much bigger relative error as the reference's reactive power is only 6.9 MVar. Among the simplified models, simplified load model 2 is the most accurate for active power and simplified load model 1 for reactive power. The basic model's active power is different from the reference as the active power represents the load pick-up at the substations. The basic model's reactive power is positive whereas the reference's is negative. Therefore, the basic load model consumes reactive power whereas the reference produces reactive power.

Table 13 Results of load flow analysis for load models

Load model	P (MW)	Q (MVar)	relative error on P (%)	Accuracy rank for P
detailed model	104.58	-6.94		
model 1	102.99	-8.12	1.52	4
model 2	104.74	-8.51	0.16	1
model 3	104.97	-8.48	0.38	2
basic model	103.80	26.02	0.74	3

The frequency analysis of all load models, seen from the 225 kV bus bar, is given on Figure 30. There is a resonance at 320 Hz for detailed and simplified load models due to the presence of both inductive and capacitive elements. On the contrary, the basic load model is only inductive so there is no resonance. The frequency analysis clearly shows that the basic model behaves very differently from the detailed and simplified models. Besides, it is interesting to notice that among the simplified models, the more simplified the model is and the lower the resonance is. This difference is not due to the approximation of the active power in the load flow analysis. Indeed, the detailed model has the highest resonance in the frequency analysis but not the lowest active power in the load flow analysis. Another element worth noticing in the frequency analysis is the dip in the impedance at 197 Hz for detailed and simplified models. This will be further studied in Section 4.2.1.

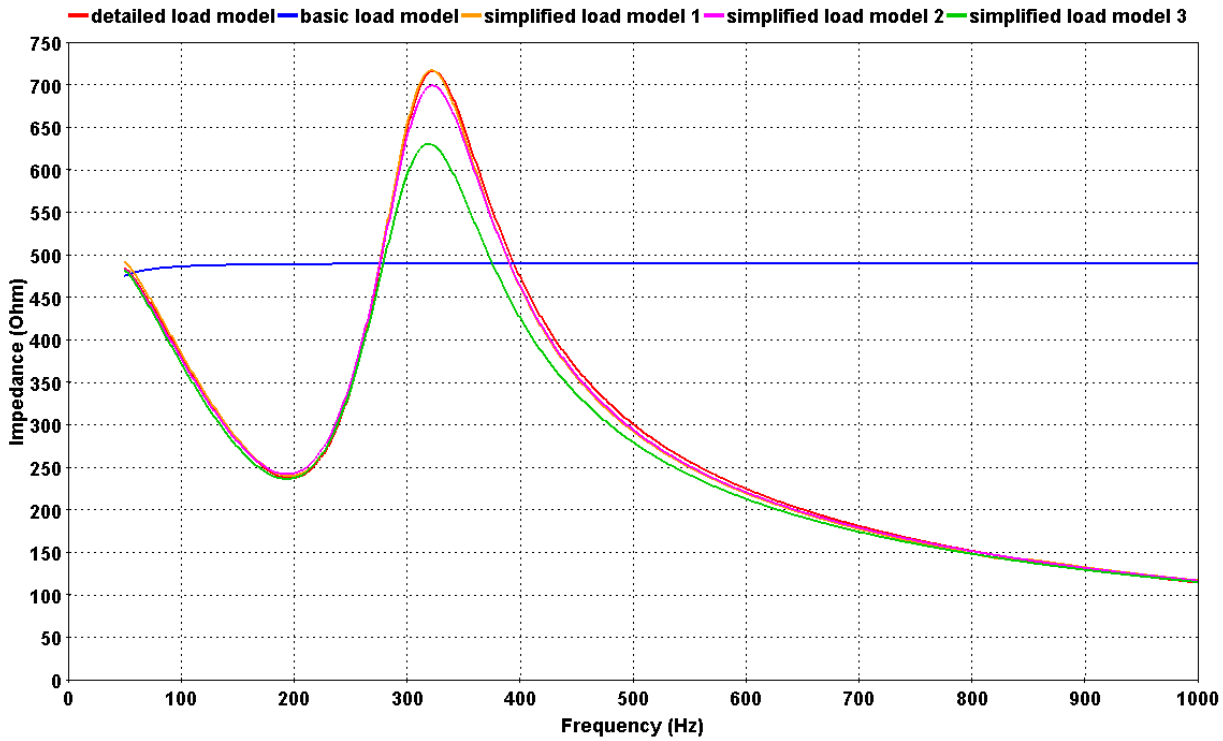

Figure 30 Frequency analysis for simplified, basic and detailed load models

3.6 Conclusion of chapter 3

The detailed load model and 3 simplified load models are build. The simplified load models require to first build the detailed load model. They are more precise than the basic load model, but less precise than the detailed load model. Load flow and frequency analysis are performed on these load models. The load flow analysis shows that, contrary to the simplified load models, the basic load model has an inductive behavior at 50 Hz whereas it should have a capacitive behavior according to the detailed load model. The frequency analysis of the detailed load model is used as a reference and the frequency analysis of the basic and simplified load models are compared with the reference. Contrary to the frequency analysis of the simplified load models, the frequency analysis of the basic load model is very different from the reference as it has no resonance.

Chapter 4. Black start study

4.1 Real backbone

4.1.1 Presentation

A black start study consists in carrying-out a time domain analysis of a backbone during the first seconds after energizing a transformer. Numerous scenarios are simulated by varying the parameters of the backbone. The scenario leading to the highest absolute overvoltage is called the worst scenario. The result of the black start study is the maximum absolute overvoltage observed in the worst scenario. It represents the maximum absolute overvoltage of a phase likely to appear at the primary of the transformer energized during the restoration process.

Time domain analysis of a backbone using different load models than the basic one have never been performed. The first aim is to find out if the load model has a significant influence on the result of the black start study. To put it differently, does the maximum overvoltage significantly change when the load model changes? The second aim is to find out if a more precise load model can improve the results of the black start study. This is done through comparisons with a reference. The reference is the result of the time domain analysis of the backbone using the detailed load model. The result of the time domain analysis of the backbone using the basic and simplified load models are compared to the reference.

In the scope of this Thesis, black start studies are carried-out using the Normandy's backbone displayed on Figure 31, following the restoration plan described in Section 2.4. It is considered that the first 6 steps of the network restoration plan have already been performed by the dispatcher and step 7 is being performed: the transformer at Remise is energized by closing the switch at Remise.

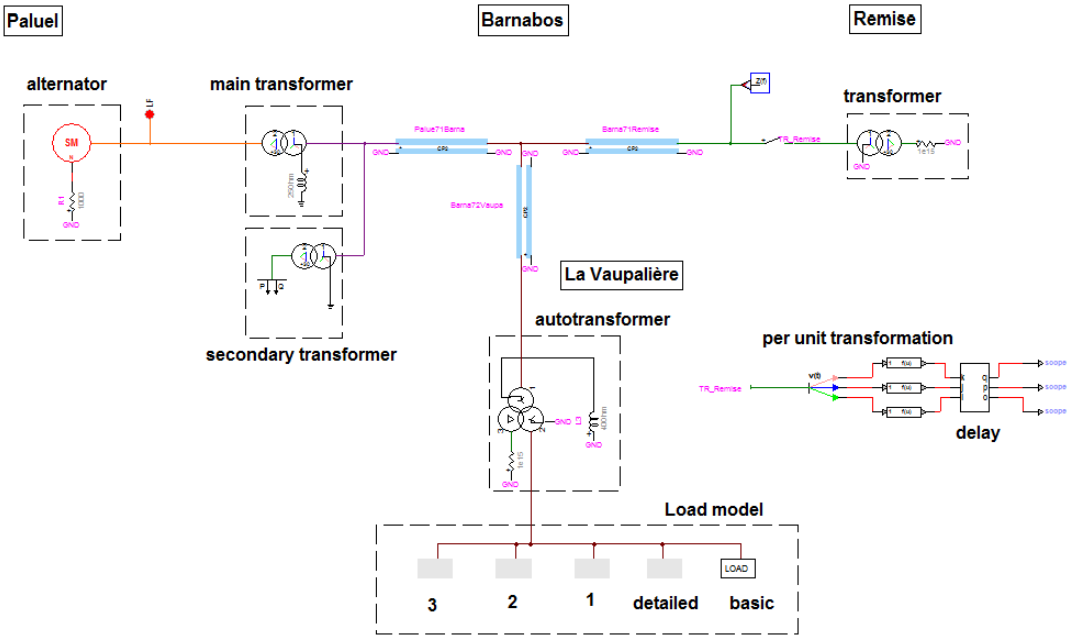

Figure 31 Normandy's backbone

The nuclear power plant at Paluel is composed of an alternator, a main transformer, a secondary transformer and an auxiliary transformer. The alternator is a rotating machine producing electricity. The main transformer levels up the voltage from 20 kV to 400 kV so as to transmit the power produced by the alternator to the 400 kV backbone. The secondary transformer feeds the auxiliary equipment (mainly pumps). The auxiliary transformer has the same role as the secondary transformer but is used only in case of a problem or a maintenance on the secondary transformer. As the auxiliary transformer is energized unloaded, it may saturate and cause transient harmonic overvoltages during the energizing of the transformer at Remise. Therefore it is not energized during restoration phase.

The information that follows about the model of the alternator and the lines, the set of parameters and the observation of the voltage is based on internal studies that have been performed by RTE in the past [4].

4.1.2 Models

Alternator

The alternator at Paluel is modeled with a synchronous machine. The network restoration plan imposes to control the voltage behind the transformer and maintain $0.9\,U_n$ so as to limit the overvoltages when energizing the transformer at Remise. A slack bus is used to initialize the alternator's steady-state voltage source. As a consequence, the voltage behind the alternator is maintained at $0.9\,U_n$ $(18\,kV)$ in steady-state. The slack bus is using the alternator's impedance at $50\,Hz$ for load flow computations.

Transformers

The models used for the transformers at Paluel and Remise are described in appendix III. The main transformer at Paluel is a 20/400 kV step-up transformer. The secondary transformer is a 400/63 kV step-down transformer and the load behind represents the auxiliary equipment such as water pumps. The transformer at Remise is a step-down transformer. The saturation of the transformer at Remise is the main cause for the appearance of overvoltages at the primary of the transformer so the value of the last segment's slope in the saturation curve is extremely important. According to preliminary previous studies, the value of the saturation inductance is around $1.021\,H$ referred to the primary. This leads to $L_{sat}^{final} = 0.21\,H$, using a factor 75 % , so as to be more conservative. The computation of L_{sat}^{final} is described in appendix I.

Lines

The representation of the lines on the 400 kV backbone is an important matter since they are very close to the transformer at Remise. Thus a frequency dependent model, called wide-band model, is used. The wide band model is further described in appendix VII.

4.1.3 Set of Parameters

Introduction

Several of the backbone's parameters are unknown during a black-start procedure. Some of these parameters can affect the saturation of the transformer. Therefore, different scenarios are considered, varying the parameters' values.

Initial flux

After a black-out, a transformer remains magnetized with different magnetizing levels in each phase. Initial flux can affect the transformer's saturation. No measurements of the initial flux are available but it is known that the flux in one phase can reach a maximum of 80% of nominal flux and that the sum of all three phases' flux is zero. Thus, the maximum flux in one phase is given by (6).

$$\boldsymbol{\varphi_{max} = 0.8\,\varphi_n^{peak} = 0.8 * \frac{V_n^{peak}}{2\,\pi\,f} = 0.8 * 420 * 10^3 \frac{\sqrt{2}}{\sqrt{3}} = 873.26\,Wb} \quad (6)$$

A set of 9 scenarios respecting the information at disposal is chosen. This set is described in appendix V.

Closing time of the switch

The saturation of the transformer's magnetizing current depends on the closing time of the switch. Figure 32 and Figure 33 show that when the switch is closed at minimum voltage (zero flux), the current in the transformer saturates less (in time and value) than when the switch is closed at zero voltage. As the voltage is periodic with a 20ms period, the closing time of phase A is varied with a set of 100 scenarios in a $20ms$ window, with a uniform distribution. Though all three phases are supposed to close simultaneously, in reality, phase B and C may close with a slight delay or advance compared to phase A. The dispersion in the phases' closing time has an influence on the saturation of the transformer's magnetizing current. That is why the closing time of phases B (t_B) and C (t_C) is varied with a normal distribution Δ centered on phase A, a standard deviation of $4.8\,ms$ and truncated at $\pm 10ms$ compared with phase A. Thus, $t_B = t_A + \Delta_b$ and $t_c = t_A + \Delta_c$

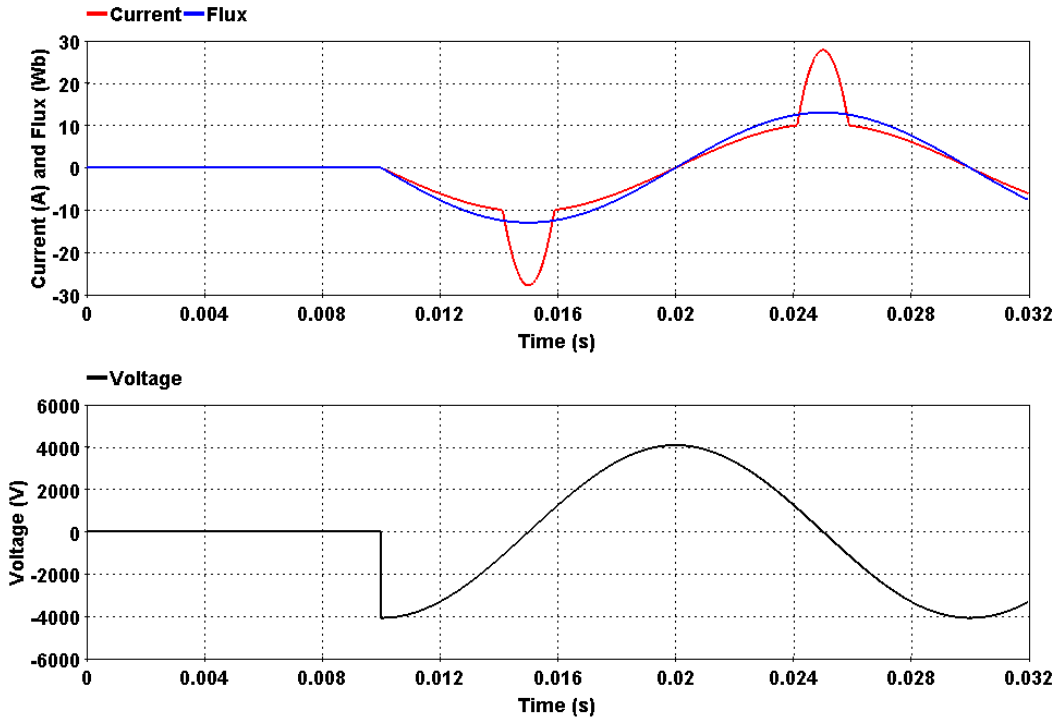

Figure 32 Switch closed at minimum voltage ($t = 10ms$)

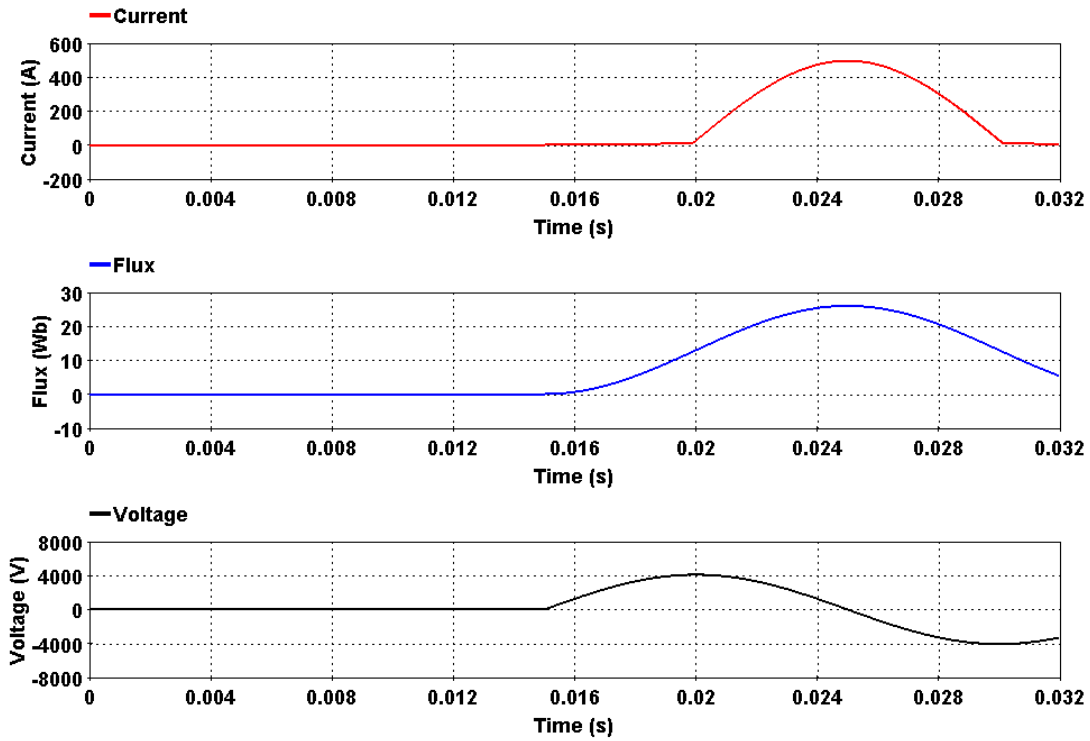

Figure 33 Switch closed at zero voltage ($t = 15ms$)

Load models

A set of 5 load models is chosen : the detailed load model, the basic load model and the three simplified load models. The load model studied is included in the backbone and all other load models are excluded.

4.1.4 Observation of the voltage

The voltage is observed at the primary of the transformer at Remise after a per unit conversion on a 343 kV base (phase to earth peak value). 420 kV is the maximal allowed phase to phase root mean square voltage value on the grid. The corresponding phase to earth peak voltage value is $\mathbf{420} * \frac{\sqrt{2}}{\sqrt{3}} = \mathbf{343}\ \boldsymbol{kV}$. The load flow states that the voltage at the primary of the transformer at Remise is 0.9 p.u. Thus, measuring $\mathbf{1}\ \boldsymbol{p.u}$ at the primary of the transformer at Remise is already an overvoltage.

With Parametric Studio[3], it is possible to visualize the maximum absolute overvoltage for each scenario. The worst scenario is determined for each load model. The corresponding value of the absolute maximum overvoltage is saved as the result.

2 kinds of overvoltages can occur when switching a transformer [4]:

- Overvoltages due to the dispersion in phases' closing time which last no more than a few milliseconds but are often very high. The equipment is set to bear these very short overvoltages so they are not a matter of interest. Such overvoltages may occur in the first 50 ms after energizing the transformer.
- Transient harmonic overvoltages due to the saturation of the transformer, the closing time of the switch and the dispersion in phases' closing time. Though such overvoltages are not as

[3] Parametric Studio is a software used to automate the simulations in EMTP.

high as the previous ones, they can last up to a few seconds and the equipment is not set to bear them. These overvoltages are of interest here.

The maximum absolute overvoltage given by Parametric Studio is very likely to be due to the dispersion in phases' closing time. To get around the problem, a solution is to add a block that puts to zeros the voltage values during the first $\mathbf{50}\ \boldsymbol{ms}$ after the closing time of phase A.

4.1.5 Simulation time

The detailed load model uses the constant parameters model for lines [5]. The time step of a scenario using the detailed load model must be smaller than the propagation time in a line. The smallest constant parameters line is between Dieppedalle and ZDiep and its propagation time is given by (7).

$$\boldsymbol{T = \sqrt{LC} = 1.4\ \mu s}\ \textbf{ with }\boldsymbol{L = 0.1\ \Omega}\textbf{ and }\boldsymbol{C = 6.366\ nF} \qquad \textbf{(7)}$$

As a consequence, the highest time step that can be used is $1.4\ \mu s$. With this time step, the CPU time of the time domain analysis for a scenario lasting $1\ s$ is $58.75\ s$. Parametric Studio performs 900 simulations with each load model so the total simulation time for the time-domain analysis of the backbone using the detailed load model is $14.6\ hours$! To shorten the CPU time, the shortest lines are changed from the Constant Parameter to the PI model. The PI model does not have a propagation time. After replacing the 7 shortest lines with the PI model, a time step of $20\ \mu s$ can be used, leading to a CPU time of $6.10\ s$ for one scenario. Therefore, the simulation time for the time-domain analysis of the backbone using the detailed load model is $1.5\ hour$. With the backbone using a simplified load model, the CPU time is further reduced by a factor three, leading to a simulation time of $30\ minutes$.

The time-domain analysis is carried-out on one scenario with the following grid parameters: $(\varphi_a, \varphi_b, \varphi_c) = (0,0,0)\ \ t_A = 0.01\ s\ \Delta_b = \Delta_c = 0.001\ s$, using the different load models. The CPU time is summarized in Table 14.

Table 14 CPU time for the time domain simulation of one scenario

Load model	Basic model	Simplified 3	Simplified 2	Simplified 1	"Detailed modified"	Detailed
Simulation time step (μs)	20	20	20	20	20	1.4
CPU Time (s)	2.04	2.07	2.09	2.15	6.10	58.75

4.1.6 Frequency and time-domain analysis

Frequency analysis

The frequency analysis of the backbone is performed seen from the transformer at Remise, using the different load models. The frequency analysis of the backbone using the detailed load model is the reference. The amplitude of the harmonic is inversely proportional to the rank. Therefore, a resonance at a low frequency is more likely to result in high transient harmonic overvoltage. Figure 34 shows the frequency analysis of the backbone, focusing on the two first resonances. The first one occurs $at\ 276\ Hz$ and the second one at $685\ Hz$.

The first resonance of the backbone with the basic load model is shifted in amplitude and frequency compared to the reference. However, the difference between the frequency analysis of the backbone using the basic load model and the reference is reduced compared to the frequency

analysis of the load model alone (see Figure 30). When the frequency analysis was carried out on the load model alone, the point of view was the $225\,kV$ bus bar at La Vaupalière. Now that the frequency analysis is carried out on the backbone using a load model, the point of view becomes the transformer at Remise. The load is $108\,km$ further away from the point of view so the influence of the load model on the frequency analysis is reduced. This explains why the difference between the frequency analysis of the backbone using the basic model and the reference is reduced.
The second resonance has a lower amplitude and occurs at a higher frequency. Therefore, it is unlikely to be significant in time-domain. Nevertheless, it is worth noticing that the frequency analysis of the backbone using the basic load model does not have this second resonance contrary to the frequency analysis of the backbones with any other load model. It highlights the inaccuracy of the basic load model in terms of frequency analysis.
The small resonance at $50\,Hz$ appearing on Figure 34 and later on the frequency analysis of the Normandy's backbones is a consequence of a bug in the model of the synchronous machine and should be disregarded. This problem was not solved here because it was not of interest.

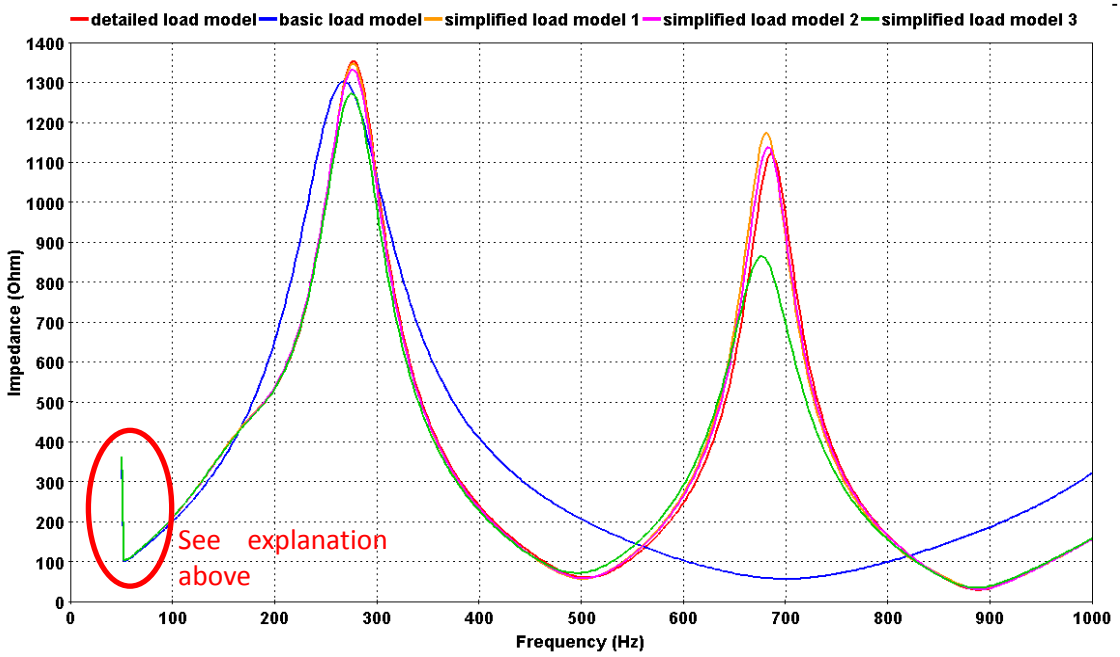

Figure 34 Frequency analysis of the backbone seen from transformer at Remise

Time-domain analysis

The time-domain analysis is carried-out on the Normandy's backbone. 9 flux combinations, 100 switching instants and 5 load models, are tested. In total, 4500 simulations are performed. Table 15 summarizes the results of the time-domain analysis. The per-unit overvoltage with a reference at $380kV$ is given in the third line of the table. Further on in the Thesis, the reference chosen is always $420kV$ as it is the usual reference used by RTE.

Table 15 Results of the time-domain analysis

Load model	Basic	Simplified 1	Simplified 2	Simplified 3	Detailed
Maximum overvoltage	1.022	1.061	1.051	1.046	1.059
Maximum overvoltage reference at 380 kV (p.u)	1.130	1.172	1.162	1.156	1.170
Absolute Relative error (%)	3.50	0.20	0.74	1.21	reference

Scenario	216	57	57	57	57
Time (s)	0.0622	0.0822	0.0822	0.0822	0.0624

There seems to be no link between the frequency and the time-domain analysis of the backbone. The amplitude of the frequency analysis at the resonance or at a frequency multiple of $50\,Hz$ is not linked to the overvoltage. The reason for this absence of link might be that the frequency analysis of the backbone using the different load models are close to one another. As a consequence, the differences in the amplitude of the resonance are not meaningful in time-domain. But this is just a guess. Another reason is given later in 4.3.4.

The scenario leading to the maximum overvoltage is the same whether the backbone uses the detailed or simplified load models but not the basic model. It can be drawn that the simplified load models are close enough to the detailed load model so that maximum overvoltage occur in the same conditions but the basic load model is so different from the detailed load model that maximum overvoltage do no occur in the same conditions. The absolute relative error supports this idea.

The overvoltages are weak so the comparison of the load models is not significant. Overvoltages are not a linear problem due to the saturation curve of the transformer energized. The conclusions drawn from the comparison of load models could be different if overvoltages were strong. Besides, the differences between the load models may be highlighted in the presence of high overvoltages. Therefore, the structure of the backbone is changed in order to enhance the overvoltage phenomenon. It is ensured that the backbone remains realistic for a restoration process.

Two parameters can enhance overvoltages:

- The length of the lines on the 400 kV backbone. As explained later, a change in the line's length moves the frequency of resonance.
- The active power of the load. A decrease in the active power of the load increases the amplitude of the resonance in the frequency analysis of the backbone.

Higher overvoltages are to be expected by moving the frequency of resonance toward low frequencies multiple of 50Hz and by increasing the amplitude of the resonance.

4.2 Evolution of the backbone

4.2.1 Increasing the line's length

The aim is to increase the length of a line between Paluel and Remise so that the resonance seen from the transformer at Remise occurs at a lower frequency, close to a multiple of 50Hz. The network map on Figure 31 shows two lines between Paluel and Remise.

Increasing the length of the line between Barnabos and Remise has the disadvantage of decreasing the effect of the load on the results of the time-domain and frequency analysis. As the line's length increases, the load gets further away from the transformer at Remise. Therefore a preferable solution is to increase the length of the line between Paluel and Barnabos

Increasing the length of the line between Paluel and Barnabos shifts the resonance's frequency to lower values, as depicted on Figure 35 and Figure 36. A longer line has higher values of inductance and capacitance so the frequency of resonance decreases, according to (8).

$$f_r = \frac{1}{\sqrt{L\,C}} \qquad (8)$$

The amplitude of the harmonic current increases when the harmonic rank decreases so resonances at low frequencies are more likely to lead to overvoltages. Figure 35 and Figure 36 both show that, as the length of the line between Paluel and Barnabos increases, the frequency of resonance is shifted to lower values. Figure 35 shows that when load model 1 is used in the backbone, the resonance is damped around 200 Hz. Actually, the damping of the resonance around 200Hz is observed when using any simplified load models or the detailed load model in the backbone. These load models have in common a dip at 200 Hz in the frequency analysis (see Figure 30) contrary to the frequency analysis of the basic load model. Thus, the damping of the resonance around 200Hz in Figure 36 is due to the dip at $200\ Hz$ in the frequency analysis of load model 1.

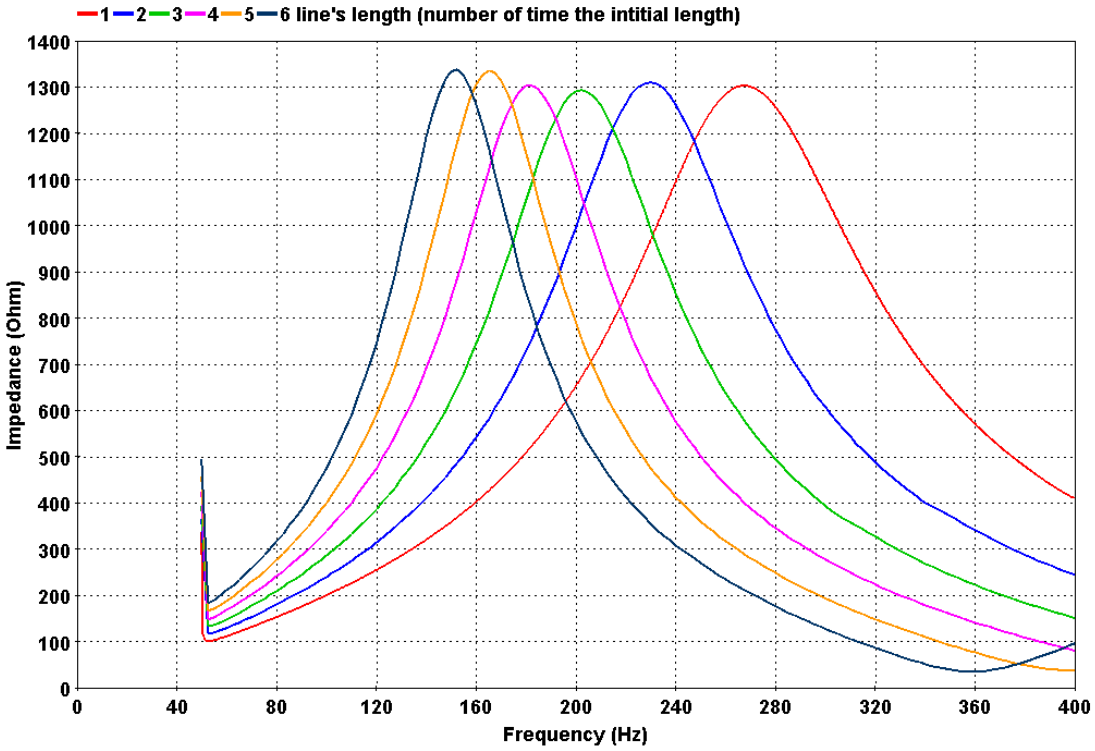

Figure 35 Effect of an increase of the length's line (Barnabos-Paluel) on the frequency of resonance (basic model used for load)

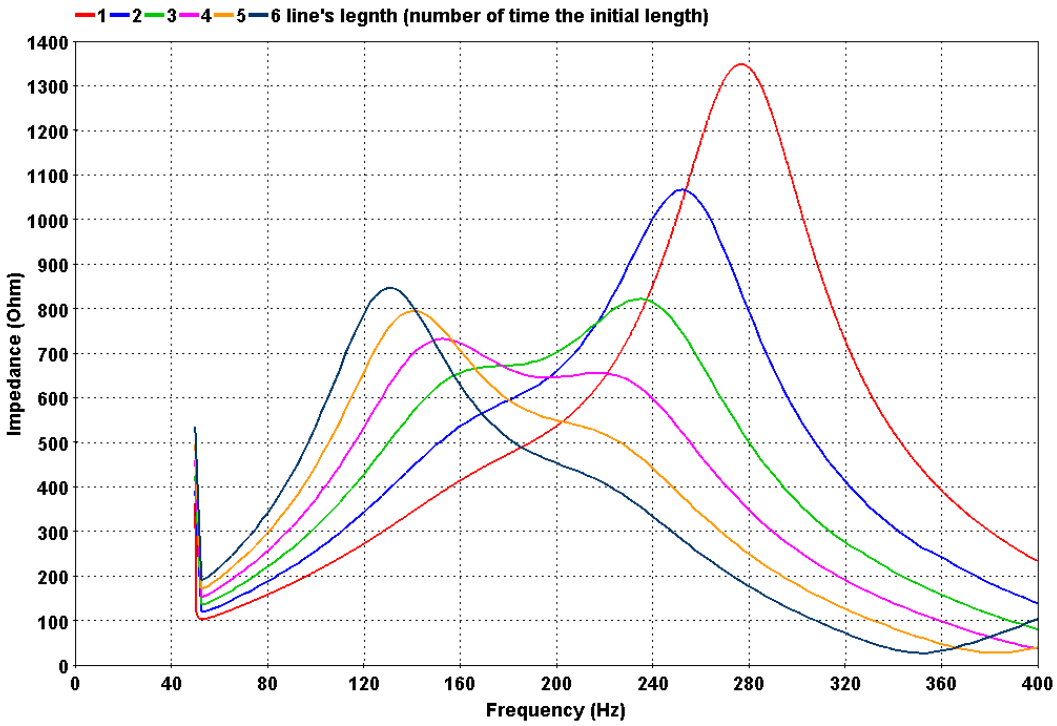

Figure 36 Effect of an increase of the length's line (Barnabos-Paluel) on the frequency of resonance (model 1 used for load)

Due to the damping of the resonance around 200Hz, the amplitude of the resonance of the backbone using a simplified load model or a detailed load model is too weak to lead to strong overvoltages. If the line's length is further increased, the voltages at the end of the line at Barnabos become unrealistic (higher than 420 kV).

Another solution to enhance overvoltages is to reduce the active power of the load at La Vaupalière.

4.2.2 Decreasing the active power of the load

Introduction

The active power consumption of the load influences the damping of the resonance. Decreasing the active power increases the amplitude of the resonance and therefore enhance transient harmonic overvoltages.
The active power is decreased with a set of 4 scenarios from 100% of the initial, maximum active power down to 10% with a step of 30%.

Detailed load model

At each substation where load is picked up, the active power is reduced with the help of a coefficient following (9).

$$\boldsymbol{P = coefficient * P_{max}} \qquad \textbf{(9)}$$

with P_{max} the active power picked up at the substation
and $coefficient = [1 \quad 0.7 \quad 0.4 \quad 0.1]$

Basic load model

The total active power is varied according to (9) with $P_{max} = 103.39\ MW$.

Simplified load model

The active power varied in the detailed load model represents the active load behind the transformers of the 90 kV grid and the 225 kV grid. The load behind the transformers of the 225 kV grid is depicted by the parameter R_{load} of the Cigré model in simplified load models 1 and 2. R_{load} is varied following (10).

$$\boldsymbol{R_{load} = \frac{R_{load,max}}{coefficient}} \qquad \textbf{(10)}$$

with $R_{load,max}$ the resistance of the initial simplified model.

A parallel RLC is used in simplified load models 2 and 3 to represent the 90 kV grid and the 225 kV grid. The parameter R represents the active load behind the transformers but also the resistance of the transformers and the lines. The active load behind the transformer is approximated with R. This approximation is reasonable since the resistance of the transformers and the lines is small compared to the resistance of the load behind the transformers. However, this approximation is not true anymore when the load pick up is low. Therefore, the scenario $P = 0$ is not considered and the lowest load pick-up scenario simulated is 10% of the initial active power. R is varied with (11).

$$\boldsymbol{R = \frac{R_{max}}{coefficient}}. \qquad \textbf{(11)}$$

Frequency analysis

The frequency analysis of the backbone with the percentage of the load active power progressively reduced is shown on Figure 37 (100%), Figure 38 (70%), Figure 39 (40%) and Figure 40 (10%). The reference is the red curve. The frequency analysis of the backbone using the basic load model (blue curve) have only one resonance up to $1000\ Hz$ whereas the reference and the frequency analysis of the backbone using the simplified load models have two to three resonances up to $1000\ Hz$. By decreasing the active power picked-up, the amplitude and the number of resonances are increased. The difference between the frequency analysis of the backbone using the basic load model and other load models around 200 Hz is particularly striking when the active power of the load picked-up is small.

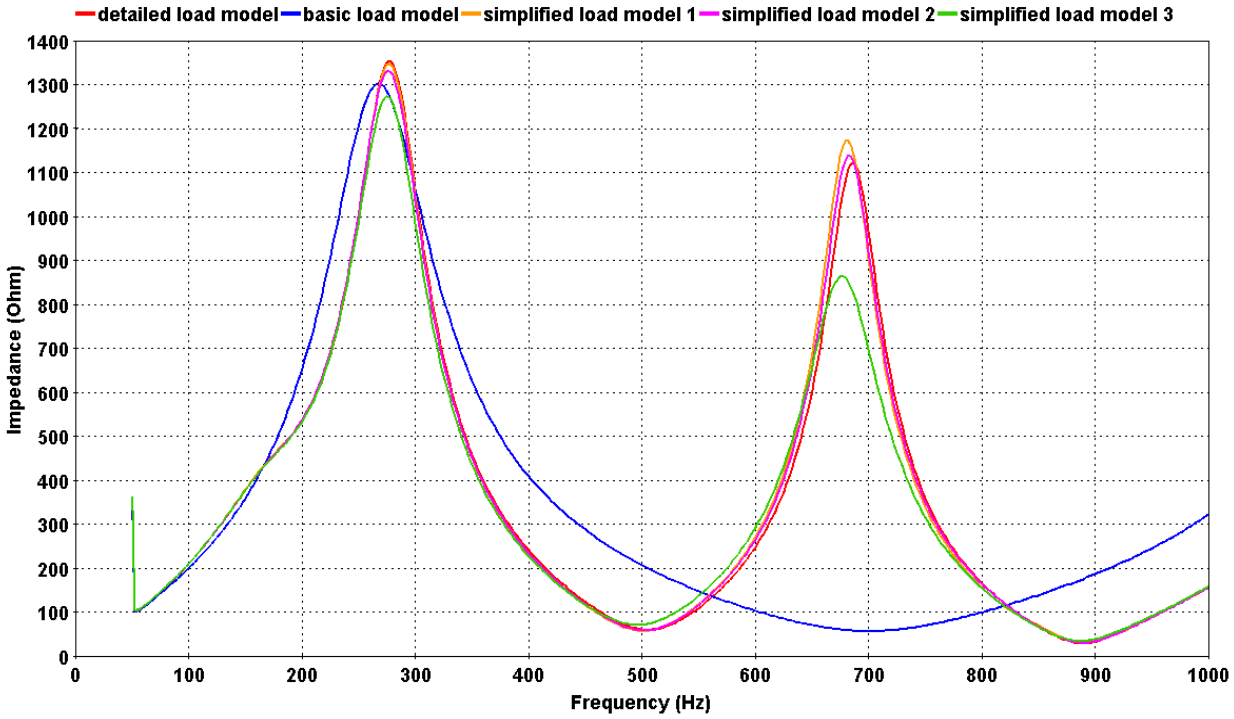

Figure 37 Fequency analysis of the backbone with 100% of the load active power

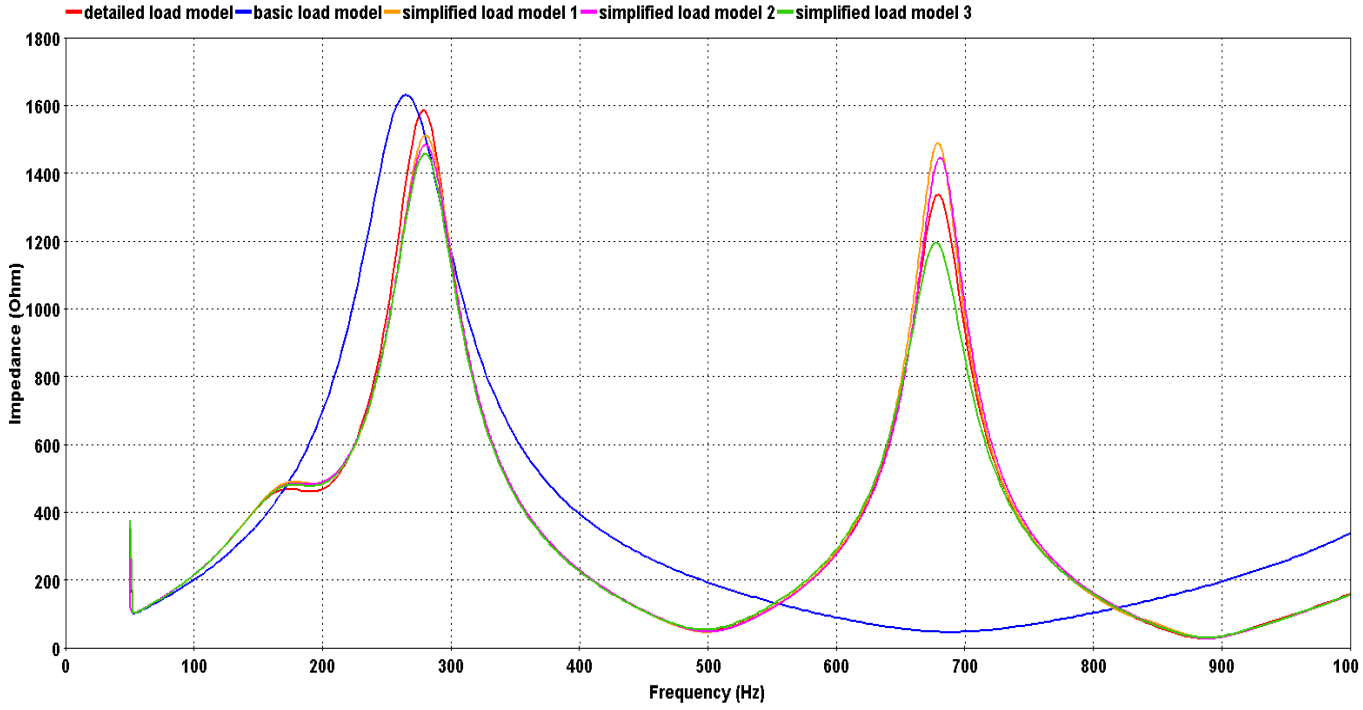

Figure 38 Frequency analysis of the backbone with 70% of the load active power

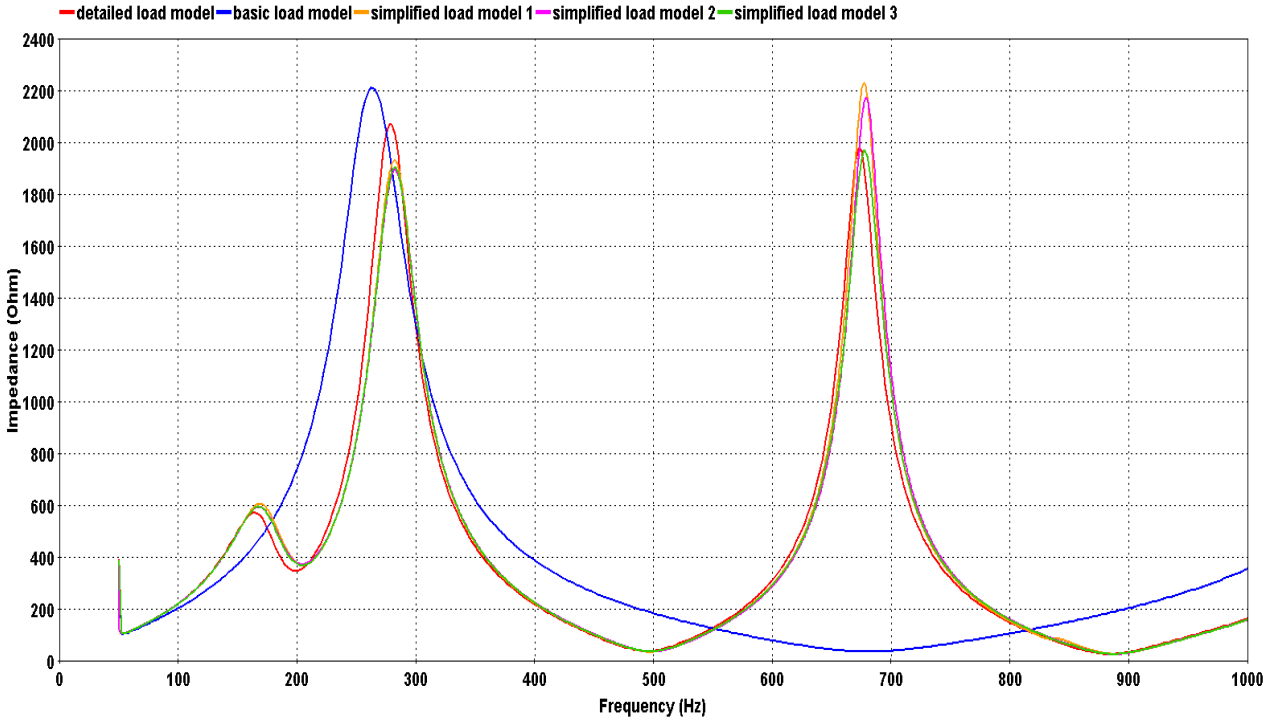

Figure 39 Frequency analysis of the backbone with 40% of the load active power

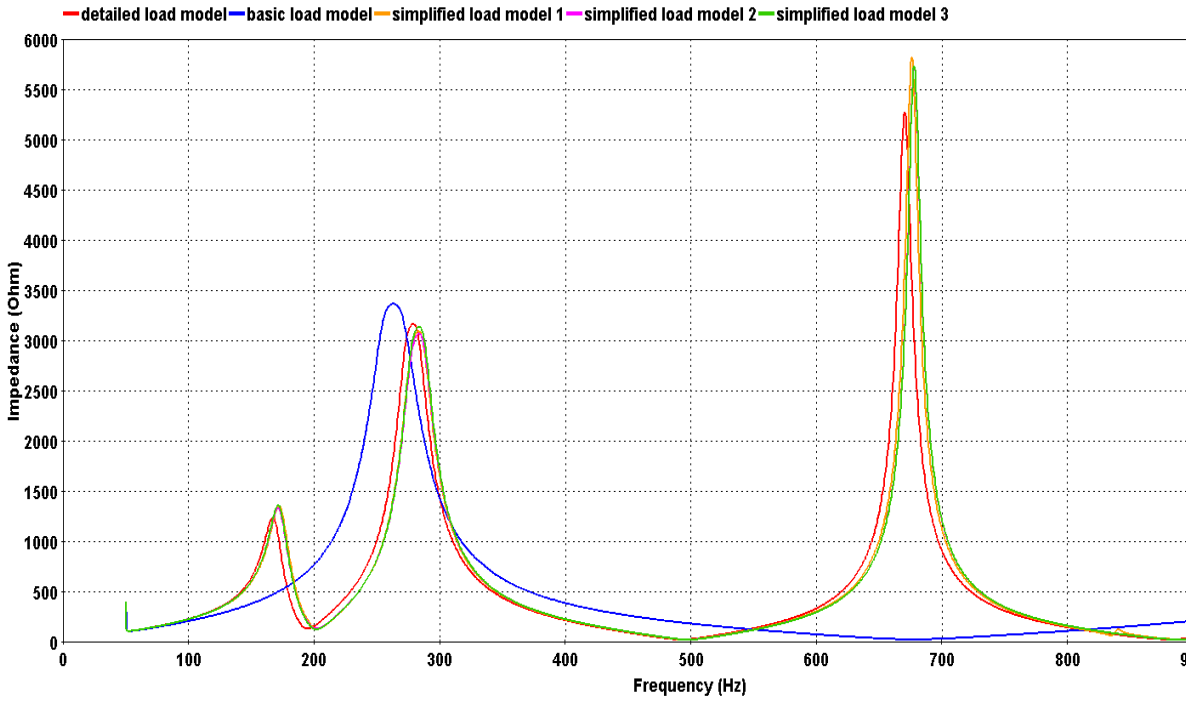

Figure 40 Frequency analysis of the backbone with 10% of the load active power

Time-domain analysis

5 load models, 3 coefficients for active power, 9 flux combinations and 100 switching instants are tested. A total of 13500 simulations are performed ($\mathbf{5 * 3 * 9 * 100}$). Table 16 summarizes the results

of the time-domain analysis. The previous results of the time-domain simulation (100% of load picked-up) are displayed in the first line. The load model leading to the best results is in bold characters in the table. The simplified load models are generally better than the basic load model. The overvoltages are enhanced by reducing the active load picked-up but they remain low: less than $\mathbf{1.15}\ \boldsymbol{p.u}$.

Table 16 Results of the time-domain analysis

Percentage of load picked-up (%)	Basic	simplified 1	simplified 2	Simplified 3	Detailed
100	1.022	**1.061**	1.051	1.046	1.059
70	1.042	1.076	**1.067**	1.065	1.071
40	1.074	1.099	1.093	**1.092**	1.090
10	**1.135**	1.146	1.141	1.144	1.130

4.3 Fictive backbone

4.3.1 Introduction

By changing the length of the line between Barnabos and Paluel, a weakness has been exposed in the basic model. When the backbone's resonance occurs around 200 Hz, the amplitude of the resonance is damped with the detailed and simplified load models but not with the basic load model. From this follows the idea of varying the frequency of resonance of the backbone as a parameter in time-domain analysis.

The real Normandy's backbone has shown its limits for the given study. Despite the efforts, the overvoltages on the Normandy's backbone remained quite low, less than $1.15\ p.u$. Therefore, it is decided to build a fictive simple grid shown in Figure 41. The grid is composed of a source and a capacitance. The source, displayed on Figure 42, is a simple voltage source with an inductance and a slack bus. Besides the grid, the load, the autotransformer at La Vaupalière and the transformer to be energized are included. The short circuit power P_{sc} sets the value of the inductance. The value of the capacitance sets the frequency of resonance of the grid f_r. By increasing the capacitance's value, the resonance of the backbone is shifted to low frequencies. Only 40% of the load active power is picked-up so as to increase the resonance.

The load has very little influence on the frequency analysis when the short circuit power is high. The frequency analysis basically only sees the source's inductance and the capacitance, resulting in a single peak set by the values of the inductance and capacitance. When the short circuit power is low, the capacitance has little influence on the frequency analysis and it is harder to shift the resonance's frequency to low frequencies. As a compromise, it is chosen a reasonable short circuit power's value for black-start of 500 MVA, so that both the load and the capacitance have influence on the frequency analysis. The inductance's value becomes $1.018\ H$ with (12).

$$L = \frac{U^2}{P_{sc}\, w} \qquad (12)$$

with $U = 400kV$

It is not interesting to choose the value of the capacitance so as to set the frequency of resonance of the backbone with one specific load model. Indeed, with the same capacitance's value, a backbone using a different load model will result in a different frequency of resonance. As a consequence, the comparison of load models does not make sense. That is why it is decided to set the frequency of resonance of the grid, instead of the backbone. Of course, the two are related: when the frequency of resonance of the grid increases, the frequency of resonance of the backbone increases and vice-versa. By varying the value of the capacitance C, the frequency of resonance of the grid is varied from $100\ Hz$ to $550\ Hz$ by steps of $50\ Hz$ with (13).

$$C = \frac{1}{w_r^2\, L}. \qquad (13)$$

with $w_r = 2 * \pi\ f_r$ and f_r the frequency of resonance of the grid

The voltage at the source is maintained at 380 kV. A load flow is performed at 50 Hz, seen from the transformer at Remise. It is checked that the voltage values are within the usual range: between 380 kV and 420 kV. Therefore, though the fictive backbone does not actually exist, it is realistic.

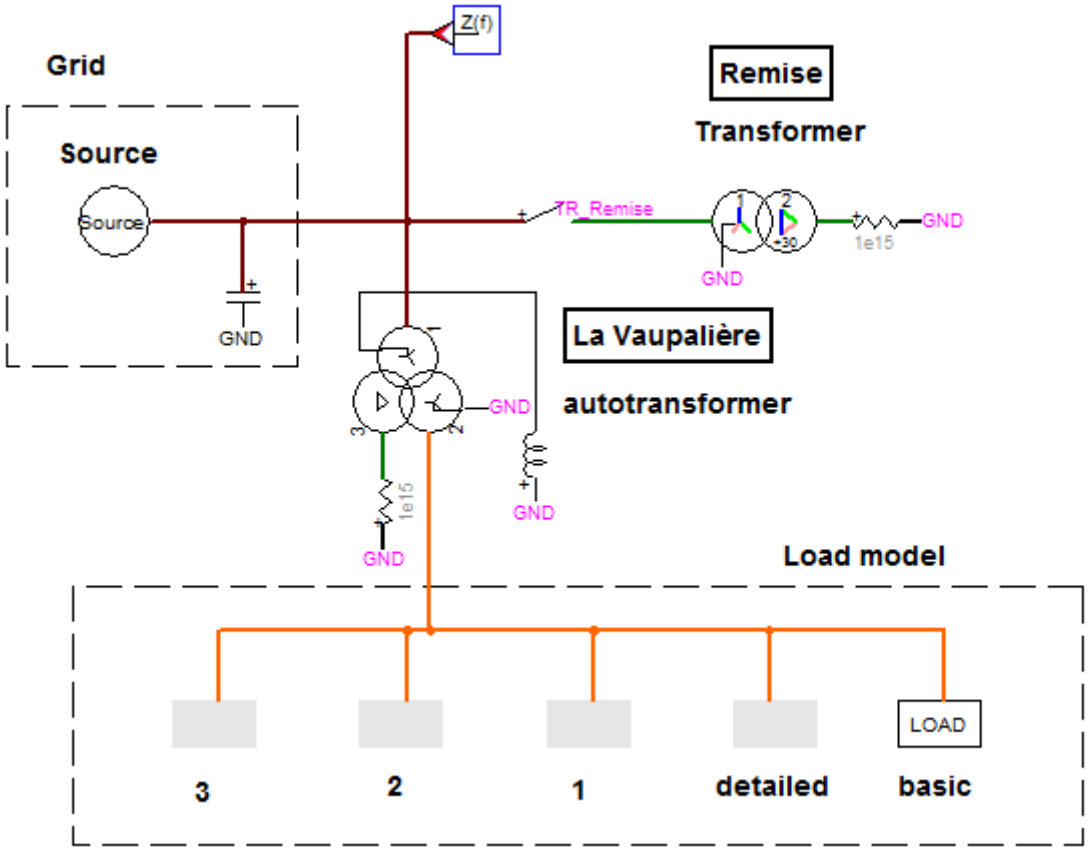

Figure 41 Fictive backbone

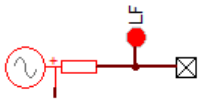

Figure 42 Source

4.3.2 Frequency and time-domain analysis

Frequency analysis

The reference is displayed on Figure 43. There are two resonances below 500Hz. As the frequency of the grid increases, the amplitude of the first resonance decreases and the amplitude of the second resonance increases. The frequency analysis of the backbone using the simplified load models have the same appearance as the reference. The amplitude of the first resonance is high, above $1300\ \Omega$ and located in the low frequencies. Therefore, the overvoltages are likely to be high and the comparison of the simplified load models may be more significant.

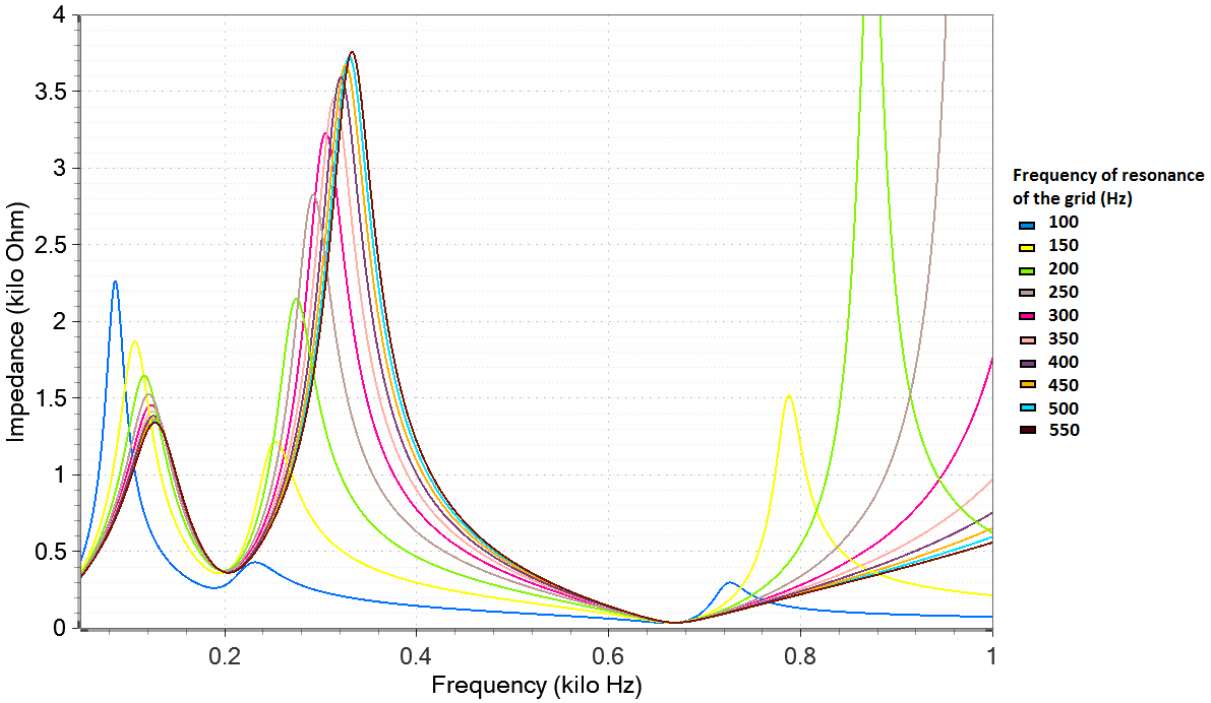

Figure 43 Frequency analysis of the backbone with the detailed load model

The frequency analysis of the backbone using the basic load model is displayed on Figure 44. As the frequency of the grid increases, the resonance of the backbone maintains about the same amplitude. Since the amplitude of the resonance is high, the overvoltages are likely to be high for low resonance's frequencies.

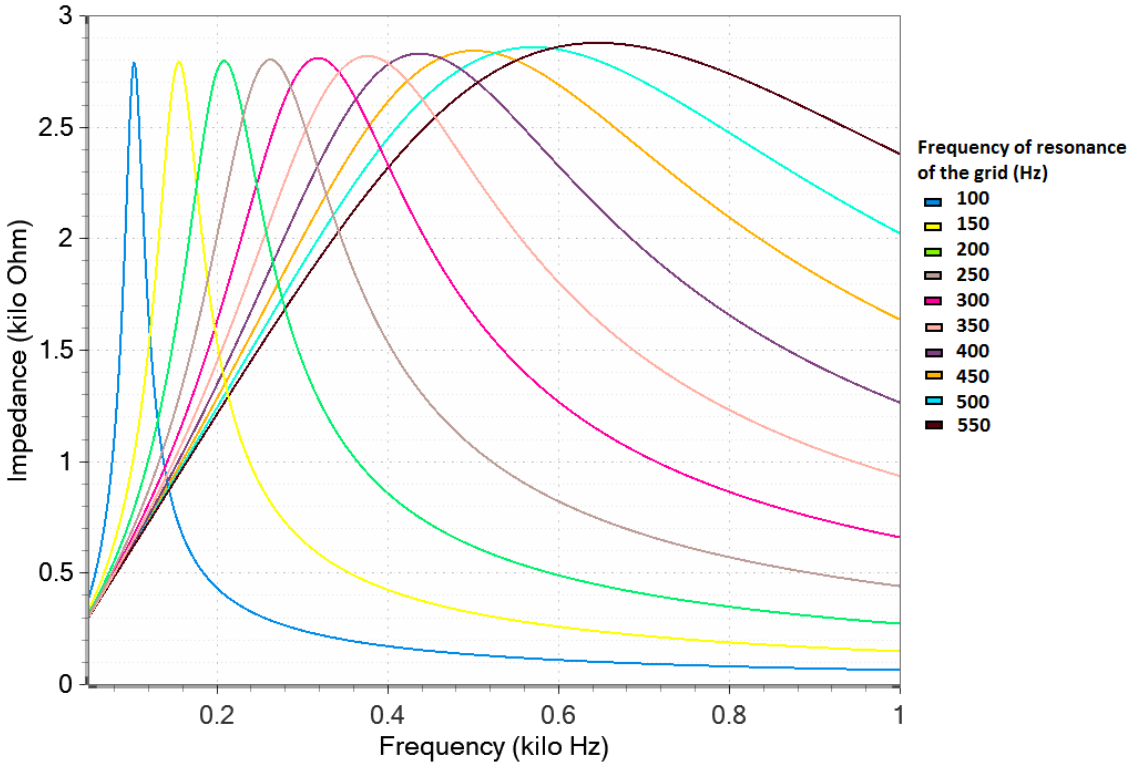

Figure 44 Frequency analysis of the backbone with the basic load model

The frequency response of the detailed and simplified load models is of order one whereas the frequency response of the basic load model alone is of order zero. This difference has an effect on the frequency response of the system composed of the backbone with the load. The Frequency response of the backbone with the detailed and simplified load models, below 1000 Hz, is of order 3, whereas the frequency response of the backbone with the basic load model is of order 1.

Time-domain analysis

The results of the time-domain analysis are shown in Table 17. The reference's results are displayed in the last column. Overvoltages were successfully enhanced up to $1.66\ p.u$. The backbone using the basic load model under-estimates the results. As the frequency of resonance of the grid increases, the overvoltage decreases. The decrease is much sharper with the backbone using the basic load model than with the backbone using any other load model. As a consequence, for high grid resonance's frequencies, the result of the time-domain analysis of the backbone using the basic load model is much lower than the reference.

Table 18 summarizes the relative errors. The biggest error is in red character and the smallest in bold black character. The time-domain analysis of the backbone using the basic load model is almost always the one with the biggest error (except for $f_r = 100\ Hz$). There is no time-domain analysis of a backbone using a simplified load model that stands out as having always a smaller error. As the behavior of the load model is a combination of the load flow at 50 Hz and the frequency analysis. Though according to the frequency analysis, simplified load model 1 is better than the others, it is not true according to the load flow at 50Hz. This might be the reason why there is not one simplified load model better than the others.

Regarding the reference, it seems that the time-domain analysis mostly sees the first resonance of the frequency analysis. From $f_r = 100\ Hz$ to $f_r = 200\ Hz$, the decrease in the amplitude of the

resonance explains the decrease in the values of overvoltage. Above $f_r = 200Hz$, the decrease in the amplitude of the first resonance is not significant anymore, that is why the overvoltage value are about the same.Regarding the backbone with the basic load model, the decrease in the overvoltages is due to the shift in the frequency of resonance toward high frequencies where there are less harmonics able to resonate.

Table 17 Results of the time-domain analysis

Frequency of the grid (Hz)	Basic	Simplified 1	Simplified 2	Simplified 3	detailed
100	1.58	1.64	1.56	1.52	1.66
150	1.28	1.37	1.33	1.33	1.43
200	1.17	1.33	1.28	1.28	1.29
250	1.10	1.30	1.30	1.30	1.27
300	1.08	1.30	1.31	1.29	1.27
350	1.05	1.26	1.27	1.27	1.25
400	1.03	1.29	1.28	1.28	1.25
450	1.00	1.30	1.30	1.30	1.25
500	0.98	1.31	1.32	1.31	1.25
550	0.98	1.27	1.27	1.26	1.22

Table 18 Relative error in percentage regarding the maximum overvoltage

Basic	Simplified 1	Simplified 2	Simplified 3
4.89	**0.84**	6.16	8.21
10.36	**3.85**	6.65	6.72
8.94	3.03	**0.23**	0.70
13.21	**2.04**	2.36	2.12
14.66	2.53	3.24	**1.51**
15.97	**1.44**	2.01	1.52
18.13	2.72	**2.48**	2.56
20.10	3.51	**3.35**	3.91
21.42	4.72	5.12	**4.40**
19.31	4.11	4.03	**3.53**

4.3.3 Comparison of load models regarding the number of scenarios leading to high overvoltages

A scenario leading to high overvoltage is defined as a scenario leading to an overvoltage higher than 90% of the maximal value. For each model and each frequency, the percentage of scenarios leading to high overvoltages among the 900 scenarios is counted. The results are summarized in Table 19.

Table 19 Percentage of scenario leading to high overvoltages

Frequency of the grid without the load (Hz)	Basic	Model 1	Model 2	Model 3	Detailed
100	22.8	**5**	10.9	10.9	5.0
150	73.1	**27.1**	32.8	32.0	19.2
200	81.8	30.9	**34.3**	37.6	35.1
250	75.0	**25.6**	19.2	20.3	39.3
300	70.8	20.9	20.8	**27.4**	36.6
350	71.0	**30.3**	26	27.8	36.1
400	70.3	22.4	**23.3**	22.8	40.2
450	100	**36.1**	36	31.8	39.3
500	100	32.4	32.6	**33.2**	35.3
550	100	48.3	48.8	**48.0**	36.7

Though the basic load model underestimates the results of the time-domain analysis, the percentage of scenarios leading to high overvoltages is bigger with the backbone using the basic load model than with the backbone using any other load model. Besides, the number of scenarios leading to high overvoltages is more realistic when any simplified load model is used in the backbone than when the basic load model is used.

4.3.4 Harmonic analysis

Chapter 2 explained that the current in the primary of the transformer at Remise is not necessarily sinusoidal, because of the non-linear characteristic of the transformer at Remise, and causes a harmonic voltage. The voltage can be decomposed, thanks to Fourier analysis, into a serie of sinusoids at the fundamental frequency and at integer multiples of the fundamental frequency. The Fourier analysis is further explained in appendix VI. Looking at the harmonic composition of the voltage for the different load models can help better understand the differences in the final value of the overvoltages.

A harmonic analysis has performed on a periodic signal but the voltage at the primary of the transformer at Remise is not a real periodic signal during transients. However, if only a few periods are considered, then the aperiodic component of the signal is negligible. Therefore, a harmonic analysis is performed on four periods and the amplitude of the voltage is computed in per unit for the six first harmonics. If the harmonic analysis had been performed on the following few periods, the amplitude of the harmonics would have been smaller, but the conclusions drawn would have been the same.

case $f_r = 200\ Hz$:

It is considered the case $f_r = 200\ Hz$. The frequency analysis of the backbone using the basic and detailed load model is displayed on Figure 43. The frequency analysis of the backbone using the simplified and detailed load model is displayed on Figure 44.Table 20 summarizes the results of the harmonic analysis.

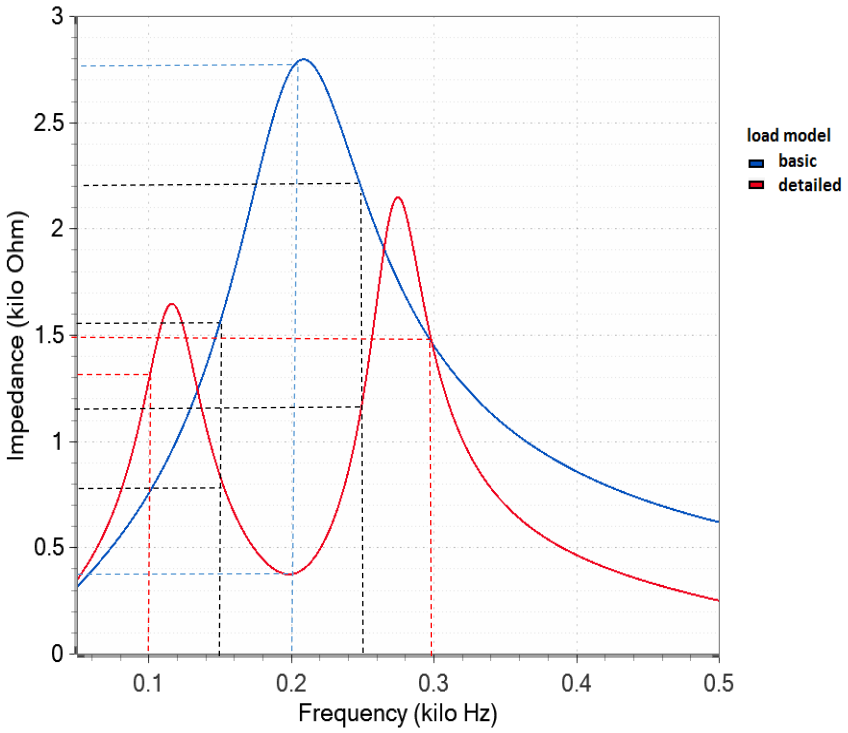

Figure 45 Frequency Analysis for $f_r = 200\ Hz$ (basic and detailed load models)

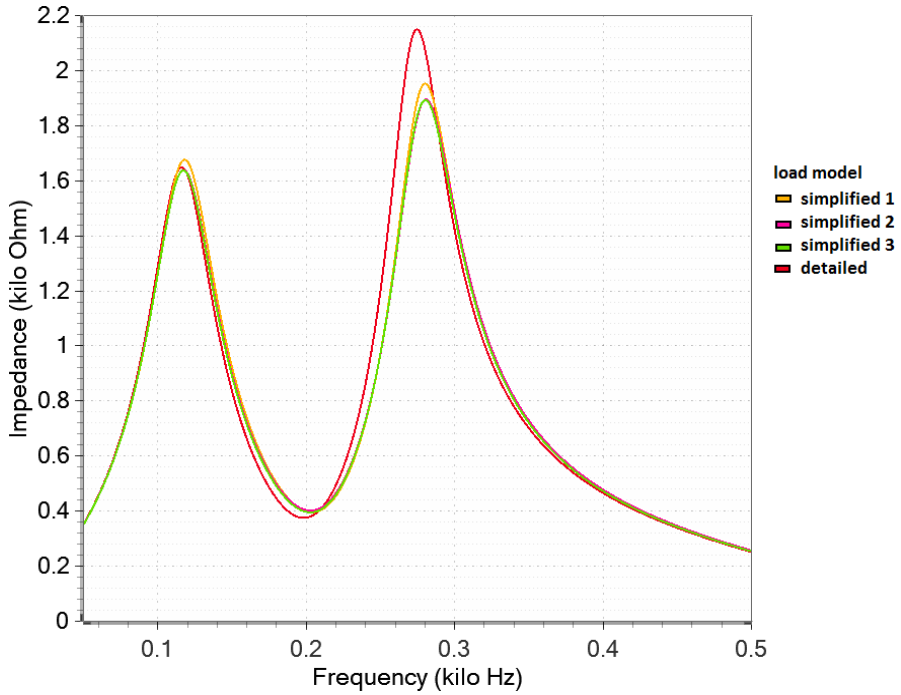

Figure 46 Frequency Analysis for $f_r = 200\ Hz$ (simplified and detailed load models)

Table 20 Harmonic analysis for $f_r = 200\ Hz$

Amplitude (p.u)	Harmonic 2	Harmonic 3	Harmonic 4	Harmonic 5	Harmonic 6
Detailed	0.378	0.044	0.021	0.018	0.051
Basic	0.159	0.134	0.127	0.147	0.052
Model 1	0.376	0.043	0.009	0.033	0.044
Model 2	0.363	0.080	0.014	0.023	0.043
Model 3	0.384	0.087	0.009	0.018	0.050

The frequency analysis of the backbone using the basic load model leads to a single peak at 210 Hz whereas the frequency analysis of the backbone using the simplified load models lead to two peaks, one below 210 Hz and one above 210 Hz, as the reference.

First, a connection can be established between the frequency and the harmonic analysis. At 100 Hz, in the frequency analysis the amplitude is higher for the reference and the backbone using the simplified load models than for the backbone using the basic load model. The result is that harmonic 2 is more amplified with the reference and the backbone using the simplified load models At 150 Hz, in the frequency analysis, the amplitude is smaller for the reference and the backbone using the simplified load models than for the backbone using the basic load model. The result is that harmonic 3 is less amplified with the reference and the backbone using the simplified load models At 300 Hz, in the frequency analysis, the amplitude is the same for the reference, the backbone using the simplified load models and the backbone using the basic load model. The result is that harmonic 6 is amplified almost equally whatever the load model used in the backbone.

Second, the composition of the harmonic voltage, shown in Table 20, shows much less harmonics 4 for the backbone using the detailed model or any simplified models than for the backbone using the basic load model. The observation stands also for the neighboring harmonics 3 and 5. This difference is explained by the frequency analysis of the load models alone which shows a dip at $200\ Hz$ for the detailed load model but not for the basic load model.

The example above shows that the backbone using the basic load model amplifies harmonics 3, 4 and 5 whereas the backbone using a simplified load model or the reference do not. This difference of behavior is explained by the frequency analysis of the load model alone.

The connection between frequency analysis and time-domain analysis or harmonic analysis is not always as simple. The frequency analysis does not include the transformer at Remise. On the contrary, the time-domain analysis includes the transformer at Remise. In the time-domain analysis, the inductance of the transformer at Remise matters: it changes the impedance of the backbone. The inductance of the transformer at Remise is the slope of the saturation curve. During time-domain analysis, the inductance of the transformer at Remise varies, depending on the position on the saturation curve. As a consequence, the frequency analysis alone is insufficient to foresee the results of the time-domain analysis.

4.4 Conclusion of chapter 4

In the Normandy's backbone, using the basic load model instead of the detailed load model influences the frequency analysis but has negligible influence on the time-domain analysis. As the phenomenon of transient overvoltages is non-linear, the results may change with high overvoltages so a fictive backbone is built to enhance the overvoltages.
In the fictive backbone, using the basic load model instead of the detailed load model significantly changes both the results of frequency and time-domain analysis. The backbone using the basic load model, contrary to the backbone using a simplified load model, under-estimates the overvoltages. Therefore, the basic load model is not always satisfactory for black start studies. Another point worth mentioning is that no simplified load model is better than the others for this black start study.

Chapter 5. A load model using equipment data

5.1 Presentation

In Chapter 4 points out that the basic load model is shown to be unsatisfactory for black start studies. Furthermore, the simplified load models cannot be used for black start studies since they require to first build the detailed load model, a long process that one would like to avoid doing if possible. Besides, if the detailed load model has been built, then a Frequency Dependent Network Equivalent of the load can be used. It will be as precise as the detailed load model and the simulation time of black start studies will be shorter. More information on the Frequency Dependent Network Equivalent is given in appendix VIII. The goal of this chapter is to see whether it is possible to find a load model for black start studies that does not require to first build the detailed load model. This model is called “load model using equipment data”.

According to chapter 4, no simplified load model is better than the others in black start studies. Simplified load model 3 is the easiest one to build so its structure is chosen for the load model using equipment data. The task is then to search for a method to estimate the values of parameters of simplified load model 3, without having to build the detailed load model first.

Let’s call S the main substation (S represents for instance La Vaupalière or Bezaumont), S_{HV} the main substation on the high voltage level and S_{LV} on the low voltage level.

- Spot the main transformer which is the transformer between S_{HV} and S_{LV} .
- Divide the grid in two: the grid behind the main transformer, called G_1 and the remaining grid called G_2. P_1 and P_2 represent the active load picked-up at the substations present in G_1 and G_2 respectively.

Data needed :

- zero devices plans on both high and low voltage level
- Load shedding plan
- lines’ capacitances
- the factory test data sheet for the main transformer

The zero devices plans are used to delimit the load pockets and thus find out at which substations load is picked-up. The value of active power picked-up is determined with the load shedding plan. The lines’ capacitances are available in RTE’s database. The inductance representing the main transformer is determined with the factory test data sheet of the transformer.

The main transformer is modeled with $L_{transformer}$.
G_1 is modeled with a parallel R_1 , L_1 , C_1. The resistance and inductance are deduced from the active and reactive power picked-up at the substations present in the grid. They are referred to the high voltage level. The capacitance is the sum of all lines’ capacitances, referred to the high voltage level. G_2 is modeled with a parallel R_2 , L_2 , C_2. The capacitance is the sum of all lines’ capacitances, referring the low voltage level lines to the high voltage level. A schema of the load model is displayed on Figure 47.

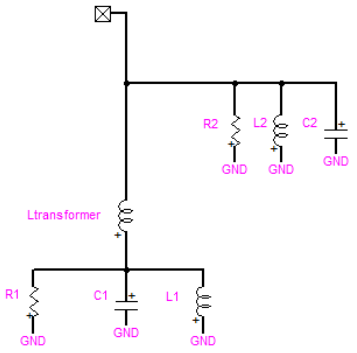

Figure 47 Load model using equipment data

$L_{transformer} = X_{sc\ HV/MV}$ (see appendix I)
$X_{sc\ HV/MV}$ is the impedance of the transformer when the high voltage winding is supplied and the medium voltage level winding is short-circuited.
$\cos(\varphi) = 0.97$
$\cos(\varphi)$ is the power factor which gives the relation between the reactive power and the active power.
$Q_j = P_j \tan(\varphi) \quad j = 1..2$

$$\boldsymbol{R_1 = \frac{U_{HV}^2}{P_1}} \quad \boldsymbol{L_1 = \frac{U_{HV}^2}{Q_1\, w}} \quad \boldsymbol{C_1 = \left(\frac{U_{LV}}{U_{HV}}\right)^2 \sum_i C_{LV,i}} \qquad \textbf{(14)}$$

$$\boldsymbol{R_2 = \frac{U_{HV}^2}{P_2}} \quad \boldsymbol{L_2 = \frac{U_{HV}^2}{Q_2\, w}} \quad \boldsymbol{C_2 = \left(\frac{U_{LV}}{U_{HV}}\right)^2 \sum_i C_{LV,i} + \sum_i C_{HV,i}} \qquad \textbf{(15)}$$

5.2 Applications of the load model using equipment data on two different loads

5.2.1 Application 1: Load at La Vaupalière

The method depicted above is applied to find a model for the load at La Vaupalière (Normandy's backbone). The values of the parameters found are very close to the values of parameters found with simplified load model 3.

Data:

- $L_{transformer\ 225/90} = 112.74\ \Omega$
- $P_1 = 63.49\ MW$
- $P_2 = 39.9\ MW$
- Values of parameters for the load model using equipment data with (14) and (15) :
  $R_1 = 797\ \Omega \quad L_1 = 10.12\ H \quad C_1 = 1.52\ 10^{-6} F$
  $R_2 = 1269\ \Omega \quad L_2 = 16.11\ H \quad C_2 = 1.46\ 10^{-6} F$

The load model using equipment data is compared with the basic and the detailed load model through load flow and frequency analysis of the load alone.

The results of the load flow and the frequency analysis of the load alone are displayed on Table 21 and Figure 48.

Table 21 Load flow analysis

Load model	P (MW)	Q ($Mvar$)
using equipment data	104.44	-12.34
basic	103.39	26.01
detailed	104.58	-6.94

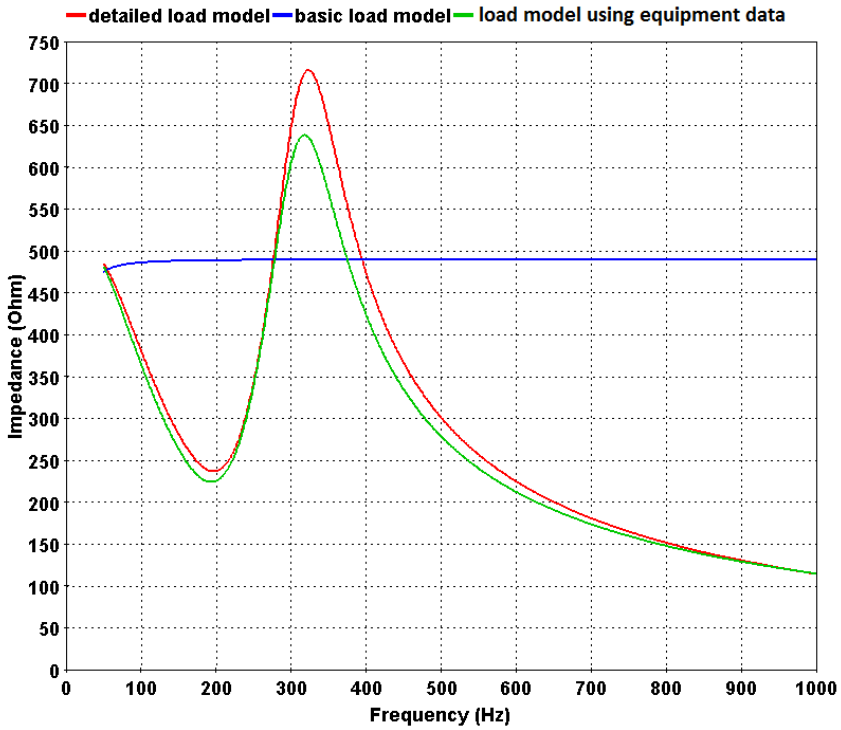

Figure 48 Frequency analysis of the load alone

In the case of La Vaupalière's load, the load model using equipment data gives satisfactory results both for load flow and frequency analysis of the load alone. It is interesting to know if, as expected, the method works on a different load. The load at La Vaupalière is picked-up in cities. For convenience reason, underground cables are often built instead of overhead lines in cities. Therefore, the load at La Vaupalière is composed of underground cables. In other areas, the load is picked-up in the countryside so there are only overhead lines. This is the case of the load at Bezaumont in Nancy's area. The method is thus applied on the load at Bezaumont.

5.2.2 Application 2: Load at Bezaumont

Data:

- $L_{transformer\ 225/63} = 85.20\ \Omega$
- $P_1 = 21.08\ MW$
- $P_2 = 79.33\ MW$
- Values of parameters for the load model using equipment data with (14) and (15) :
  $R_1 = 2401\ \Omega \quad L_1 = 30.50\ H \quad C_1 = 9.10\ 10^{-8} F$
  $R_2 = 638\ \Omega \quad L_2 = 8.11\ H \quad C_2 = 1.72\ 10^{-6} F$

The frequency analysis of the load models alone is displayed on Figure 49. For the purpose of comparing the load model using equipment data with the reference and the basic load model, the detailed and basic load models are built. It is important to highlight that the detailed load model was not used for building the load model using equipment data, as it was built independently. The reference is the frequency analysis of the detailed load model, in red on Figure 49. The frequency analysis of the load model using equipment data, in green, is almost always under-evaluated whereas the frequency analysis of the basic load model, in blue, is always highly over-evaluated. The results of the frequency analysis of the load using the load model using equipment data on Nancy's backbone are satisfactory. The load model using equipment data is definitely an improvement compared to the basic load model. However, the results are a bit disappointing compared to Normandy's backbone. The reason is that the representation of grids with a parallel RLC gives better results for frequency analysis if the grid is composed of underground cables than if the grid contains only overhead lines.

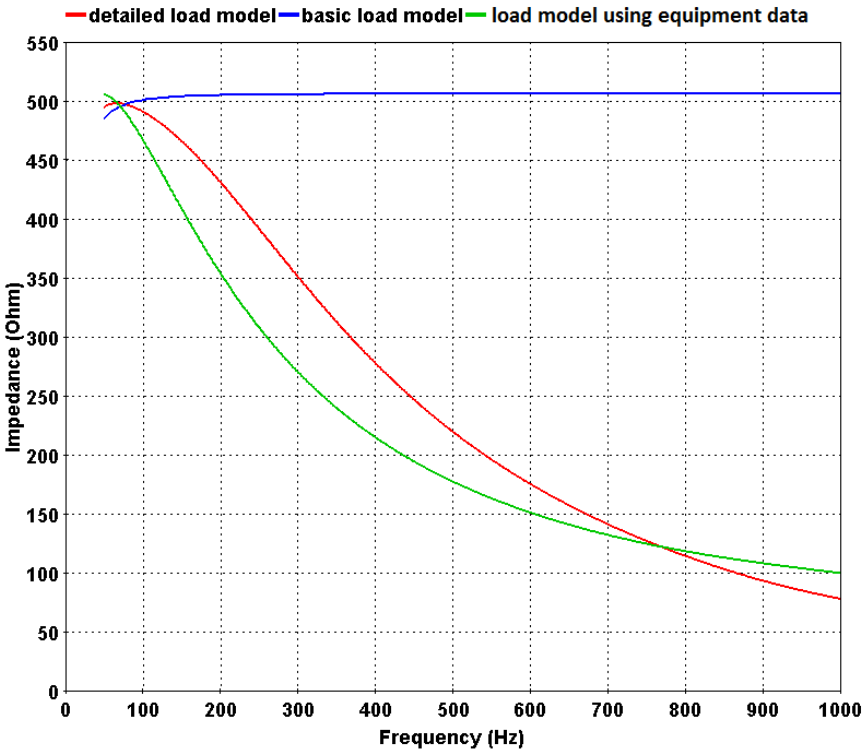

Figure 49 Frequency analysis of the load alone

The detailed load model is shown on Figure 50**.**

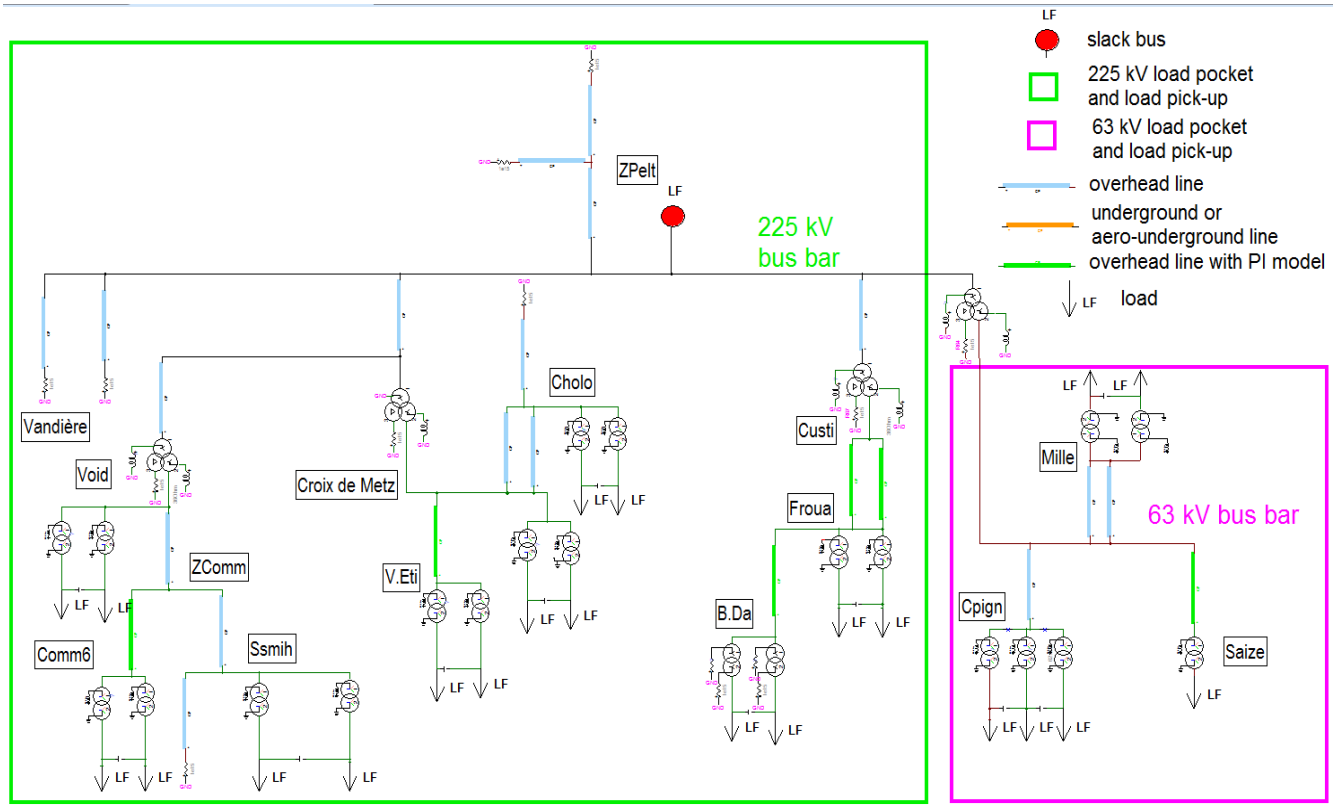

Figure 50 Detailed load model for Nancy's backbone

5.3 Black start studies

5.3.1 Backbones using the load at La Vaupalière

The black start study is performed on Normandy's backbone and the fictive backbone, with the basic load model and the load model using equipment data of La Vaupalière and comparing it to the reference. The results of the black start studies are shown on Table 22 and Table 23 respectively. The results are very close to the results of the backbones using the simplified load model 3 (Table 15 and Table 17). The load model using equipment data brings a significant improvement in almost all cases.

Table 22 Results for Normandy's backbone

Basic load model (reminder)	Load model using equipment data	Detailed load model (reminder)	Error for basic load model (%)	Error for load model using equipment data (%)
1.02	1.05	**1.06**	3.77	0.94

Table 23 Results for the fictive backbone

Frequency of resonance of the grid without the load (Hz)	Basic load model (reminder)	Load model using equipment data	Detailed load model (reminder)	Error for basic load model (%)	Error for load model using equipment data (%)
100	**1.58**	1.50	1.66	4.82	9.64
150	1.28	**1.34**	1.43	10.49	6.29
200	1.17	**1.29**	1.29	9.30	0.00
250	1.10	**1.31**	1.27	13.39	3.15
300	1.08	**1.29**	1.27	14.96	1.57
350	1.05	**1.28**	1.25	16.00	2.40
400	1.03	**1.30**	1.25	17.60	4.00
450	1.00	**1.32**	1.25	20.00	5.60
500	0.98	**1.32**	1.25	21.60	5.60
550	0.98	**1.27**	1.22	19.67	4.10

5.3.2 Backbones using the load at Bezaumont

A black start study has already been performed by RTE on Nancy's backbone, using the basic load model of Bezaumont. The studies have shown that the overvoltages are low. Therefore, the results of the time-domain analysis will not be significant and the comparison of load models will not be meaningful. The results of the frequency and time-domain analysis are displayed in appendix IX.

Since the problem is non-linear the results may be different with high overvoltages. Therefore the black start study is performed on the fictive backbone, using the load at Bezaumont.

A frequency and a time-domain analysis are carried-out on the fictive backbone, with the basic load model, the load model using equipment data and detailed load model. The results of the frequency analysis are shown from Figure 51 to Figure 53 and the results of the time-domain analysis are

displayed in Table 24. The most accurate results are in bold black characters. The load model using equipment data is almost always closer to the reference than the basic load model (except for $f_r = 100\ Hz$). Besides, the backbone with the load model using equipment data gives higher overvoltages than the backbone with the basic load model. Therefore, the load model using equipment data is conservative.

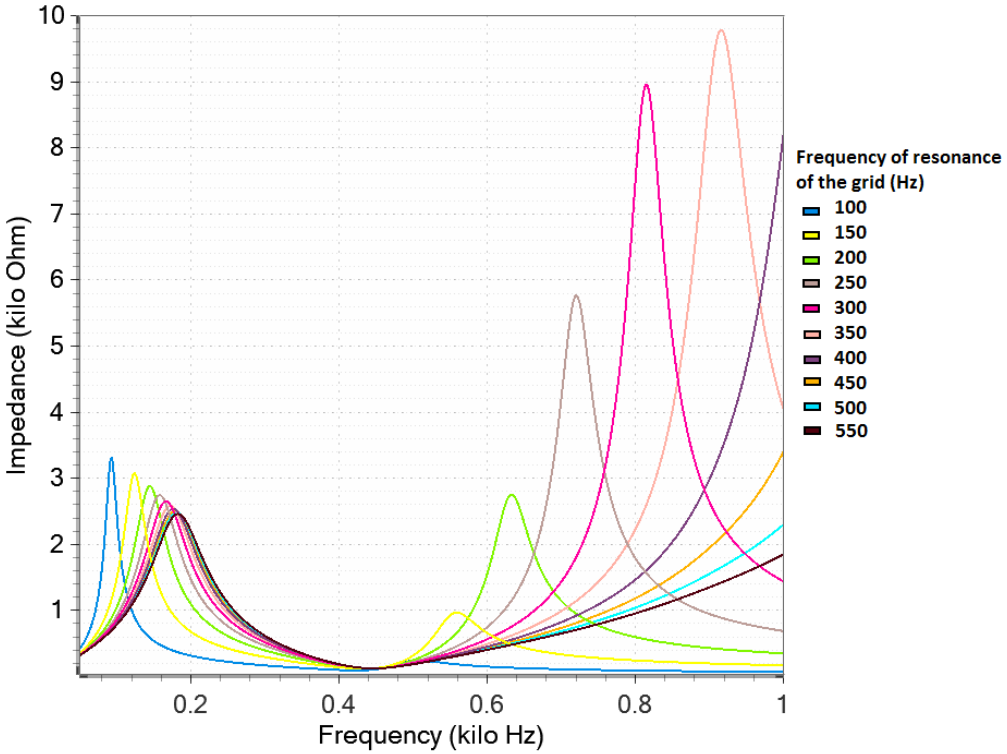

Figure 51 Frequency analysis of the fictive backbone using the detailed load model

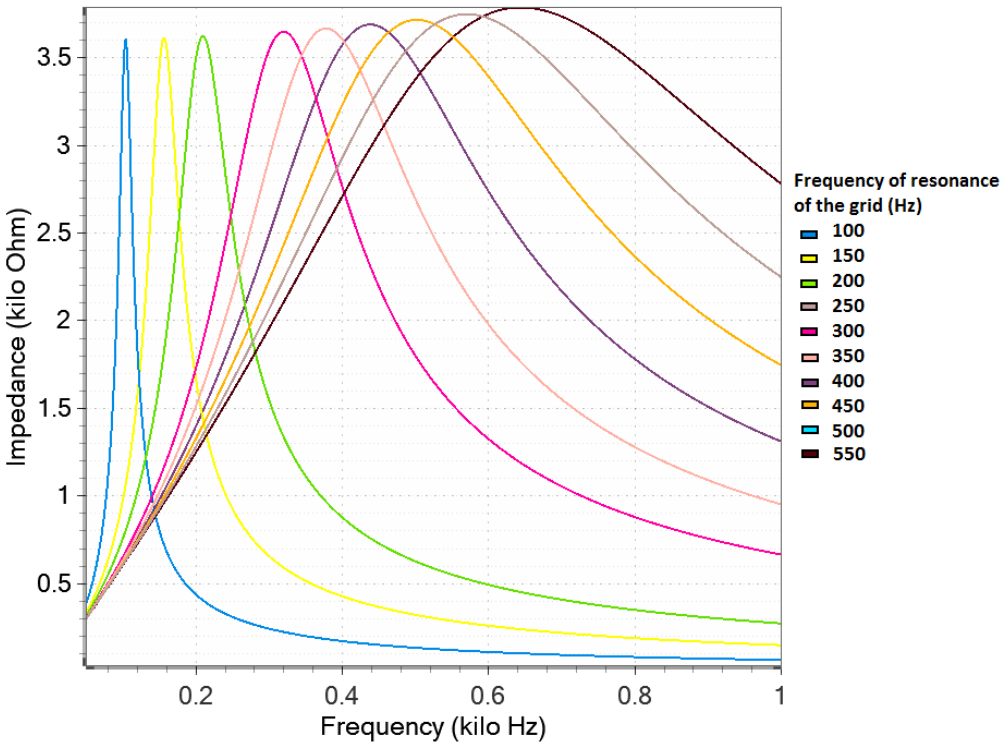

Figure 52 Frequency analysis of the fictive backbone using the basic load model

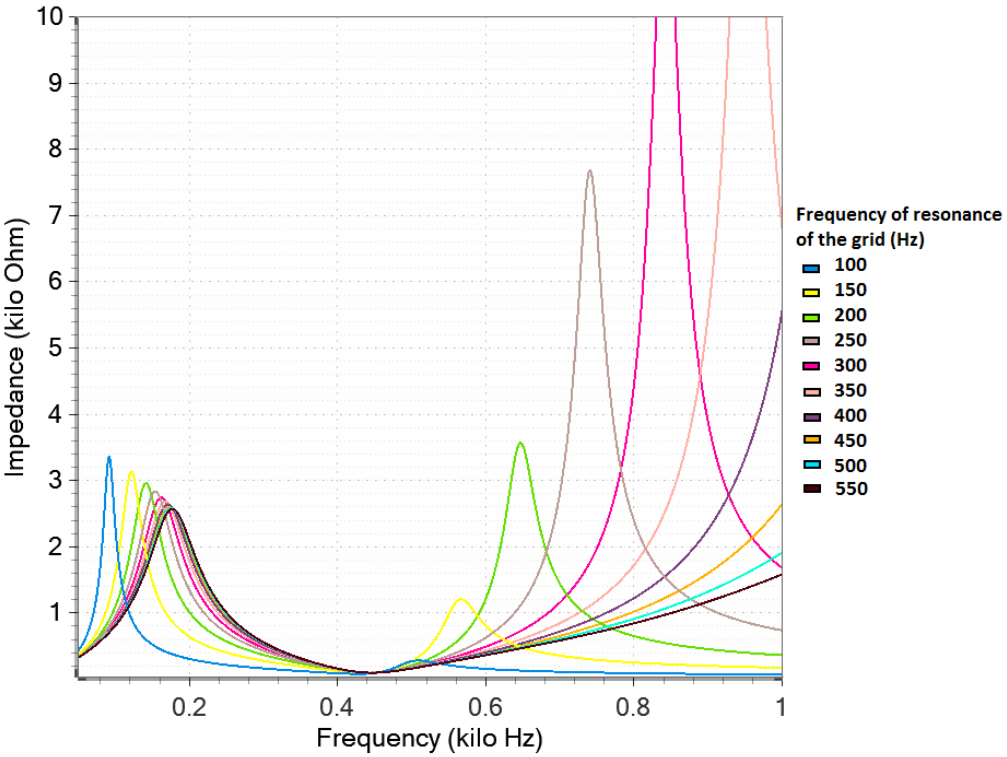

Figure 53 Frequency analysis of the fictive backbone with the load model using equipment data

Table 24 Time-domain results for the fictive backbone

Frequency of resonance of the grid without the load (Hz)	Basic load model	Load model using equipment data	Detailed load model	Error for basic load model (%)	Error for the load model using equipment data (%)
100	**1.33**	1.30	1.48	10.14	12.16
150	1.11	**1.16**	1.19	6.72	2.52
200	1.07	**1.11**	1.09	1.83	1.83
250	1.04	**1.13**	1.09	4.59	3.67
300	1.02	**1.11**	1.08	5.56	2.78
350	1.00	**1.10**	1.06	5.66	3.77
400	0.98	**1.08**	1.05	6.67	2.86
450	0.96	**1.12**	1.08	11.11	3.70
500	0.95	**1.12**	1.08	12.04	3.70
550	0.94	**1.16**	1.08	12.96	7.41

5.4 Conclusion of chapter 5

As the basic load model is not always satisfactory when used in black-start studies, it is looked for a new load model for black-start studies. This new load model is based on equipment data so it is called “load model using equipment data”. The results of the black-start studies using the simplified load models are satisfactory so it is decided to keep the structure of the most simplified load model, load model 3, for this new load model. Then, a method is given so as to build the load model using equipment data without having to first build the detailed load model. The method is applied on two very different loads, La Vaupalière and Bezaumont. The frequency analysis of the load without the whole backbone, gives satisfactory results. Black-start studies are carried-out on scenarios leading to high overvoltages in order to have a meaningful comparison of the load models. The time-domain analysis shows that the use of the load model using equipment data instead of the basic load model in the backbone almost always significantly improves the results. Besides, the results with the load model using equipment data are conservative.

Conclusions

The current load model used in black start studies is very basic. It consists in a parallel resistance and inductance. A black start study performed on a real backbone shows that, though the frequency response is deteriorated when the basic load model is used, the results of the time-domain analysis using the basic and simplified load models do not significantly change compared to the reference. The real backbones that have been studied do not lead to strong overvoltages. However, strong overvoltages may occur in other real backbones. That is why a backbone leading to strong overvoltages has been built for the purpose of carrying out black-start studies. The black-start studies show that both frequency response and time-domain results are deteriorated when using the basic load model compared to the reference. Therefore, the basic load is not satisfactory and another load model is needed.

The study of three simplified load models shows that simplified load model 3 is a good candidate for a new load model. A method is determined to estimate the values of the parameters of simplified load model 3, without having to build the detailed load model first.

This new load model, called “load model using equipment data”, is applied on two different loads and used in scenarios leading to strong overvoltages. The use of this load model instead of the basic one significantly improves the results of the time-domain analysis. Therefore, the MESH division, where I carried out this Thesis, decided to use the load model using equipment data in future black-start studies.

Future work

The solution of the Frequency Dependent Network Equivalent for the load model was put aside in the scope of this Thesis because it is time consuming. It is still necessary to build the detailed load model if FDNE tools are planned to be used. A tool exists to automatically transpose the 400 kV grid from Convergence to EMTP. Similarly, it could be envisaged to partly automatically transpose the detailed load model from Convergence to EMTP. The method requires beforehand to define the boundaries of the detailed load model and gather information on the load picked-up or details on transformers that are not in Convergence. It would be interesting to compare the time-consumption of this method with the load method using equipment data.

Bibliography

[1] RTE, (2004), ***Mémento de la sûreté du système électrique.***

[2] RTE, (2011), C. Trudu, R. Berta, C. Chapel, ***« Plan de reconsitution du réseau – Organisation, principes et mise œuvre »*****, DIR-S2-DPSAR-GPES-10-00290.**

[3] Cigré, (2013), ***Special Aspects of AC Filter Design for HVDC Systems,*** **Working Group B4.47.**

[4] RTE, (2014), ***Reconstitution de l'ossature EST depuis cattenom : Enclenchement d'un autotransformateur 300MVA au poste 400kV de Logelbach*****, NT-ING-CNER-DP-3EP-14-00247-Ossature SEE Logelbach**

[5] RTE, Documentation helps of EMTP "CPline"

[6] Atef Morched, Bjmn Gustavsen, Manoocher Tartibi (July 1999), ***A universal model for accurate calculation of electromagnetic transients on overhead lines and underground cables,*** **IEEE Transactions on Power Delivery, Vol. 14, No. 3.**

[7] Ilhan Kocar, (2009), ***Wideband modeling of transmission lines and cables (Thèse de doctorat, École Polytechnique de Montréal)***

Appendices

Appendix I : Autotransformer Yyd

Computation of parameters $R_{HV}, R_{MV} R_{LV}, X_{HV}, X_{MV}, X_{LV}, R_m$

The following data are required on EMTP for autotransformers 400/225 kV YYD :

- Primary, secondary and tertiary phase to phase voltage, respectively U_{HV}, U_{MV}, U_{LV}
- Primary, secondary and tertiary resistance, respectively R_{HV}, R_{MV}, R_{LV}
- Primary, secondary and tertiary reactance, respectively X_{HV}, X_{MV}, X_{LV}
- Magnétisation resistance R_m
- Saturation curve $\Phi_m(i_m)$

Taking the example of the autotransformer 400/225 kV at La Vaupalière, it is shown how to calculate the parameters X_{HV}, X_{MV}, X_{LV} , R_{HV}, R_{MV}, R_{LV} and R_m

The one phase model of the autotransformer 400/225 kV at La Vaupalière is shown on Figure 54.

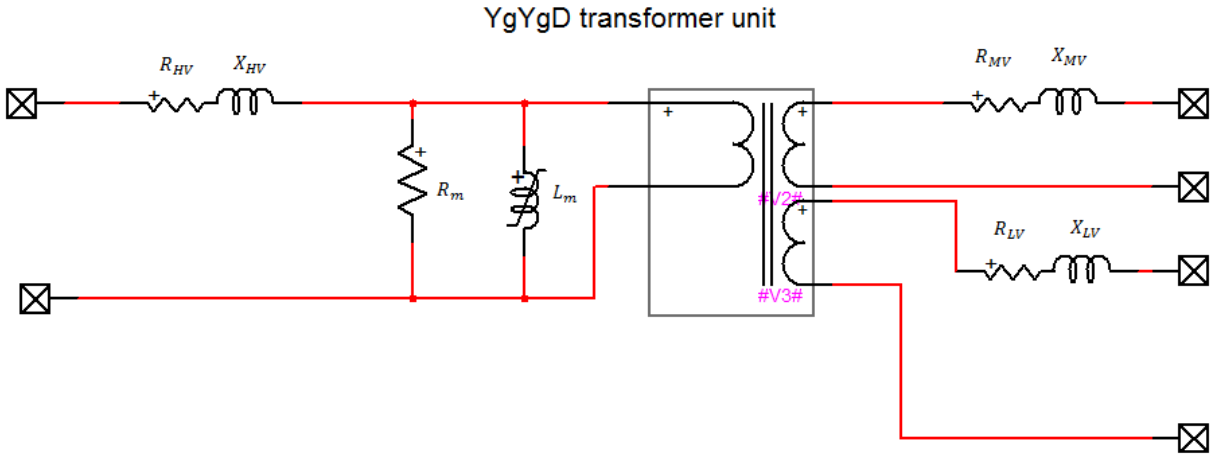

Figure 54 Transformer YYD one phase model

<u>Data for the autotransformer 400/225 kV at La Vaupalière:</u>

- High voltage phase to phase $U_{HV} = 405\ kV$
- Medium voltage phase to phase $U_{MV} = 240\ kV$
- Low voltage phase to phase $U_{LV} = 21\ kV$
- Apparent power $S = 600\ MVA$
- iron losses $P_{iron} = 108.160 kW$

<u>Short-circuit test data :</u>

- High Voltage supplied, medium voltage short-circuited :
  $U_{scHV/MV} = 19.277\ kV, \quad I_{scHV/MV} = 285\ A, \quad P_{scHV/MV} = 127.9\ kW$
- High Voltage supplied, low voltage short-circuited :
  $U_{sc\ HV/MV} = 14.583\ kV, \quad I_{sc\ HV/MV} = 46.3\ A, \quad P_{sc\ HV/MV} = 19.3\ kW$

- Medium Voltage supplied, low voltage short-circuited :

$$U_{sc\ HV/MV} = 5.737\ kV, \qquad I_{sc\ HV/MV} = 78.2\ A, \qquad P_{sc\ HV/MV} = 17.29\ kW$$

Winding i and j's short-circuit reactance referred to the primary side is :

$$X_{sc\ i/j} = \sqrt{\frac{U_{sc\ i/j}}{I_{sc\ i/j}\sqrt{3}} - \frac{P_{sc\ i/j}}{3I_{sc\ i/j}^2}}$$

Winding i and j's short-circuit resistance referred to the primary side is :

$$R_{sc\ i/j} = \sqrt{\frac{P_{sc\ i/j}}{3I_{sc\ i/j}^2}}$$

$$with\ (i,j) = (HV,MV),(HV,LV),(MV,LV)$$

Solving the system :

$$X_{scHV/MV} = X_{HV} + X_{MV}\frac{U_{HV}}{U_{MV}}$$

$$X_{sc\ HV/LV} = X_{HV} + X_{LV}\frac{U_{HV}}{\sqrt{3}\,U_{LV}}$$

$$X_{sc\ MV/LV} = X_{MV} + X_{LV}\frac{U_{MV}}{\sqrt{3}\,U_{LV}}$$

gives the values :

$$X_{HV} = 50.14\ \Omega, \qquad X_{MV} = -3.89\ \Omega, \qquad X_{LV} = 1.06\ \Omega$$

Solving the system :

$$R_{scHV/MV} = R_{HV} + R_{MV}\frac{U_{HV}}{U_{MV}}$$

$$R_{sc\ HV/LV} = R_{HV} + R_{LV}\frac{U_{HV}}{\sqrt{3}\,U_{LV}}$$

$$R_{sc\ MV/LV} = R_{MV} + R_{LV}\frac{U_{MV}}{\sqrt{3}\,U_{LV}}$$

gives the values :

$$R_{HV} = 0.42\Omega, \qquad R_{MV} = 0.036\ \Omega, \qquad R_{LV} = 0.021\ \Omega$$

The magnetising resistance is : $R_m = \frac{U_{HV}^2}{P_{iron}} = 1\,516\,503\ \Omega$

The saturation curve $\Phi_m(i_m)$

The saturation curve gives the magnetizing flux as function of the current in the magnetizing branch i_m . Open-circuit tests results are performed. The tertiary winding of the transformer is energized at three different voltage levels, while primary and secondary windings are open-circuited. The current in the tertiary winding is measured.

$$V_{LV}^1 = 18.9\ kV \quad i_{LV}^1 = 3.43\ A$$
$$V_{LV}^2 = 21\ kV \quad i_{LV}^2 = 6.61\ A$$
$$V_{LV}^3 = 23.1\ kV \quad i_{LV}^3 = 23.82\ A$$

The flux corresponding to each voltage level is computed. The factor $\frac{\sqrt{2}}{\sqrt{3}}$ changes the voltage rms phase to phase value in a peak phase to ground value. Given that the voltage V_{LV}^i is referred to the

tertiary winding, the factor $\frac{U_{HV}}{\sqrt{3}U_{LV}}$ refers the voltage to the primary winding. The result gives the flux peak value referred to the primary winding. $\Phi_m^i = V_{LV}^i * 10^3 \frac{\sqrt{2}}{\sqrt{3}} \frac{1}{2\,\pi\,f} \frac{U_{HV}}{\sqrt{3}U_{LV}}, \;\; i = 1..3$
The corresponding current value is deduced using a dichotomie method.

A fourth point is added to the saturation curve so as to fix the value of the last segment's slope in the saturation curve.

It is assumed a conservative value of 0.4 p.u for the saturation inductance. The base value of the inductance is : $L_{base} = \frac{U_{HV}^2}{P_{HV} * 2\,\pi\,f} = 0.870\ H$. As a consequence, the saturation inductance referred to the primary is $L_{sat} = 0.348\ H$. However, this value includes both the magnetizing inductance and the inductance of the primary winding, as it was computed using U_{HV}. A small value of the saturation curve's slope is responsible for the current saturation. For backbone studies, it is preferred to slightly overestimate the phenomenon of overvoltage than underestimate it. Regarding the value of the saturation curve's slope, it means that a lower value is a safer choice. That is why the final value is reduced to 90%.

$$L_{sat}^{final} = 0.9 * L_{sat} - L_{HV} = 0.154\ H$$

Appendix II : transformer 90/21 kV Yy and modeling of the load behind

Transformer 90/21 kV Yy

There are several transformers 90/21 kV in the detailed load model used for Normandy's backbone. However, they do not belong to the transmission grid but to he distribution grid. As a consequence, the results of the short circuit and open circuit test of these transformers are not available at RTE. All of the transformers's apparent power is 36 MVA and all but two belong to Jeumont Schneider manufacturer and were built from 1973 to 1998. It was possible to find in RTE's data base the results of the tests for a transformer 90/21 kV of same technology which was built later in 2007. Transformers B.GUI-Y413 belongs to "Le Transformateur Ste Anonyme" and was built in 1963. Transformer BZGAY-Y411 belongs to "Alsthom-Savoisienne" and was built in 1970. No results of tests were found for transformers of these two manufacturers in RTE's data base so it was decided to use Jeumont-Schneider's transformer which has the same technology.

The following data is required on EMTP for transformer 90/21 kV Yy :

- Primary and secondary phase to phase voltage, respectively U_{HV}, U_{MV}
- Primary and secondary resistances, respectively R_{HV}, R_{MV}
- Primary and secondary reactances, respectively X_{HV}, X_{MV}
- Magnetization resistance R_m
- Saturation curve $\Phi_m(i_m)$

The one phase model of transformer YY is shown on Figure 55.

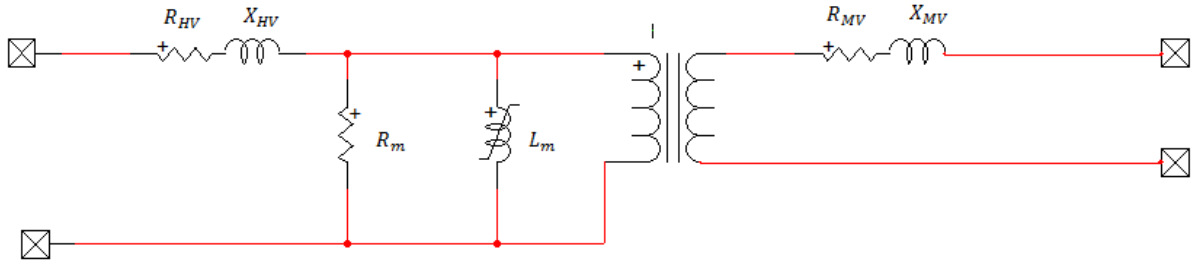

Figure 55 Transformer YY one phase model

The transformer is represented on tap 9. The reason for using tap 9 is explained in 3.1.4.

Data for TR ERDF :

- High voltage phase to neutral $V_{HV} = 89.5\ kV$
- Medium voltage phase to neutral $V_{MV} = 21\ kV$
- Iron losses : $P_{iron} = 18.48\ kV$

Short-circuit test data :

High Voltage supplied, medium voltage short-circuited :

$$V_{sc\ HV/MV} = 7597.93\ kV, \qquad I_{sc\ HV/MV} = 198.39\ A, \qquad P_{sc\ HV/MV} = 131.2kW$$

Primary and secondary's windings reactance refered to the primary side is :

$$X_{scHV/MV} = \sqrt{\frac{U_{scHV/MV}}{I_{scHV/MV}} - \frac{P_{scHV/MV}}{I^2_{scHV/MV}}}$$

Primary and secondary's windings resistance refered to the primary side is :

$$R_{scHV/MV} = \sqrt{\frac{P_{scHV/MV}}{I^2_{scHV/MV}}}$$

which gives :

$$X_{sc\ HV/MV} = 38.15\ \Omega \text{ and } R_{sc\ HV/MV} = 3.33\ \Omega$$

The ratio of the short-circuit reactance and resistance refered to the primary side is chosen as $w_p = 0.9$

$$X_{HV} = w_p\, X_{scHV/MV} = 34.34\ \Omega$$

$$X_{MV} = (1 - w_p) X_{scHV/MV} \frac{V_{MV}}{V_{HV}} = 0.21\ \Omega$$

$$R_{HV} = w_p R_{scHV/MV} = 3.00\ \Omega$$

$$R_{MV} = (1 - w_p) R_{scHV/MV} \frac{V_{MV}}{V_{HV}} = 0.018\Omega$$

The magnetising resistance is :

$$R_m = \frac{V^2_{HV}}{P_{iron}} = 433\ 455\ \Omega$$

For the saturation curve $\Phi_m(i_m)$, refer to appendix I.

Modeling of the load behind the transformer 90/21 kV

It is assumed that there is no loop in the structure of the load. It means that for a substation where there are several loads, each load is behind one single transformer 90/21 kV and is not connected to another transformer. If the transformer fails, the load behind that transformer is lost. An example of a substation with two loads and a no-loop structure is displayed on Figure 56. The validity of the no-loop structure assumption was checked with the DSO.

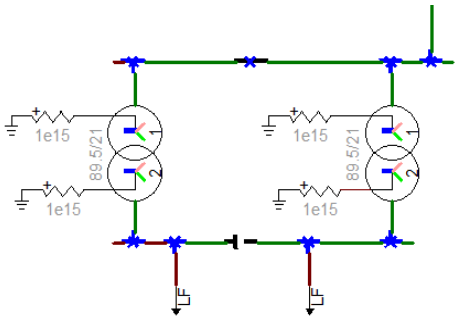

Figure 56 Substation with two loads and a no-loop structure

Appendix III : Transformer 225/21 kV YDD and YD

Equivalence

In the detailed load model of La Vaupalière, the factory test data sheet of the transformer 225/21 kV at Hotel-Dieu does not give the short-circuit tests results for the YDD transformer but for an equivalent YD transformer.

A transformer YDD under the following conditions :

- Same load on the medium and low voltage windings
- Same coupling

is equivalent to a transformer YD with double power at the secondary winding.

Transformer 225/21 kV at Hotel-Dieu YDD 1 data is :

$$U_{HV} = 227\ kV, \qquad U_{MV1} = U_{MV2} = 15.75\ kV$$
$$S_{HV} = 80\ MVA, \qquad S_{MV1} = S_{MV2} = 40\ MVA$$
$$X_{scHV/MV1} = 246.54\ \Omega \text{ and } X_{scHV/MV2} = 245.71\ \Omega \text{ aproximately equal}$$

Therefore, it is equivalent to a transformer 225/21 kV YD with :

$$U_{HV} = 227\ kV, U_{MV} = 15.75\ kV$$
$$S_{HV} = 80\ MVA, S_{MV} = 80\ MVA$$

Transformer 225/21 kV YD

The following data is required on EMTP for transformer 225/21 kV YD:

- Primary and secondary phase to phase voltage, respectively U_{HV}, U_{MV}
- Primary and secondary resistances, respectively R_{HV}, R_{MV}
- Primary and secondary reactances, respectively X_{HV}, X_{MV}
- Magnétisation resistance R_m
- Saturation curve $\Phi_m(i_m)$

The one phase model of a transformer YD is given on Figure 57 :

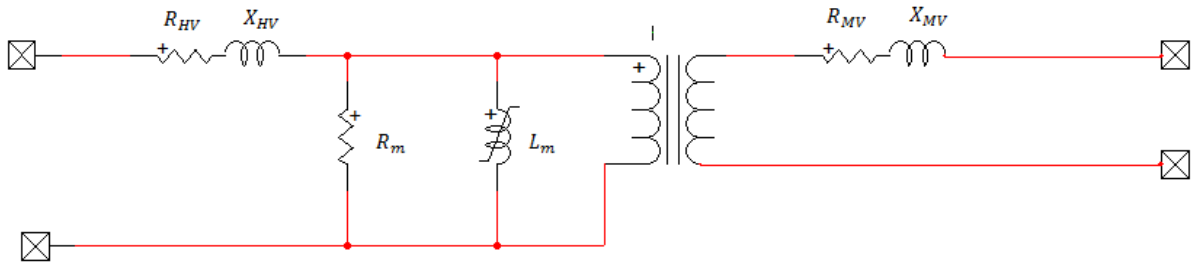

Figure 57 Transformer YD one phase model

Short-circuit test data for YD1 at Hotel Dieu:

High Voltage supplied, medium voltage short-circuited :

$$U_{sc\ HV/MV} = 22.47\ kV, \qquad I_{sc\ HV/MV} = 100\ A, \qquad P_{sc\ HV/MV} = 98.7\ kW$$

Primary and secondary's windings reactance refered to the primary side is :

$$X_{scH/MV} = \sqrt{\frac{U_{scHV/MV}}{\sqrt{3}\ I_{scHV/MV}} - \frac{P_{scHV/MV}}{3\ I_{scHV/MV}^2}}$$

Primary and secondary's windings resistance refered to the primary side is :

$$R_{scHV/MV} = \sqrt{\frac{P_{scHV/MV}}{3\ I_{scHV/MV}^2}}$$

which gives :

$$X_{scHV/MV} = 129.73\ \Omega \text{ and } R_{scHV/MV} = 0.00987\ \Omega$$

The ratio of the short-circuit reactance and resistance refered to the primary side is chosen as $w_p = 0.9$

$$X_{HV} = w_p\ X_{scHV/MV}$$

$$X_{MV} = (1 - w_p) X_{\frac{scHV}{MV}}\ \frac{\sqrt{3} U_{MV}}{U_{HV}}$$

$$R_{HV} = w_p\ R_{scHV/MV}$$

$$R_{MV} = (1 - w_p) R_{scHV/MV} \frac{\sqrt{3} U_{MV}}{U_{HV}}$$

The magnetising resistance is $R_m = \frac{U_{HV}^2}{P_{iron}}$

For the saturation curve $\Phi_m(i_m)$, refer to appendix I.

Appendix IV : short-circuit and open-circuit tests

To check the values of the transformer's parameters, short circuit tests are simulated. There are three short-circuit tests in the case of a three windings transformer and one in the case of a two windings transformer. In Table 25 are summarized the data and results for the short-circuit tests in the case of autotransformer AT762 (Appendix I). The short-circuit test 1 simulated on EMTP is displayed on Figure 58. The high voltage winding is energized, the secondary winding short-circuited and the tertiary winding open-circuited.

Short circuit test :

Table 25 Data and results of short-circuit tests for AT762

Winding energized and Voltage (kV)	Winding short-circuited	I (A)	I(A) measured	P_{sc} (W)	P_{sc} (W) measured
HV: 19.277	MV	285	284.99	127 900	127 895
HV : 14.583	LV	46.3	46.3	19 300	19 300
MV : 5.737	LV	78.2	78.2	17 290	17 290

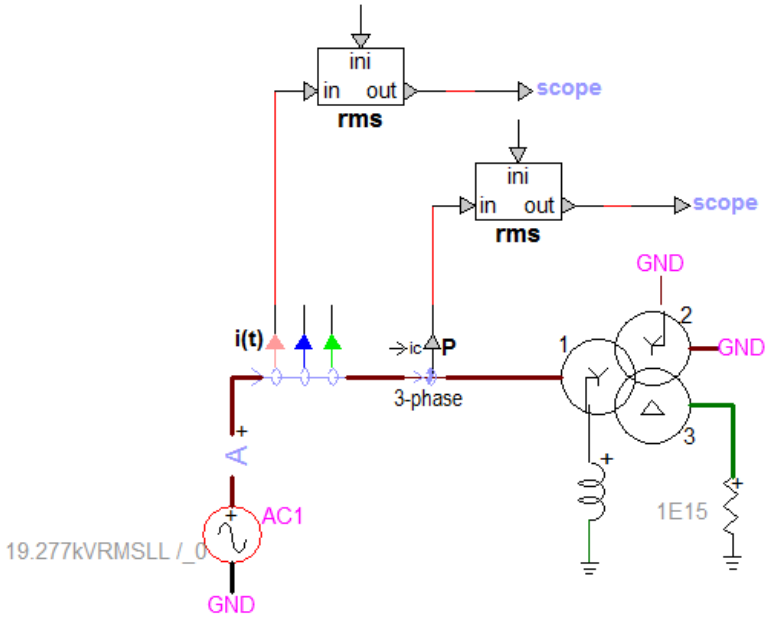

Figure 58 Short-circuit test 1 : HV winding energized, MV winding short-circuited

To check the saturation curve's values for the current, open circuit tests are simulated. There are 3 open-circuit tests. In the case of a three winding transformer, the tertiary winding is energized and the primary and secondary windings are open-circuited. In the case of a two windings transformer, the secondary winding is energized and the primary winding is open-circuited. In Table 26 are summarized the data and results for the open-circuit tests in the case of autotransformer AT762 (Appendix I). The short-circuit test 1 simulated on EMTP is displayed on Figure 58. The tertiary voltage winding is energized at 18.9 kV, the primary and secondary windings are short-circuited.

Open circuit test :

Table 26 Data and results of open-circuit tests for AT762

Voltage (kV)	I (A)	I (A) measured on EMTP
18.9	3.43	3.379
21	6.61	6.638
23.1	23.82	23.56

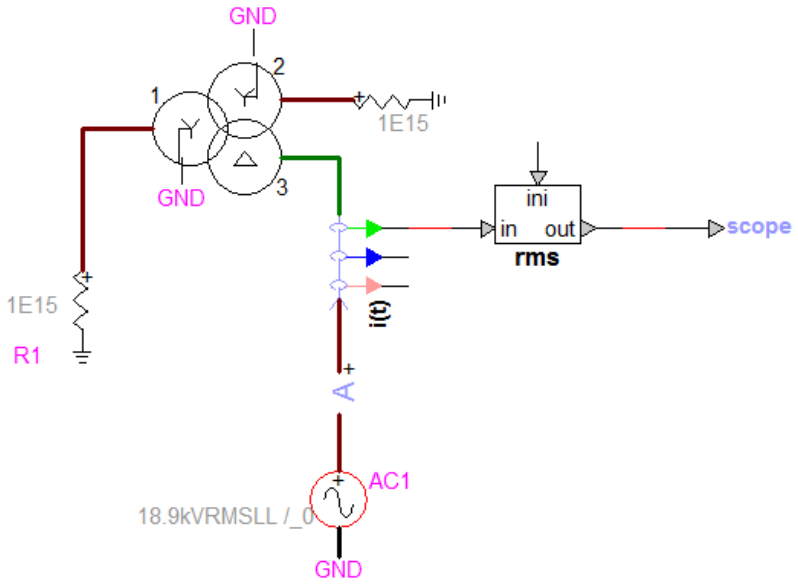

Figure 59 Open circuit test with tertiary winding energized at 18.9 kV

Appendix V : Sets of parameters for Parametric Studio

Table 27 Set of parameters for variation of flux

scenario	$\varphi_a^{initial}\,(Wb)$	$\varphi_b^{initial}(Wb)$	$\varphi_c^{initial}(Wb)$
1	0	0	0
2	873.26	-436.63	-436.63
3	0	873.26	-873.26
4	-873.26	436.63	436.63
5	0	-873.26	873.26
6	436.63	-218.32	-218.32
7	0	436.63	-436.63
8	-436.63	218.32	218.32
9	0	-436.63	436.63

Table 28 Set of parameters for variation of closing time of the switch phases'

$T_{close,A}\ (s)$	$T_{close,B}\ (s)$	$T_{close,C}\ (s)$
0.03	0.0056836	0.00243369
0.015	0.00432016	-0.00340534
0.029	-0.00268551	-0.00347781
0.02	-0.00331685	-0.00049584
0.014	-0.00880294	0.0005225
0.012	-0.00170144	0.00237582
0.028	0.00191445	0.0060135
0.022	-0.00282793	-0.00632518
0.011	-0.00291354	0.00218191
0.03	0.00293381	0.0027932
0.018	0.00083513	-0.0043977
0.016	0.00258263	5.57E-05
0.015	-2.50E-05	-0.00133695
0.023	-0.00539314	-0.00397357
0.024	-0.00918989	0.00481989
0.012	-0.00500636	-0.00163027
0.014	0.0044933	0.00131247
0.023	0.00558046	0.00311833
0.017	-0.00565989	0.00668102
0.024	-0.00238957	0.00564747
0.02	-0.00050082	0.00433379
0.018	-0.00440535	0.00232425
0.024	-0.00192052	-0.00034026
0.025	-0.00036805	5.23E-05
0.017	0.00110002	-0.00441718
0.017	0.00269777	0.00326221
0.023	-0.00068677	-0.00210772
0.028	0.00159368	0.00434919
0.012	0.00516457	-0.00437154
0.013	0.00155314	0.00270183
0.025	-0.00895552	0.00736565
0.012	-0.00067101	-0.00264034
0.028	0.00312313	0.00206041
0.018	-0.00666625	-0.00340751
0.026	-0.00138332	-0.00210845
0.018	0.00125213	-0.00446817
0.027	-0.0005288	-0.00279759
0.028	-0.00150016	-0.00421108
0.027	-0.00494359	-0.00648722
0.01	-0.00472	-0.00370637
0.028	-0.00474444	0.0020857
0.029	-0.00072129	-0.00264165
0.011	-0.00398463	0.0008666
0.01	-0.00403053	-0.00755712
0.027	-0.0030159	-0.00164594
0.015	-0.00190976	-0.00309595
0.029	-0.00244803	0.00773679
0.017	0.00243837	-0.00214652
0.023	0.00275812	-0.00171989
0.013	0.00362254	-0.0079508
0.017	-0.00265576	0.0029629
0.022	0.00602931	-0.00173545
0.014	0.00739668	-0.00738887
0.029	-0.00047803	-0.00679205
0.023	0.00101894	0.00205166
0.014	-0.00988108	0.00474853
0.011	-0.00637093	0.00293428
0.022	0.00431114	0.00670895
0.029	-0.00552207	0.00588393
0.016	-0.00620876	-0.00123931
0.025	0.00297164	0.00068324
0.019	-0.00467127	0.00243639
0.015	-0.00147601	-0.0047614
0.025	0.00123672	0.00209012
0.026	0.00146221	-0.00694788

$T_{close,A}\ (s)$	$T_{close,B}\ (s)$	$T_{close,C}\ (s)$
0.019	0.00709001	-0.00033947
0.011	0.00304339	0.00025332
0.028	0.00327366	-0.00482698
0.012	0.00223619	-0.00010351
0.026	-0.00107887	-0.00234942
0.022	-0.00721895	0.00108585
0.027	-0.00483209	0.00792221
0.027	0.0030959	0.00213048
0.022	0.00247669	0.00176833
0.029	-0.00061818	0.0006276
0.029	-0.00155274	-0.00436153
0.016	-0.00744078	-0.00434522
0.02	0.00252637	0.00582954
0.022	0.00261232	-0.00158842
0.029	0.001368	-0.00697702
0.028	-0.00653624	-0.00079162
0.015	-0.00504062	-0.00281147
0.02	0.00126667	-0.00557648
0.028	-0.00182845	0.00144021
0.02	-0.0053793	-0.00319053
0.026	0.00715715	0.00423023
0.023	-0.00274899	-0.00288829
0.024	-0.00590541	-0.00068118
0.013	0.00328444	0.00079844
0.029	0.00449718	-0.00833851
0.022	-0.00018871	0.00166989
0.024	0.00080208	0.00944916
0.015	0.00136327	-0.00880673
0.028	0.0042902	0.00558929
0.028	-0.00737501	0.0013302
0.021	-0.00335946	0.0058861
0.023	0.00136643	0.00203466
0.014	0.00192635	0.00427486
0.011	-0.00014312	0.00601768
0.024	-0.00487802	-0.001346

Appendix VI Harmonic analysis

According to Fourier, a periodic signal of period T_0 can be decomposed into a serie of cosinus and sinus at the fundamental frequency and at integer multiples of the fundamental frequency:

$$s(t) = a_0 + \sum_{n=1}^{\infty} a_n \cos(n2\pi f_0 t) + \sum_{n=1}^{\infty} b_n \sin(n2\pi f_0 t)$$

with

$$a_0 = \frac{1}{T_0}\int_{t=0}^{T_0} s(t)dt$$

$$a_n = \frac{2}{T_0}\int_{t=0}^{T_0} s(t)\cos(n2\pi f t)dt\,, n \geq 1$$

$$b_n = \frac{2}{T_0}\int_{t=0}^{T_0} s(t)\sin(n2\pi f t)\,dt,\ n \geq 1$$

Using a complex representation for the signal $\overline{s(t)}$, this expression becomes :

$$\overline{s(t)} = c_0 + \sum_{n=-\infty}^{+\infty} c_n e^{jn2\pi f t}$$

with

$c_0 = \frac{1}{T_0}\int_{t=0}^{T_0} s(t)dt$ the mean value of the signal $s(t)$

$$c_n = \frac{1}{T_0}\int_{t=0}^{T_0} s(t)e^{in2\pi f t}dt\,, |\, n \,| \geq 1$$

In the complex representation, negative harmonics appear.

The relation between the real coefficients a_n, b_n and the complex coefficients is :

$$c_n = \frac{a_n - i\, b_n}{2} = c_{-n}^{*}, n \geq 1$$

In the scope of the Thesis, the signal is the overvoltage at the primary of the transformer energized, so it is a real signal. The harmonic analysis represents the amplitude of the complex coefficient c_n as function of the rank of the harmonic n. As the signal is real, there are no negative harmonics c_n .

Appendix VII Line models

Infinitesimal portion of a line

An infinitesimal portion of a line is depicted on Figure 60.
$\bar{Z}$ and $\bar{Y}$ are defined as:
$\bar{Z} = R' + jwL'$ the impedance matrix,
$\bar{Y} = G' + jwC'$ the admittance matrix
$R', L', G' and\ C'$ are the parameters of the infinitesimal portion of the line dx.

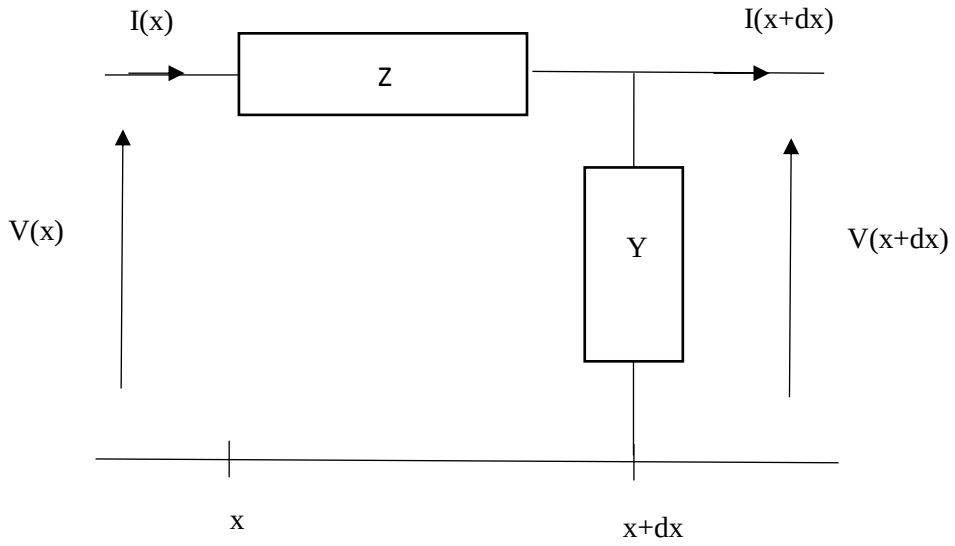

Figure 60 infinitesimal portion of a line

Constant parameter model

The CP model [5] neglects the frequency dependence of the resistance, the inductance and the capacitance. It assumes that the shunt conductance is zero, the line continuously transposed and parameters LC distributed. It first assumes a lossless line and then includes the losses. Reference 6] provides more information on the propagation equations in the case of a line using the constant parameter model.

It is defined:

$$I_{k_h} = \frac{V_k(t)}{Z_c} - I_k(t)$$
$$I_{m_h} = \frac{V_m(t)}{Z_c} + I_m(t)$$

The EMTP lossless distributed parameter single phase line model is assembled in Figure 61 from equations (7) and (8) :

$$I_{k_h} = \frac{V_m(t-T)}{Z_c} - I_m(t-T)$$

$$I_{m_h} = \frac{V_k(t-T)}{Z_c} + I_k(t-T)$$

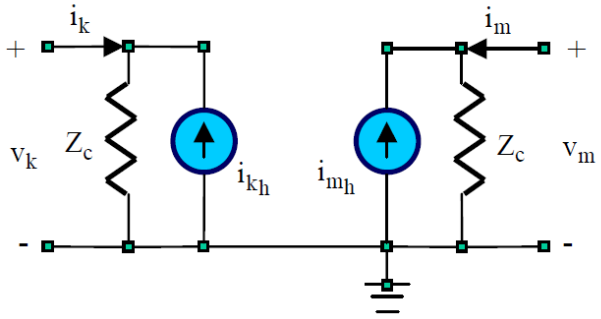

Figure 61 EMTP lossless distributed parameter single phase line model

The losses are modeled by separating the line into two lossless lines of halved equal propagation time and distributing the total line resistance into three, a quarter of resistance at both ends of the line and half a resistance in the middle.

The multiphase version is a generalization of the single phase line model.

Wideband model

The model takes into account the frequency dependence of parameters R(w) and L(w) as well as the distributed nature of the line. The model is used for the 400 kV lines in the black start study. The 400 kV lines are often not transposed in France. This causes the phase voltage to be slightly different.

$\overline{Z(w)} = R(w) + jwL(w)$ the impedance matrix
$\overline{Y(w)} = G + jwC$ the admittance matrix

$$\begin{cases} \overline{Z(w)}\,\overline{I(x,w)}\,dz = \overline{V(x,w)} - \overline{V(x+dx,w)} \\ \overline{I(x,w)} - \overline{I(x+dx,w)} = \overline{Y(w)}\,\overline{V(x+dx,w)} \end{cases}$$

$$\begin{cases} \overline{Z(w)I(x)} = -\frac{d\overline{V(x,w)}}{dx} \\ \overline{Y(w)V(x,w)} = -\frac{d\overline{I(x)}}{dx} \end{cases}$$

So the line propagation equations are :

$$\begin{cases} \frac{d^2\overline{V(z,w)}}{dx^2} = \overline{Z(w)}\ \overline{Y(w)}\ \overline{V(z)} \quad (1) \\ \frac{d^2\overline{I(x)}}{dx^2} = \overline{Y(w)}\ \overline{Z(w)}\ \overline{I(x,w)} \quad (2) \end{cases}$$

if index k represent the sending end and m the receiving end of a line of length l, then a solution to equations (1) and (2) in frequency domain is:

$$\begin{cases} \overline{Y_c}\,\overline{V_k} - \overline{I_k} = \overline{H}\,(\overline{Y_c}\,\overline{V_m} - \overline{I_m}) \quad (1') \\ \overline{Y_c}\,\overline{V_m} + \overline{I_m} = \overline{H}\,(\overline{Y_c}\,\overline{V_k} + \overline{I_k}) \quad (2') \end{cases}$$

these equations can be seen as incident current waves (1') and reflected current wave (2') with :

$\Gamma(w) = \sqrt{Y(w)Z(w)}$
$\overline{Y_c} = Z^{-1}\sqrt{Z(w)\,Y(w)}$ the characteristic matrix
$H = e^{-\Gamma(\omega)l}$ the propagation function

H and Y_c are frequency dependent quantities which characterizes the lines in the frequency domain. The frequency domain equations can directly be used for steady state analysis but for transient analysis they should be converted into time domain.
An efficient approach is to replace H and Y_c by low order rational function approximations. References 6]-[7] provide more information on the wideband model.

Appendix VIII Frequency Dependent Network Equivalent

A frequency dependent network equivalent (FDNE) is an equivalent of a part of the grid with the same frequency response. The exact admittance function is approximated by a rational function using vector fitting. A frequency equivalent of the detailed model is an excellent simplified model. The FDNE was not considered as long as it was tried to avoid having to build the detailed model.

The CPU time for the time-domain analysis of one scenario: $(\varphi_a, \varphi_b, \varphi_c) = (0,0,0)$ $t_A = 0.01\ s$ $\Delta_b = \Delta_c = 0.001\ s$, with a simulation time step of $20\ \mu s$, is $2.32\ s$. The computer used is a regular computer (CPU with $2.8\ GHz$). Though the CPU time is slightly higher than the CPU time of the same backbone using a basic or simplified load models, it remains much lower than the CPU time of the backbone using the detailed load model ($6.10\ s$ according to Table 14).

Time-domain analysis is carried out on the Normandy's backbone using the FDNE load model. The results, summarized in Table 29, are all better than with the basic load model and generally better than with the simplified models (except for 40% load pick-up).

Table 29 Time-domain results of Normandy's backbone with FDNE load model

Percentage of active load picked-up (%)	Overvoltage (p.u)	Error (%)
100	1.057	0.16
70	1.069	0.25
40	1.086	0.41
10	1.127	0.28

The FDNE load model used in a black start simulation gives very accurate results and requires short simulation time. The disadvantage is that the detailed load model has to be built first in order to know the exact admittance function and the process for building the detailed load model is long. Besides, all information is not available so assumptions have to be made.

Appendix IX Results of frequency and time-domain analysis on Nancy's real backbone

The network restoration plan for Nancy's backbone gives the different steps for the restoration phase, depicted on Figure 62. The nuclear power plant at Cattenom is used for black start.

1- Vigy 400 kV is energized.
2- Bezaumont 400 kV is energized.

The distance between the transformer to be energized at Logelbach and the last transformer energized at Cattenom, 232 km, is higher than the critical distance (95 km) so energizing an autotransformer at Logelbach can lead to transient harmonic overvoltage. It is decided to pick-up 100 MW load at Bezaumont so as to damp the resonance and thus limit the risk of transient overvoltages.

3- An autransformer 400/225 kV is energized. After energizing the autotransformer at Bezaumont, the 225 kV load pocket is automatically energized.
4- Priority load is picked-up at Void, Croix de Metz and Custines .
5- Transformer 225/63 kV is energized. Bezaumont 63 kV load pocket is automatically energized.
6- Priority load is picked-up at Millery and Saizerais.
7- Houdreville is energized
8- Logelbach is energized and the autotransformer 400/63 kV at Logelbach is energized. The distance between the autotransformer to be energized at Logelbach and the last autotransformer energized at Bezaumont is higher than the critical distance but the 100 MW load picked-up at Bezaumont limits the risk of overvoltages.

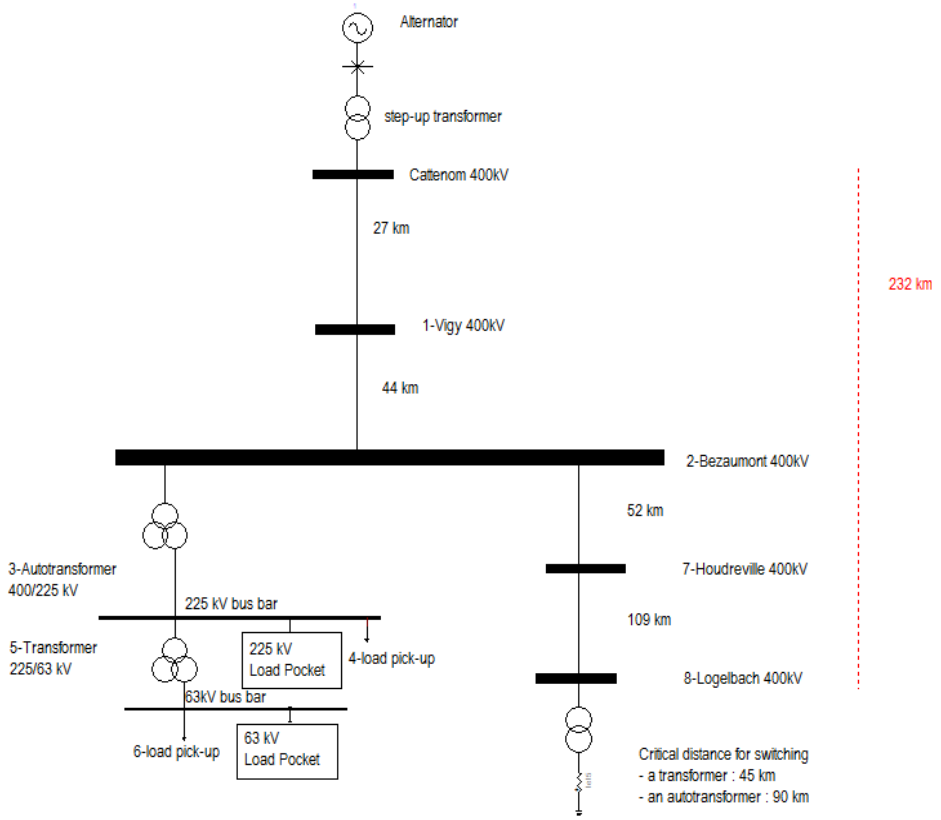

Figure 62 network restoration plan for Nancy

RTE performed a study using for the load at Bezaumont the basic load model with $P = 100\ MW$ and $Q = 30\ MVar$. The active load power picked-up was then reduced. This study was performed with a more robust method than the method described in chapter 3 because two parameters from the grid were varied : the sub transitoire reactance of the synchronous machine X_d" and the phase to earth capacity of the 400 kV lines. As a result an additional set of 9 scenarios was simulated. The set of parameters for the initial flux is the same as the one used in chapter 4. The set of parameters for the closing time of the switch is generated randomly as described in chapter 4. Though the values are not equal to those displayed in Appendix V, the set checks the properties described in chapter 4. The delay set to remove the overvoltages due to the phases' dispersion. The voltage is measured at the primary of the transformer at Logelbach.

The black start study was carried-out with the detailed direct and basic load model at Bezaumont. The method is not as robust because it is chosen not to take the sub transient reactance of the synchronous machine as a parameter to shorten the simulation time. However, there is one additional parameter, the load model. It is justified to neglect the sub transient reactance of the synchronous machine because it has little influence on the results of the time-domain simulation.

A frequency analysis is carried-out on the real Nancy's backbone, using the basic, direct and detailed load model and varying the active load picked-up. The results are shown on Figure 63 to Figure 66.

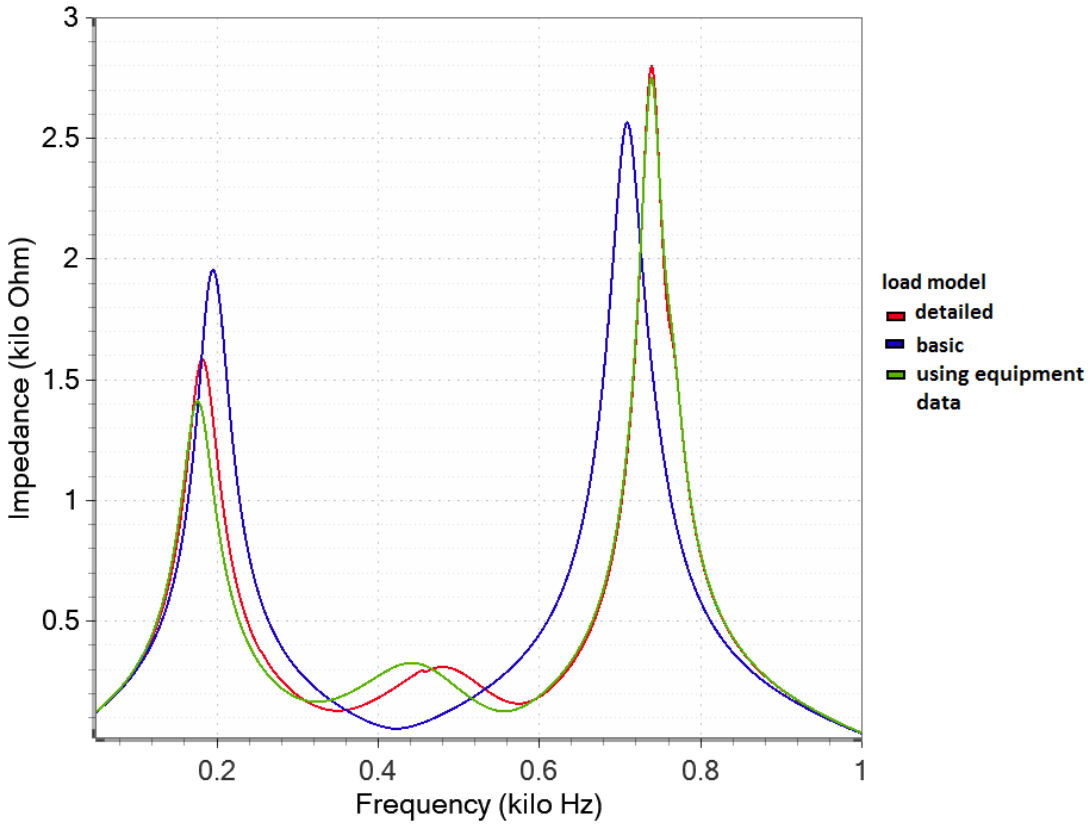

Figure 63 Frequency analysis of Nancy's backbone with 100% of the active load of Bezaumont

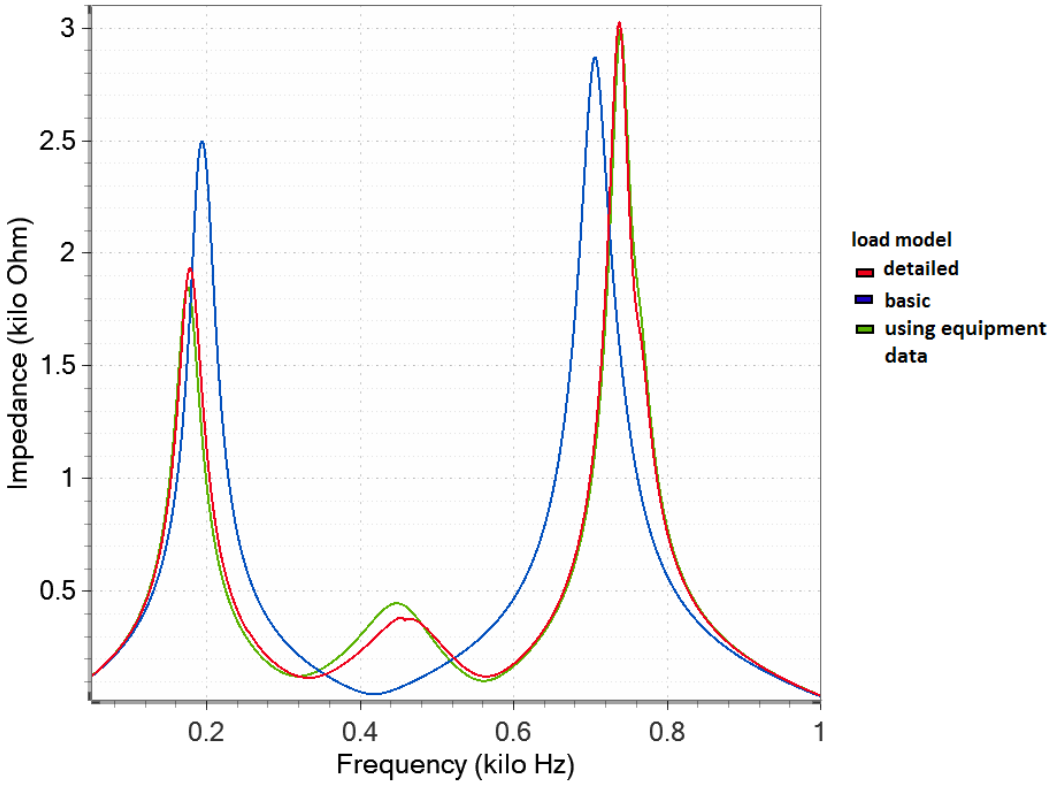

Figure 64 Frequency analysis of Nancy's backbone with 70% of active load of Bezaumont

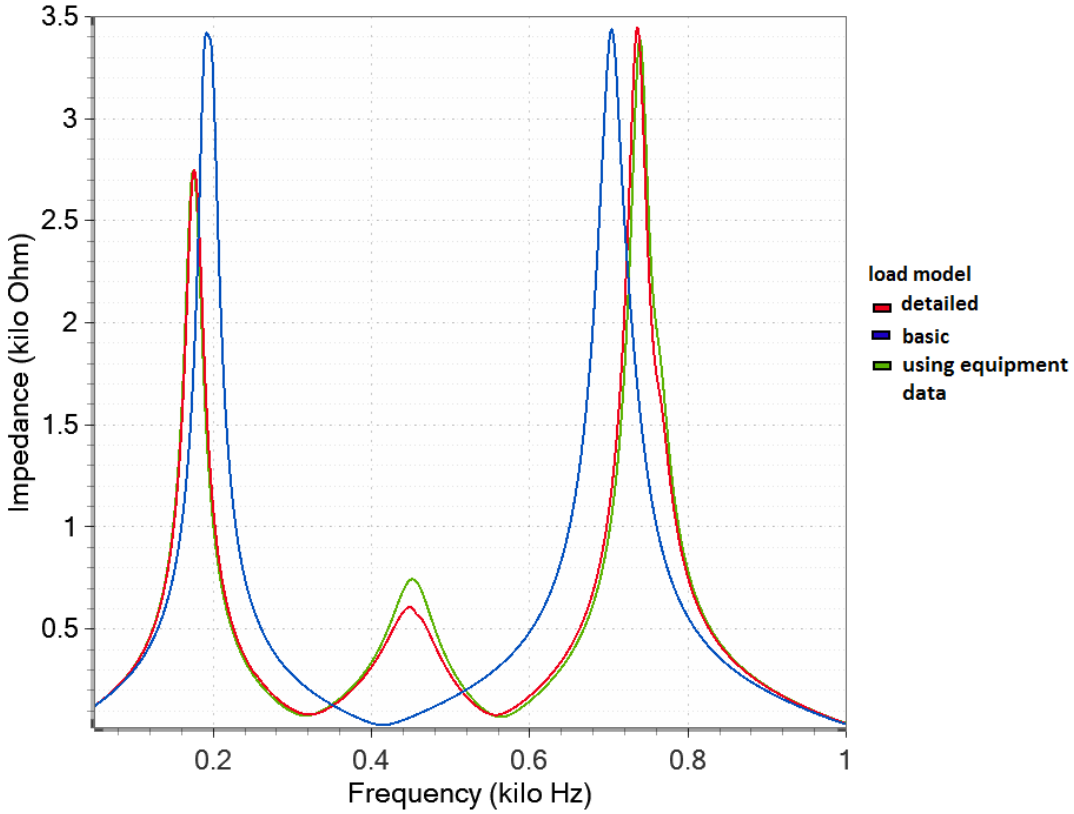

Figure 65 Frequency analysis of Nancy's backbone with 40% of active load of Bezaumont

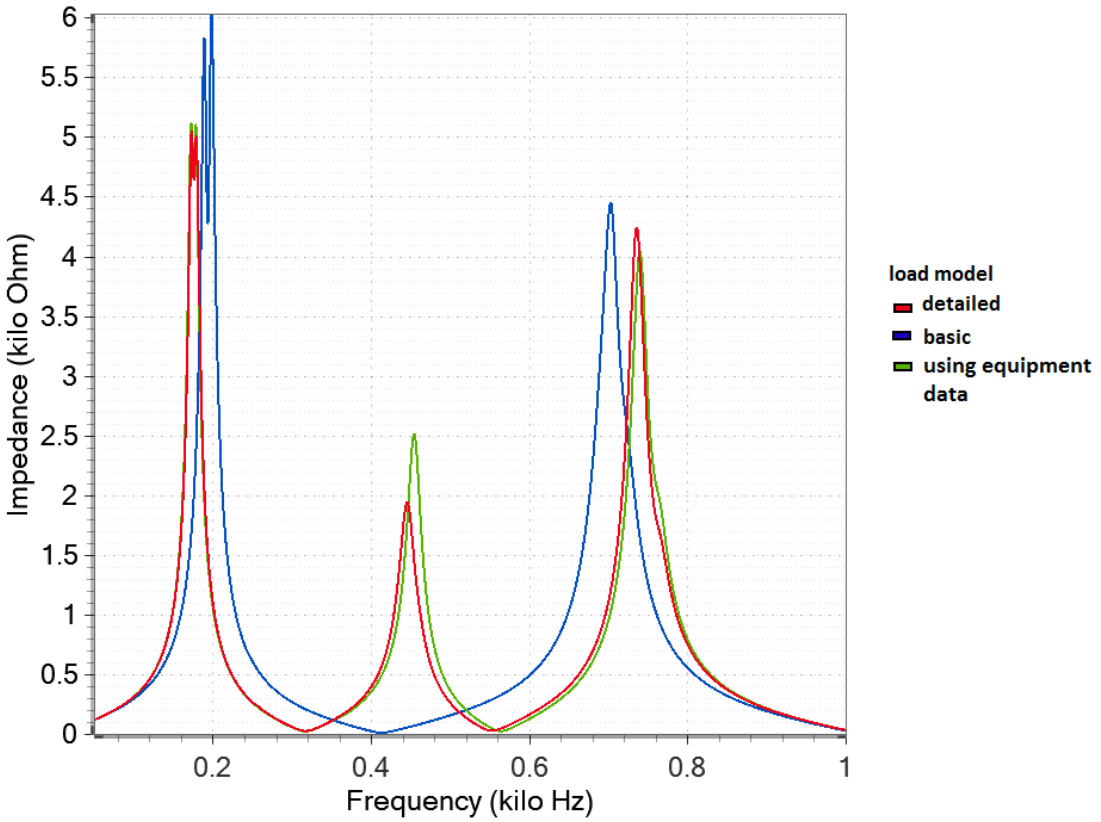

Figure 66 Frequency analysis of Nancy's backbone with 10% of active load of Bezaumont

The results of the time-domain analysis are summarized in

Table 30. As expected, the overvoltages are weak, less than $1.11\ p.u$ according to the reference. Therefore, the comparison of load models is not meaningful. That is why in 5.3 a black-start study is carried-out on a fictive backbone using the load of Bezaumont.

Table 30 Phase to earth overvoltages values when energizing the autotransformer at Logelbach

Active load (MW)	Basic load model	Direct load model	Detailed load model
100	1.08	1.01	1.09
70	1.09	1.02	1.09
40	1.16	1.03	1.10
10	1.32	1.06	1.10